

EFFECTIVENESS OF ULTRAFILTRATION ON THE RECOVERY AND REUSE OF
LIQUID ENZYMES IN THE PRODUCTION OF BIODIESEL

A Thesis
by
REBECCA HOBDEN

Submitted to the Graduate School
at Appalachian State University
in partial fulfillment of the requirements for the degree of
MASTER OF SCIENCE

May 2013
Department of Technology and Environmental Design

EFFECTIVENESS OF ULTRAFILTRATION ON THE RECOVERY AND REUSE OF
LIQUID ENZYMES IN THE PRODUCTION OF BIODIESEL

A Thesis
by
REBECCA HOBDEN
May 2013

APPROVED BY:

Jeffrey E. Ramsdell
Chairperson, Thesis Committee

Eric Allain
Member, Thesis Committee

Marie Hoepfl
Member, Thesis Committee

Jeffrey S. Tiller
Chairperson, Department of Technology and Environmental Design

Edelma D. Huntley, PhD
Dean, Graduate School and Research & Sponsored Programs

Copyright by Rebecca Hobden 2013
All Rights Reserved

Abstract

EFFECTIVENESS OF ULTRAFILTRATION ON THE RECOVERY AND REUSE OF LIQUID ENZYMES IN THE PRODUCTION OF BIODIESEL

Rebecca Hobden,
B.S., Manhattan College
M.S., Appalachian State University

Chairperson: Jeffrey E. Ramsdell

Biodiesel is a transportation fuel that has similar characteristics to petroleum diesel, but is made from natural fats and oils, making it a more renewable and sustainable alternative. The most sustainable biodiesel uses low quality waste streams, such as waste vegetable oils, animal fats, soapstocks, and brown grease as feedstock. Traditional biodiesel production involves a transesterification reaction to convert feedstock to biodiesel using an acid or base catalyst. Enzymatic catalysts and the role they can play in production of biodiesel have begun to be researched because they are more environmentally benign, produce higher value co-products, require less energy, and produce cleaner biodiesel as compared to acid or base catalysts. The major drawback of enzymatic catalysts is their high cost. Therefore, to make enzymes a feasible and affordable alternative, the producer must be able to recover and reuse them. This research looks at two techniques to effectively and efficiently recover enzymes so they can be reused to catalyze multiple batches.

Two runs were analyzed, each of which used one dose of enzymes to catalyze four consecutive batches. Enzyme recovery and reuse techniques of a simple settling method versus ultrafiltration were compared. The initial batch in each run reacted feedstock,

methanol, water, glycerol, and fresh enzyme over a 24 hour period. At the completion of the reaction, batches were allowed to settle. After two hours of settling, two phases formed: a biodiesel phase and an aqueous phase, the latter of which contained the enzymes. In the filtration method, at this point the aqueous phase passed into a tangential flow filtration module where enzymes were retained by the membrane, resulting in an enzyme-rich retentate that was used to catalyze the next batch in the run. This technique was compared to a technique that allowed a longer settling time of 24-72 hours, during which the enzymes concentrated in a thin layer between the two phases. This enzyme layer was recovered with a portion of the aqueous phase and used to catalyze the next batch in the run.

Samples were taken throughout the batches and the FAME was analyzed for free fatty acids. Gas chromatography was used to determine bound glycerin content. Additionally, at the 24-hour period, samples of the aqueous phase were analyzed for enzyme activity. Analysis showed that both techniques resulted in some loss of enzymes, but the overall loss in activity was 46.8% using ultrafiltration compared to 72.7% with settling. This loss of enzymes in the settling technique is also seen by a more significant reduction in reaction rates from one batch to the next as compared to the rates of consecutive batches with enzymes recovered using the ultrafiltration technique. Although findings are preliminary, this study shows promise for enzyme catalysts as an economically feasible alternative for biodiesel producers, particularly when using ultrafiltration as a way to recover and reuse enzymes. Additional research and optimization of this process is one step in making enzymatic biodiesel production a reality.

Dedication

To Mary Elizabeth Scherger, to whom I owe an eternal debt of gratitude for the love and support that has allowed me to find a career and life path that I truly love. Thank you.

To my parents, Bonnie and Jim Hobden, for their unconditional love and support through it all.

Acknowledgements

Many knowledgeable and passionate people have contributed to this thesis. I would like to express my gratitude for their dedication to enzymatic biodiesel and to me; without them, this work would not have been possible.

I would like to acknowledge first and foremost Paul Eudy, whose knowledge of chemistry, biodiesel production, research and analysis techniques, grammar, life, and just about everything, his resourcefulness, his willingness to answer yet another call from me, his ability to *almost* always be right, and his willingness to share all this with me made him an invaluable partner in this endeavor. And to Paul and Summer for allowing me to be their most favorite houseguest. Thank you.

I would also like to acknowledge Rachel Burton for giving me the opportunity to partner with Piedmont Biofuels for this research. More importantly for being an inspiration as a strong female leader who is able to speak confidently about her long acquired knowledge in the field of biodiesel production and for her dedication to improving our sustainability portfolio by engaging in research and development of innovative technologies.

I would like to thank Mark Vanderhoff for his commitment to improving biodiesel production with the use of ultrafiltration technology, even in the wee hours of the morning. Additionally, for his support and his assistance in helping me find an opportunity where I can continue to grow in the field of enzymatic biodiesel production and beyond. Thank you.

I would like to express my thanks to Dr. Jeff Ramsdell for his support and guidance throughout my graduate career here at Appalachian State University. His confidence in my abilities and high expectations have pushed me to develop the skills and knowledge to the extent that I have over these past two years.

Thanks also to Dr. Eric Allain, an excellent teacher who has shared his vast knowledge of enzymes and his interest in their industrial application.

Thanks to Dr. Marie Hoepfl for her input on this thesis work, she has read through the many versions of this thesis more than any other person.

Thanks to Zack Hobbs who has been my friend from day one. He helped me as a skilled engineer, chemist, biodiesel producer, handy man, dog lover, mechanic, and all around nice guy. I will miss you next year.

Table of Contents

Abstract.....	iv
Dedication.....	vi
Acknowledgements.....	vii
List of Tables.....	xii
List of Equations.....	xiii
List of Figures.....	xiv
Chapter 1: INTRODUCTION.....	1
Statement of the Problem.....	3
Purpose of the Study.....	4
Research Hypothesis and Related Research Question.....	4
Limitations of the Study.....	5
Significance of the Study.....	6
Glossary of Terms.....	7
Symbols & Abbreviations.....	9
Chapter 2: REVIEW OF RELATED LITERATURE.....	11
Feedstocks.....	11
Virgin versus waste feedstock.....	12
Saturation and degumming.....	14
Traditional Biodiesel Production.....	14
Catalysts.....	16
Reactions of triglycerides and free fatty acids to form fatty acid methyl esters.....	16
Alkali catalyst.....	17
Acidic catalyst.....	20
Two-step process.....	20
Enzymes.....	23
Physical characteristics of enzymes.....	23
Enzymes as catalysts.....	23
Enzyme kinetics.....	28
Rate of reaction.....	29
Ping pong bi-bi mechanism.....	32
Specificity.....	33
Specificity constant.....	33
Enzyme inhibition.....	34
Enzyme Catalyzed Biodiesel Production.....	34
Lipases.....	37
α/β hydrolase fold superfamily.....	37
Lipase subfamily.....	40
Interfacial activation and the lid.....	40

Active site triad	41
Lipase mechanism.....	43
Regioselectivity of lipases.	46
Enzyme inhibition and other considerations.....	47
Alcohol inhibition.	48
Ping pong bi-bi mechanism with competitive inhibition.....	48
Water content.....	50
Use of solvents.....	51
Liquid versus immobilized enzymes.	52
Enzyme loading.	55
Recovery and Reuse of Liquid Enzymes	55
Membrane-based ultrafiltration.	56
Tangential flow filtration.	58
Tangential flow filtration unit.....	59
Chapter 3: METHODOLOGY.....	62
General Overview of the Research Design.....	62
Collaboration with Piedmont Biofuels.....	64
Previous Research on Callera Trans	65
Previous Research on Enzyme Recovery via TFF.....	67
Characterization of Inputs.....	67
Apparatus	68
Transesterification Reactor	68
Validating Dosing Pump Configuration.	69
Tangential Flow Filtration Unit	69
Cleaning the tangential flow filtration unit between runs and NWP.....	73
Procedure	73
First-Batch Transesterification Reaction	73
Recovery and Reuse of Enzyme via Selective Aqueous Phase Reduction.....	75
Recovery and Reuse of Enzyme via Tangential Flow Filtration	77
Analysis of Feedstock and Biodiesel	79
Determining Free Fatty Acids.....	79
Determining Monoglycerides, Diglycerides, Triglycerides, Bound Glycerin.....	79
Determining Methanol	80
Analysis of Aqueous Phase.....	81
Determining Water.....	81
Determining Glycerol	81
Determining Methanol.....	82
Determining Enzyme Activity in Reduction and Permeate.....	82
Filtration Performance	83
Chapter 4: FINDINGS AND DISCUSSION.....	84
Introduction.....	84
Free Fatty Acid	84
Initial Batches	87
Selective Aqueous Phase Reduction.....	90
Tangential Flow Filtration	93
Enzyme Activity in Permeate	95

Reuse Batches	97
Methanol discrepancy.	97
SAPR reactions.	98
TFF reactions.	100
FAME Production.....	103
Chapter 5: CONCLUSIONS.....	105
Research Hypothesis.....	105
Introduction.....	105
Implications for Enzyme Use in Biodiesel Production.....	105
Suggestions for Further Research	107
Final Remarks	108
REFERENCES	110
Vita.....	115

LIST OF TABLES

Table 2.1. Range of FFA in Various Feedstocks and Oils.....	13
Table 2.2. Comparison of Reaction Conditions and Performance for Various Types of Catalysts Used in Transesterification of WVO.....	22
Table 2.3. Variables Affecting Enzyme Reactions.....	27
Table 2.4. Summary of Research Conducted on Biodiesel Production with Various Lipases.....	35
Table 2.5. Important Features of Lipases.....	43
Table 3.1. First-Batch Recipe.....	74
Table 4.1. SAPR Reduction Content.....	91
Table 4.2. TFF Permeate Flux.....	93
Table 4.3. TFF Permeate Content.....	94
Table 4.4. TFF Parameters.....	95
Table 4.5. Methanol Discrepancies in SAPR and TFF Runs.....	98
Table 4.6. SAPR Model and Rate Decrease with Associate Residual Sum of Squares Error.....	99
Table 4.7. TFF Model and Rate Decrease with Associate Residual Sum of Squares Error.....	101

LIST OF EQUATIONS

Equation 2.1. Michaelis-Menton Constant.....	30
Equation 2.2. Rate of Reaction.....	30
Equation 2.3. Maximum Rate of Reaction.....	31
Equation 2.4. Michaelis-Menton Equation.....	31
Equation 2.5. Rate of Reaction with Alcohol and Substrate Inhibition	50
Equation 2.6. Permeate Flux Rate.....	59
Equation 3.1. Permeate Flux Rate.....	73
Equation 3.2. Mass percentage of for Individual Glyceride in Sample.....	80
Equation 3.3. Bound Glycerin Contribution from Monoglycerides.....	80
Equation 3.4. Bound Glycerin Contribution from Diglycerides.....	80
Equation 3.5. Bound Glycerin Contribution from Triglycerides.....	80
Equation 4.1 Model 1 for Bound Glycerin Consumption.....	88
Equation 4.2 Model 2 for Bound Glycerin Consumption	88

LIST OF FIGURES

Figure 2.1. Hydrolysis of triglycerides to form free fatty acid.....	12
Figure 2.2. Transesterification is the primary reaction in the production of FAME.....	17
Figure 2.3. Three step progression of triglycerides to fatty acid methyl esters.....	18
Figure 2.4. Esterification of free fatty acids to produce FAME and water.....	19
Figure 2.5. Saponification of free fatty acids to form soaps.....	19
Figure 2.6. Transition state diagram of a catalyzed and an uncatalyzed reaction.....	25
Figure 2.7. Transition state diagram for an enzyme catalyzed reaction and an uncatalyzed reaction.....	27
Figure 2.8. Simplest form of an enzyme-catalyzed reaction with rate constants.....	29
Figure 2.9. Graph of rate, v , versus substrate concentration, $[S]$	31
Figure 2.10. Ping pong bi-bi mechanism.....	32
Figure 2.11. Secondary structure diagram of a ‘canonical’ α/β hydrolase fold.....	38
Figure 2.12. Variability of the secondary structure of α/β hydrolase fold.....	39
Figure 2.13. Structure of <i>Mucor miehei</i> lipase in closed and open form.....	42
Figure 2.14. Catalytic mechanism of the serine proteases.....	44
Figure 2.15. Oxanion hole found in lipases.....	46
Figure 2.16. Regioselectivity of lipases.....	47
Figure 2.17. Schematic representation of the ping pong bi-bi mechanism with competitive inhibition by both alcohol and acid substrates.....	49
Figure 2.18. Filtration type versus pore size.....	56

Figure 2.19. Dead-end filtration versus cross-flow filtration.....	58
Figure 2.20. Tangential Flow Filtration module where feed stream flows tangentially to the membrane layers.....	60
Figure 2.21. System design for TFF unit for thermally sensitive materials.....	61
Figure 3.1. Three distinct phases formed during initial trials using Callera Trans to esterify virgin soy bean oil to produce FAME.....	63
Figure 3.2. A fully enzymatic biodiesel production consists of two steps: transesterification of TG followed by esterification of FFA.....	66
Figure 3.3. Purosep Phoenix Pilot Scale Filtration Unit in conjunction with the CONSEP® 3000 filter module and manifold.....	70
Figure 3.4. CONSEP® 3000 membrane details.....	71
Figure 3.5. Phase separation after 2 hours and after 24 - 72 hours of settling.....	76
Figure 3.6. Diagram of the set-up for recovering enzymes using the SAPR technique.....	77
Figure 3.7. Diagram of the set-up for recovering enzymes using the TFF technique.....	78
Figure 4.1. Lipase transesterification involves hydrolysis followed by esterification.....	85
Figure 4.2. FFA content over the course of the initial reaction of the SAPR run.....	86
Figure 4.3. FFA content over the course of the initial reaction of the TFF run.....	86
Figure 4.4. BG content over the course of the initial SAPR run.....	89
Figure 4.5. BG content over the course of the initial TFF run.....	89
Figure 4.6. Samples from SAPR1 versus SAPR4.....	92
Figure 4.7. Enzyme activity in SAPR and TFF Permeates based on FFA and FAME.....	96
Figure 4.8. Rate of BG consumption post methanol dosing to 24 hour point for SAPR run.....	99
Figure 4.9. Rate of BG consumption post methanol dosing to 10 hour point for SAPR run.....	100

Figure 4.10. Rate of BG consumption post methanol dosing to 24 hour point for TFF run.....	101
Figure 4.11. Rate of BG consumption post methanol dosing to 10 hour point for TFF run.....	102
Figure 4.12. Rate decrease between adjacent batches for SAPR and TFF runs.....	102
Figure 4.13. Overall rate decrease from initial to final batches SAPR and TFF runs.....	104
Figure 4.14. Performance curve for the enzyme.....	104

Chapter 1: INTRODUCTION

The dependence of modern communities on convenient transportation fuels creates a mounting dilemma as the cost, insecurity and environmental degradation of obtaining petroleum fossil fuels increases. According to the US Energy Information Administration (USEIA), the United States consumed 18.8 million barrels per day (MMbd) of petroleum products during 2011. One way this dependence is being curbed is through the gradual adoption of alternative fuels. Biodiesel is one such alternative fuel that can be used in existing diesel engines, is a renewable energy, particularly when produced from waste oil streams, and is a non-toxic, biodegradable resource.

Because of the increasing acceptance and demand for biodiesel, production numbers for 2011 reached over one billion gallons (approx. 0.07 MMbd) according to a year-end report published by the US Environmental Protection Agency. While this number is a small fraction of the overall petroleum consumption, its use is a growing trend. To date there are 151 production plants registered with the National Biodiesel Board (NBB) in the United States, with more than half of those reporting production capacity of less than 5,000,000 gallons per year. These production plants are small compared to other biodiesel producers, some of whose yearly production capacity exceeds 100,000,000 gallons, but they, none the less, play an important role in bringing biodiesel into the communities of mainstream culture.

A defining characteristic of many of these smaller biodiesel producers is a mission that considers the environmental and community benefits, as well as economic ones. The environmental benefits of biodiesel are realized in the diversion of waste streams, such as

waste vegetable oil (WVO), chicken fat, and pork fat; production of a renewable resource to displace fossil fuels; reduction of emissions such as carbon monoxide, ozone-forming hydrocarbons, hazardous diesel particulate, and sulfur dioxide during combustion; and its biodegradable and nontoxic nature. Communities benefit from the production of biodiesel in the creation of jobs in a growing sector of business; decrease in reliance on foreign oil imports; and enhancement of rural economies by providing a market for excess production of vegetable oils and animal fats (Akoh, Chang, Lee, & Shaw, 2007; Burton & Fan, 2009; Shah, Sharma, & Gupta, 2003; Wang, Ou, & Zhang, 2007).

As with any commercial endeavor, a balance between the mission and the economics must be met to ensure success. Economic considerations and costs include how quickly feedstock can be converted to clean biodiesel, availability and quality of feedstock, inputs other than feedstock, energy inputs required for heating processes, downstream purification and input recovery, labor, and quality control.

Traditionally, biodiesel production uses a base or acid catalyst to convert triglycerides (TG) and free fatty acids (FFA) found in fat and oil feedstocks into fatty acid acyl esters (FAAE) or biodiesel. Once converted the FAAE requires purification from contaminants and byproducts, such as glycerol, soaps, water, catalyst and excess methanol. The expense and availability of feedstock and downstream processes, which are costly and create a large volume of contaminated wastewater, are major limitations to the success of any small scale commercial producer. Therefore, choice of catalyst, which influences quality of feedstock that can be used and the presence and interaction of by-products during the reaction and purification process, can influence the overall success of the producer.

More recently enzymatic catalysts have been researched as an attractive option in biodiesel production. The use of enzyme catalysts, rather than traditional chemical catalysts, has the potential to offer an economic advantage by utilizing lower quality (and often cheaper) feedstocks from more varied sources. Additionally, research has shown the enzyme catalyzed process to produce a higher value co-product of technical grade glycerol, react under milder conditions, and thus more energy efficient conditions, and produce a cleaner biodiesel product requiring less downstream purification (Akoh et al., 2007; Shah et al., 2003). However, to make costly enzymes truly an affordable alternative, the producer must be able to recover and reuse them. The optimization of the recovery and reuse process currently being explored by industry and academics will help make enzymatic biodiesel production for the small scale producer feasible.

Statement of the Problem

In spite of the many benefits of using enzyme catalysts, cost has been a constraining factor in their widespread adoption (Fjerbaek, Christensen, & Norddahl, 2009). One way to offset some of the cost associated with enzymes is to recover and reuse the initial dosage of enzymes for several biodiesel batches. This has prompted recent research in immobilized enzymes as they are bound to a carrier and thus easy to extract via a simple screening process. However, immobilized enzymes are much more costly and the bulky carrier can lead to a decrease in enzyme activity (Fjerbaek et al., 2009). Liquid or soluble enzymes are cheaper and often times a more effective catalyst than immobilized enzymes, however the difficulty in removing and reusing them has been a deterrent to their use.

Two emerging techniques in which liquid enzyme catalysts have been recovered are through gravity settling and decantation of by-products, enzymes and biodiesel or with an

ultrafiltration system. In the first technique referred to as selective aqueous phase reduction or SAPR the aqueous phase, composed predominantly of glycerol co-product, excess methanol, water, and enzyme, is allowed an extended period of settling time during which the enzyme can separate from the more dense material. The second technique is defined by the use of tangential flow filtration or TFF, a form of ultrafiltration. In this technique the aqueous phase is circulated through the filtration unit, which retains the enzyme and allows glycerol, water, and methanol to be removed as permeate.

Purpose of the Study

This research aimed to quantify the effectiveness of using these enzyme recovery technologies on a pilot-scale representative of and easily scalable to small commercial producers. Comparisons were made in the use of a TFF system to SAPR as a recovery technique of one form of the enzyme *Thermomyces lanuginosus* lipase after its use and reuse as a catalyst for the transesterification of triglycerides (TG) with methanol to make fatty acid methyl esters (FAME) or biodiesel. The percent conversion of TG to FAME was determined using gas chromatography throughout and at the completion of each of four consecutive batches made with one dose on enzymes. The FAME yield as well as enzyme activity tests performed on the permeate (for TFF) or reduction (for SAPR) streams was used to determine the recovery rate of active enzyme from the previous batch.

Research Hypothesis and Related Research Question

This research is guided by the following hypothesis:

H1: Tangential Flow Filtration (TFF) is a more effective method for the recovery of active, liquid enzymes from the transesterification of waste vegetable oil with up to 10% free fatty acid (FFA) into fatty acid methyl esters (FAME) catalyzed by a commercially available

formulation of the enzyme *Thermomyces lanuginosus* lipase as compared to the simpler separation technique of selective aqueous phase reduction (SAPR).

Limitations of the Study

The limitations of this study can be categorized into factors that affect accurate data collection and analysis and factors that may have affected enzyme activity and/or the reaction rate. Due to the large volume of aqueous phases, pre- and post-reaction, exact quantification was difficult. Using measurements based on volume, rather than mass, allowing limited time for phase separation, resulting in residual FAME suspended in the aqueous phase, and, using rough graduated marks on the side of a 5 gallon carboy all contributed to inaccuracies in reported aqueous phase quantities.

The limitations that may have influenced the recovery of active enzymes and the reaction rates stem from quality of feedstock and inadequate apparatus. Discrepancies in methanol dosing rates and volumes from their target values may have affected the reaction rates as well as caused deactivation of enzymes. These discrepancies stemmed from the unavailability of a high quality dosing pump that could meet the target dosing rate, rather a configuration of three imprecise dosing pumps plumbed together was used to approximate the target dosing rate. The effects of this were minimized by regularly measured and adjusted dosing rates.

In the membrane selection process a conservative molecular weight cutoff (MWCO) was used to assure the enzymes were retained. However, this small MWCO contributed to slow permeate flux rates, long filtration times, and higher gel layer formation. To counteract this, transmembrane pressures and pump speed were increased, which resulted in system temperatures that exceeded the recommended temperatures for the enzyme. While

temperatures were not elevated for long periods of time, some enzymes may have been deactivated during this process.

Finally, the lack of available yellow grease or waste vegetable oil feedstock led to the use of a 50/50 mixture of distiller's dry grain corn oil with WVO. All previous bench-scale research that contributed to this research was performed using either virgin soy oil or yellow grease. It is suspected that the DDG corn oil had compounds which made phase separation more difficult at the larger pilot scale volume.

Significance of the Study

This research will be most useful to small scale commercial producers of biodiesel that produce less than 5,000,000 gallons/year looking for an alternative to chemical catalysts. It may also hold interest for an industry or research community interested in the use, mechanism, and kinetics of enzymes, particularly the *Thermomyces lanuginosus* lipase, as a biocatalyst. The impact of this study on the production of biofuels could be widespread, if it allows the industry to move closer to using enzymes, a more environmentally benign, energy efficient and economically profitable catalyst for biodiesel production.

Glossary of Terms

Activation energy. The minimum energy needed for reaction to occur.

Active site. The region of an enzyme in which catalysis takes place.

Acyl group. A portion of a molecule with the formula $-\text{COR}$, where R is an alkyl group.

Acylglycerols. An ester of glycerol and fatty acids that occurs naturally as fats and fatty oils.

α -helix. A regular secondary structure of polypeptides, with 3.6 residues per right-handed turn, a pitch of 5.4 Å, and hydrogen bonds between each backbone N-H group and the backbone C=O group that is four residues earlier.

Amide. Any of a class of organic compounds derived from ammonia or an amine by replacement of hydrogen with an acyl group.

Amino acid. A compound consisting of a carbon atom to which are attached a primary amino group, a carboxylic acid group, a side chain (R group), and a hydrogen atom.

β -sheet – a regular secondary structure in which extended polypeptide chains form interstrand hydrogen bonds. In parallel β sheets the polypeptide chains all run in the same direction; in anti-parallel β sheets, the neighboring chains run in opposite directions.

Carboxylesterase. An enzyme that is capable of hydrolyzing the ester bond in a wide variety of carboxylic acid esters to form an alcohol and a carboxylic acid.

Carboxylic acid. A chemical compound of the type $\text{R}-\text{COOH}$, where R is an alkyl group.

Conformation. In a molecule, a specific orientation of the atoms that varies from other possible orientations by rotation or rotations about single bonds; generally in mobile equilibrium with other conformations of the same structure.

Enzyme. A large molecule that is a biological catalyst; most enzymes are proteins.

Ester. A chemical compound of the type R_1-COOR_2 , where R_1 and R_2 are an alkyl group.

Esterification. The reaction between alcohols and carboxylic acids to make esters.

Free energy (G). A thermodynamic quantity whose change at constant pressure is indicative of the spontaneity of a process. For spontaneous processes, $\Delta G < 0$, whereas for a process in equilibrium $\Delta G = 0$.

Ground state. The lowest energy or most stable state of a molecule

Histidine. An amino acid with an imidazole functional group.

Hydrolysis. The cleavage of chemical bonds by the addition of water.

Ligand. A small molecule that binds to a larger molecule.

Lipid. Any member of a broad class of biological molecules that are largely or wholly hydrophobic and therefore tend to be insoluble in water but soluble in organic solvents such as hexane.

Nucleophile. A group that contains unshared electron pairs that readily react with an electron-deficient group (electrophile).

Peptide bond. An amide linkage between the alpha-amino-acid of one amino acid and the alpha-carboxylate group of another. Peptide bonds link the amino acid residues in a polypeptide.

Ping pong reaction. A group transfer reaction in which one or more products are released before all substrates have bound to the enzyme.

Polypeptide. A polymer consisting of amino acid residues linked in linear fashion by peptide bonds.

Regioselectivity. The property of a chemical reaction of producing one structural isomer (isomers which have their atoms arranged in a completely different order) in preference to others that are theoretically possible.

Residue. A monomeric unit of a polymer.

Secondary structure. The highly regular sub-structures (α helix and strands of β sheet) which are locally defined and contribute to the three-dimensional form of enzymes.

Serine proteases. A peptide-hydrolyzing enzyme characterized by a reactive serine residue in its active site.

Stereoselectivity. The property of a chemical reaction of producing one stereoisomer (isomers which have their atoms connected in the same sequence but differ in the way the atoms are oriented in space) in preference to others that are theoretically possible.

Superhelical twist. A molecular structure in which a helix is itself coiled into a helix

Transesterification. The reaction that exchanges the R group of an ester with the R group of an alcohol.

Transition state. The particular arrangement of reactant and product molecules at the point of maximum energy in the rate-determining step of the reaction.

Symbols & Abbreviations

Asp	Aspartic acid residue
ASTM	American Society for Testing and Materials
CSTR	Continuously stirred-tank reactor
DDG	Distillers Dry Grain
FAAE	Fatty Acid Acyl Ester
FAME	Fatty Acid Methyl Ester
FFA	Free Fatty Acid
Glu	Glutamic acid residue
Gly	Glycine residue

His	Histidine residue
kD	kilo-Dalton; unit of molecular mass
LMH	liter/m ² /hour; unit of flux
MWCO	Molecular Weight Cut Off
PBR	Packed Bed Reactor
SAPR	Selective Aqueous Phase Reduction
Ser	Serine residue
TFF	Tangential Flow Filtration
TG	Triglycerides
WVO	Waste Vegetable Oil

Chapter 2: REVIEW OF RELATED LITERATURE

Feedstocks

In the small-scale, commercial production of biodiesel, feedstock selection is the first of many factors that influence the quality of biodiesel produced and the overall success of a biodiesel production facility. When considering which feedstock(s) to use, availability, quality and cost all play an important role in the decision. The composition (i.e. the amount of free fatty acids versus triglycerides) determines the best mechanism, catalyst, and process to use to optimize the production of clean fuel that meets the American Society for Testing and Materials (ASTM, 2012) specifications and to enhance the economic viability of the production facility. Higher quality feedstocks come from refined vegetable oil, and lower quality feedstocks typically come from a waste stream. “[I]n order to compete with diesel fuel and survive in the market, lower-cost feedstocks are preferred, including waste cooking oil (WCO), grease, [and] soapstocks, since feedstock costs are more than 85% of the cost of biodiesel production” (Burton & Fan, 2009, p. 100). Other researchers have shown the high cost of feedstock having considerable economic impact on the total cost of biodiesel production (Yan, Salley, & Ng, 2009; Zhang, Dube, McLean, & Kates, 2003b).

In lipid feedstocks the molecules that are converted to biodiesel are acylglycerols, referred to as glycerides in the biodiesel industry, and free fatty acids. The major constituent in lipids, triglycerides (TG), is an ester composed of three moles of fatty acid chains, which are long hydrocarbon side chains bound to a one-mole glycerol backbone (Kovac, Scheib, Pleiss, Schmid, & Paltauf, 2000; Lam, Lee, & Mohamed, 2010). When a TG molecule

undergoes hydrolysis caused by the presence of water, free fatty acids (FFA), which are carboxylic acids that contain a long chain hydrocarbon side chain, are released, as well as monoglycerides, diglycerides or glycerol; one of these reactions is shown in Figure 2.1.

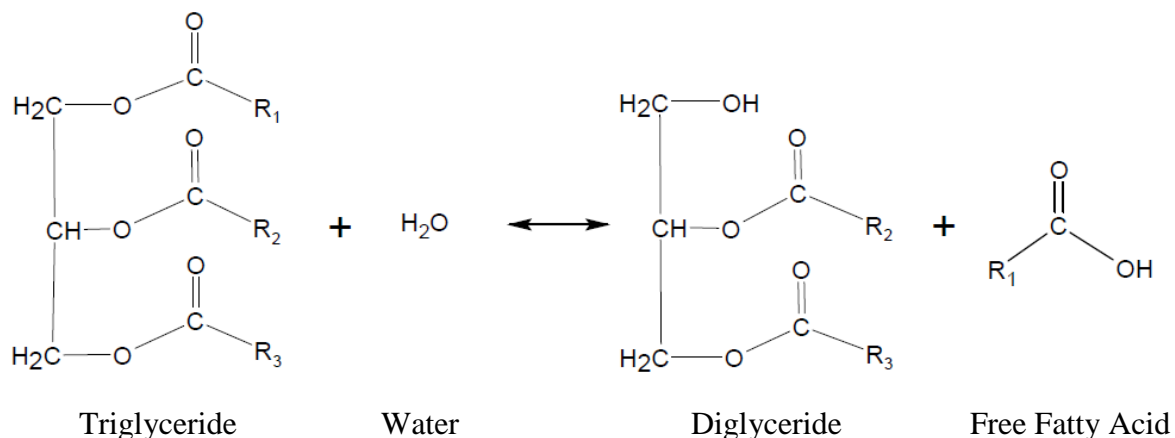


Figure 2.1. A triglyceride can be hydrolyzed to form a diglyceride and a free fatty acid. Similarly a diglyceride or monoglyceride can be hydrolyzed to form free fatty acids and a glyceride or glycerol (not shown). In all reactions the reverse (synthesis) reaction can combine a diglyceride, monoglyceride, or glycerol with fatty acid(s) to form a triglyceride.

There may also be contaminants present, such as water and particulate matter depending on the source of the feedstock; these should be removed in a production facility in the pre-treatment step(s).

Virgin versus waste feedstock.

In traditional biodiesel production facilities, virgin oil feedstock is a more desirable feedstock because the conversion of pure TG to FAME is high, and the reaction time is relatively short (Wang et al., 2007). This is true in part because the low FFA content of virgin oils, which is between 0-1%, results in a chemically simple mechanism (Kemp, 2006; Lam et al., 2010). That being said, the high cost of virgin feedstocks, such as soybean, canola, palm, peanut, olive, sunflower and jatropha oils (Nielsen, Brask, & Fjerbaek, 2008) can make this a cost prohibitive option for a small-scale producer.

Waste oils, such as waste vegetable oils (WVO), grease, soapstock or acid oils, animal fats (poultry, pork, lard, and tallow), and distillers dry grain oils are appealing as low cost feedstock (Burton & Fan, 2009; Nielsen et al., 2008). In addition to the lower cost of waste oils, the productive use of a waste stream and the debate between land-use for food versus fuel gives a compelling argument to avoid using virgin vegetable oils as feedstock (Akoh et al., 2007; Al-Zuhair et al., 2011). The drawback is a lack of purity, including a higher FFA and water content. The FFA content of waste oils most commonly acceptable for commercial biodiesel production ranges from 0.5 – 15% (Lam et al., 2010), but can be as high as 100%. The range of FFA content and the relative costs of a variety of oils are presented in Table 2.1. “[I]f waste cooking oil is to be made feedstock for biodiesel production, the amount of polar compound in the waste cooking oil, especially FFA, must be taken into consideration as it will greatly affect the transesterification reaction” (Lam et al., 2010, p. 504).

Table 2.1. *Range of FFA in Various Feedstocks and Oils.*

Feedstock Oil/Fat	Free Fatty Acid Level	Relative Cost
Refined Vegetable Oil (Soybean, Canola)	0 - 1%	Highest
Waste Fryer Oil/Fat	2 - 7%	Low
Animal Fats (Beef Tallow, Lard)	5 - 30%	Low
Yellow Grease	7 – 30%	Moderate
Brown Grease	greater than 30%	Very Low

Adapted from (Kemp, 2006, p. 108)

Saturation and degumming.

Other naturally occurring elements or phenomena may influence the success of producing biodiesel from lipids. The two largest of these influences in the production of biodiesel are saturation of fatty acids and presence of phospholipids. Animal fats or tallow contain higher levels of saturated fatty acids, or double bonds in the fatty acid chain, which causes them to solidify at higher temperatures. Degumming is the process of removing phosphatides, also known as phospholipids, which are similar to TG, but have a phosphate ester bound to the glycerol backbone rather than a fatty acid chain. Phospholipids are natural emulsifiers, which makes separation of products post reaction difficult. The processing of vegetable oils for use as food typically removes these contaminants, but this is not always the case when lipids are being processed for feedstock (Institute of Shortening and Edible Oils, 2006).

Traditional Biodiesel Production

Most commercial biodiesel production processes follow the same general steps: pre-treatment of feedstock, chemical reaction, separation of products and byproducts and finishing or washing of biodiesel product. However, the mechanisms, associated costs, and time spent on each step are unique to a production facility. To understand how those factors influence the success of a facility, an overview of the processes and of the variables specific to a facility is important.

Pretreatment of a single source or a mixture of feedstocks is a significant first step in that it removes impurities, most importantly water, but also food and other particulate matter. This step can be done with centrifugation or simple decantation, and is not a comparatively costly step.

The next step is the chemical conversion of feedstock to biodiesel and glycerol. The TG (as well as mono- and diglycerides) and FFAs react with an alcohol in the presence of a catalyst to produce fatty acid acyl esters (FAAE) or biodiesel and glycerol. The most common alcohol used is methanol due to its low cost (Al-Zuhair, 2006; Jain, Sharma, & Rajvanshi, 2011; Lam et al., 2010), in which case the FAAE produced is a fatty acid methyl esters (FAME). The reaction of TGs with alcohol is referred to as transesterification. The reaction of FFA with alcohol is esterification. This reaction is carried out in a heated reactor with agitation or mixing. “Several aspects, including type of catalyst, alcohol/oil molar ratio, temperature, purity of reactants and free fatty acid content influence the course of the reaction” (Schuchardt, Sercheli, & Vargas, 1998, p. 200).

Once close to a complete conversion, the reaction mixture is allowed to cool to room temperature and settle under gravity. The heavier glycerol falls to the bottom and the FAME remains in the upper layer. “Traces of glycerol can remain suspended in the ester phase along with small amounts of tri-, di-, and monoglycerides, while the residual catalyst and unreacted alcohol are distributed between the two layers” (Saleh, 2011, p. 21). Decantation is a typical method for separating the two phases. Density meters and electrolysis may be employed to help make a precise separation, but are not often used. The FAME is water washed to remove residual glycerol, catalyst and possibly soap. The methanol and water still present in the FAME is removed via distillation, heat and surface area exposure, use of a magnesium silicate adsorbent, and/or with ionic exchange columns. This last purifying and polishing step helps produce biodiesel that meets ASTM Standard D6751-2012: “Standard Specification for Biodiesel Fuel Blend Stock for Middle Distillate Fuels,” which producers are required to meet in order to legally sell the fuel to costumers.

The variables that are most often and successfully controlled in this process include reaction temperature, ratio of alcohol to oil, amount of catalyst, mixing intensity, feedstock used, and type of catalyst (Marchetti, Miguel, & Errazu, 2007; Ngo, Xie, Kasprzyk, Haas, & Lin, 2011). For commercial biodiesel producers the challenge is in figuring out the most profitable process in terms of their feedstock(s), raw materials, equipment availability, economic and technological constraints, and mission.

Catalysts.

Both the transesterification and esterification reactions are catalyst driven. Many different types of catalyst have been studied for this process and have successfully converted TGs and FFAs to high levels of FAME, including alkali, acid, enzyme, super critical acids, and others. The purpose of the catalyst is simply to speed up the reaction without changing the end product. (Bender & Brubacher, 1973).

The most common catalysts used in commercial biodiesel production are alkali and/or acidic; therefore, we will use those catalysts to describe the mechanisms and kinetics of reactions that TGs and FFAs undergo in the production of biodiesel. The use of enzymes as catalysts is being developed and is the basis of this research; the characteristics of enzymes as a catalyst will be elaborated upon in a later section.

Reactions of triglycerides and free fatty acids to form fatty acid methyl esters.

In biodiesel production transesterification refers to the process in which one mole of carboxylic ester (TG) reacts with three moles of methanol to form three moles of FAME (Figure 2.2). This is an equilibrium reaction, and an excess of methanol is used to drive the reaction forward to achieve a high yield of FAME. In a well-designed process, reactants are well mixed, and a 90-98% conversion of TG to FAME occurs. According to ASTM

specifications, the final biodiesel product should contain less than 0.2% by mass of glyceride back bones.

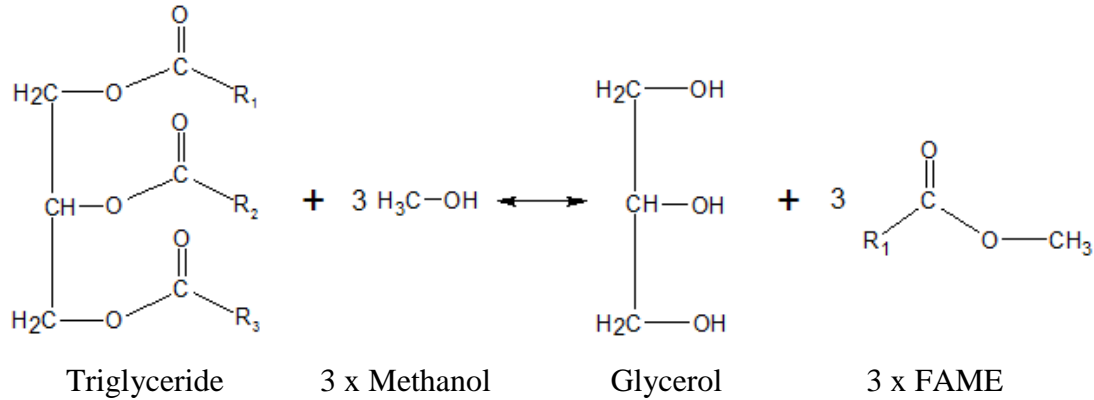


Figure 2.2. Transesterification is the primary reaction in the production of biodiesel. Glycerides and methanol combine to produce fatty acid methyl esters and glycerol.

The overall process from TG to FAME consists of three steps where di-glycerides and mono-glycerides are intermediates. The steps of this process are outlined in Figure 2.3. R_1 , R_2 , R_3 are fatty acid chains containing 16-18 carbons and 0-3 double bonds. In addition to TG many feedstocks contain FFAs, which undergo conversion to FAME via esterification. This reaction is shown in Figure 2.4.

Alkali catalyst.

Common alkali catalysts used by small-scale, commercial biodiesel producers are sodium hydroxide (NaOH) and potassium hydroxide (KOH), because they are both cheap and widely available. Additionally, alkali catalysis is favored in production because of its relatively short reaction time (30-90 min), high yield (90-98%), purity of the FAME produced, and relatively low reaction temperature (50-60 °C). The alcohol-to-oil molar ratio can vary from 1:1 to 6:1, but the optimal ratio was found to be 6:1, which gives the best

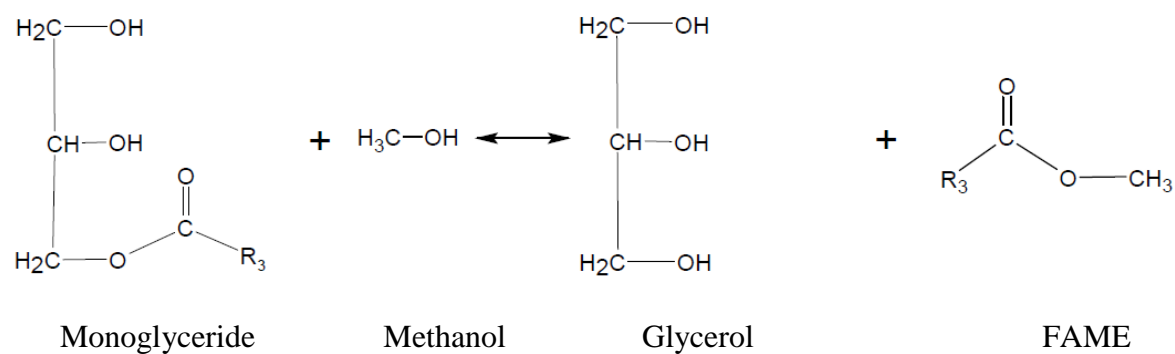
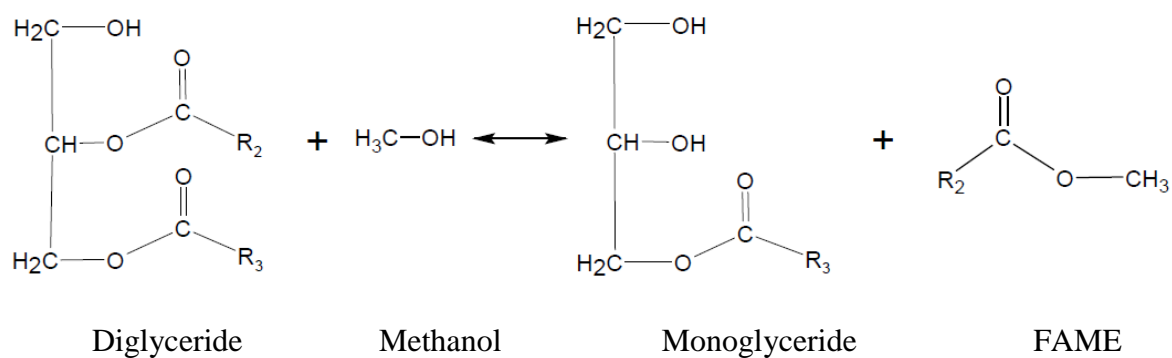
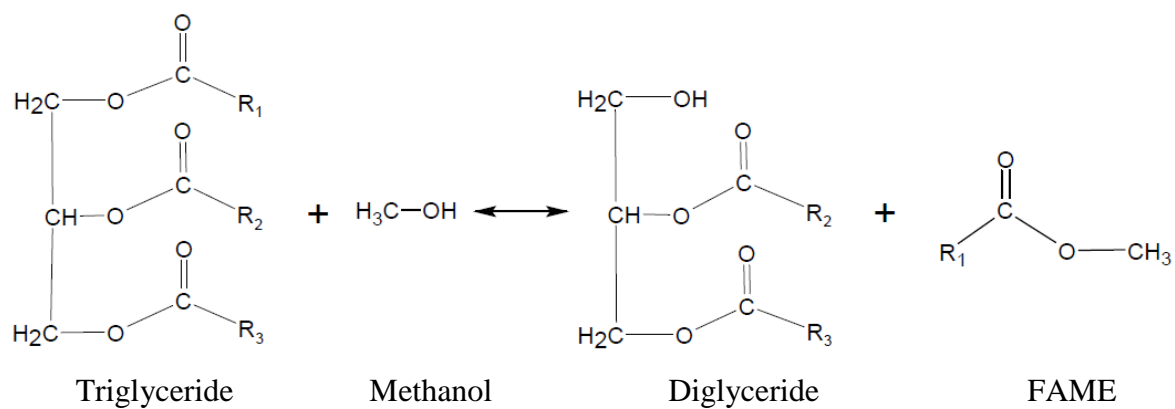


Figure 2.3. Three step progression of triglycerides to fatty acid methyl esters.

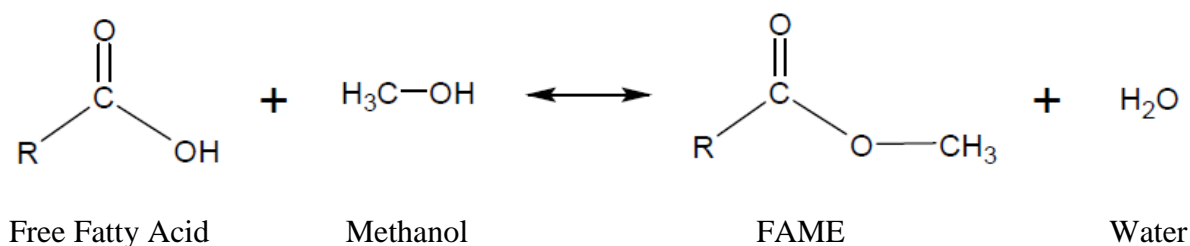


Figure 2.4. Esterification is the reaction in the production of biodiesel where free fatty acids and methanol combine to produce fatty acid methyl esters and water.

conversion rate to excess methanol used. The dosage of base used is 0.5-2% by weight of feedstock (Jain et al., 2011; Lam et al., 2010; Marchetti et al., 2007; Schuchardt et al., 1998; Wang et al., 2007; Zhang, Dube, McLean, & Kates, 2003a).

A limitation with using an alkali catalyst is the required purity of the reactants. That makes alkali catalyst unfavorable for use with waste oils because of their higher FFA and water content. A feedstock with a FFA value higher than 0.5% leads to problems (Lam et al., 2010; Marchetti et al., 2007; Wang et al., 2007). The problem with a high FFA and water content in the feedstock when it is base catalyzed is that the FFA reacts with whatever water may be present and the base catalyst to form soaps. Soap formation reduces FAME yields by consuming FFA and creates an emulsification with the glycerol, which makes downstream separation of products difficult. This saponification reaction is shown in Figure 2.5.

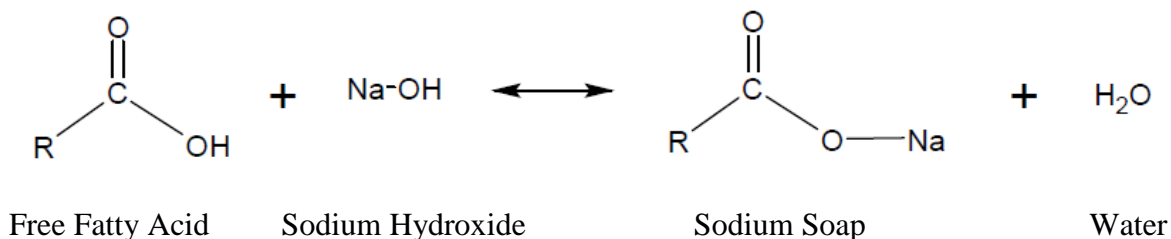


Figure 2.5. Saponification is an unwanted reaction that occurs when alkali catalyst are used. Free fatty acids react with the base catalyst to form soaps.

Acidic catalyst.

Using acid as a catalyst is a better option when there is a high level of FFA content in the feedstock, which is typically found to be true in waste oils (Marchetti et al., 2007; Schuchardt et al., 1998; Zhang et al., 2003a). “Acid catalyzed transesterification holds an important advantage with respect to base-catalyzed process: acid catalyst is insensitive to the presences of FFAs in the feedstock and can catalyze esterification and transesterification simultaneously” (Lam et al., 2010).

The most common acid used in this process is sulfuric acid (H_2SO_4). The drawbacks of using acid catalysis include the slower reaction time to reach complete conversion (3-18 hours), higher temperature required (55-100 °C), and the fact that an alcohol-to-oil molar ratio on a scale closer to 30:1 is required to drive the reaction forward (Marchetti et al., 2007; Schuchardt et al., 1998). An acid dosage of 1.5-3.5 mol% is typically used (Zhang et al., 2003a).

While acid catalysis does alleviate the problem with high FFA, the associated costs of this catalyst are higher. This is due in part to the larger dose, longer time, and higher temperature required, which makes it more energy intense. In addition, more expensive stainless steel equipment is required to handle the corrosive acid. This last point also brings to light safety issues that arise when using sulfuric acid in a production facility (Wang et al., 2007).

Two-step process.

A two-step system where the feedstock is first reacted with an acid catalyst to reduce FFA content, then reacted with an alkali catalyst has been shown to be effective on waste oils (Lam et al., 2010; Ngo et al., 2011; Wang et al., 2007; Zhang et al., 2003a). “The advantage

of this two-step process is that it can increase reaction rate by using alkaline catalysts and avoid soap formation by applying acid catalysts” (Burton & Fan, 2009, p. 101). Jain et. al (2011) studied the kinetics of this two-step process when used in India to convert waste oil to FAME at different temperatures, reaction times, and catalyst dosage. Wang et al. (2007) successfully applied this two-step process using a less volatile acid, ferric acid, followed by potassium hydroxide with a 97% conversion.

Drawbacks to this system stem from the extra steps involved to esterify the FFAs with acid. This part of the process leaves an effluent containing sulfuric acid and the recovery of catalyst is difficult; in addition, there is the high cost of the reaction equipment need for acidic reactions (Ngo et al., 2011; Wang et al., 2007). “The drawback of this two-step process is even more pronounced due to the requirement of extra separation steps to remove the catalyst in both stages. Although [the] problem of catalyst removal from the first stage can be avoided by using base catalyst from the second stage through a neutralization process, the use of extra base catalyst will add to the cost of biodiesel production” (Lam et al., 2010, p. 508). A summary of the reaction parameters and FAME yield for alkali or base catalysis, acidic catalysis and a two-step process are presented in Table 2.2.

Table 2.2. Comparison of Reaction Conditions and Performance for Various Types of Catalysts Used in Transesterification of WVO

Catalyst	Reaction Conditions				Performance	Reference
	Temp, C	Type of alcohol	Catalyst loading, wt. %	Reaction time, h		
<i>Homogeneous base catalyst</i>						
NaOH	60	Methanol (7:1)	1.1	0.33	Yield = 88.8%	Leung and Guo (2006)
KOH	87	Methanol (9:1)	6	2	Yield = 87%	Demirbas (2009)
<i>Homogeneous acid catalyst</i>						
H ₂ SO ₄	95	Methanol (20:1)	4	20	Conversion = 90%	Wang et al. (2006)
H ₂ SO ₄	70	Methanol (245:1)	41.8	4	Yield = 99%	Zheng et al. (2006)
H ₂ SO ₄	65	Methanol (30:1)	1	69	Conversion = 99%	Freedman et al. (1984)
<i>Two-step: Acid catalyst followed by base catalyst</i>						
Ferric sulfate followed by KOH	Acid: 95	Methanol (10:1)	2	2	Conversion = 97%	Wang et al. (2006)
	Base: 65	Methanol (6:1)	1	1		
Ferric sulfate followed by KOH	Acid: 100	Methanol (9:1)	2	2	Yield = 96%	Patil et al. (2010)
	Base: 100	Methanol (7.5:1)	0.5	1		
Ferric sulfate followed by CaO	Acid: 60	Methanol (7:1)	0.4	3	Yield = 81.3%	Wan Omar et al. (2009)
	Base: 60	Methanol (7:1)	Not clearly specified	3		

Adapted from (Lam et al., 2010)

Enzymes

The production of biodiesel using an enzymatic catalyst offers many advantages, with the one major drawback being their high price. Some advantages include insensitivity to high FFA content, milder and less energy intense (lower temperature) reaction conditions, elimination of soap formation, cleaner product streams and easier purification steps of FAME to obtain ASTM (2012)-standard biodiesel. An additional economic advantage is the production of a higher value co-product of technical grade glycerol compared to the less pure glycerol byproduct in traditional chemical catalysis processes (Al-Zuhair, 2006; Fjerbaek, Christensen, & Norddahl, 2009; Lam et al., 2010; Yucel, 2012).

Physical characteristics of enzymes.

To better understand enzymes' role in the production of biodiesel, it is helpful to have a basic understanding of what enzymes are and their catalytic behaviors. Enzymes, in general, are large protein molecules with molecular weights ranging in size of several thousand to several million g/mol. Comparing this to the other molecules in transesterification, where TG's molecular weight is in the range 675 to 975 g/mol, methanol has a molecular weight of 32 g/mol and FAME ranges in weight from 200 to 300 g/mol. Enzymes have active site(s) where the chemical reaction occurs, and the rest of the enzyme acts as scaffolding or is used to direct the substrate to the active site on the enzyme (Silverman, 2000).

Enzymes as catalysts.

In general enzymes yield higher reaction rates, perform under milder reaction conditions, and have greater reagent specificity. Enzyme catalysts affect both the mechanism and the kinetics of a chemical reaction. The mechanism refers to the course of events during

a chemical reaction, and kinetics refers to the rate at which the reaction occurs. “In general, catalysts stabilize the transition state relative to the ground state, and this decrease in activation energy is responsible for the rate acceleration” (Silverman, 2000, p. 13). Enzymes affect the transition state of a reaction by bringing together two or more substrates in an organized manner in which they normally would not be, by forming an intermediate state with the substrate that is bound, and by decreasing the activation energy (Silverman, 2000).

In any reaction, the reactants (A + B) and/or products (P + Q) are in states of minimum free energy, and the transition state (X^\ddagger) corresponds to a maximum free energy, or the highest point on the transition state diagram in Figure 2.6. The activation energy, also called the free energy of activation, ΔG^\ddagger is the difference between the free energy of the transition state and the free energy of the reactants. Enzyme catalysts provide a reaction pathway with a transition state whose free energy is lower than that in the uncatalyzed reaction. The difference between the ΔG^\ddagger for the uncatalyzed and the catalyzed reaction ($\Delta G^\ddagger_{\text{cat}}$), indicates the efficiency of the catalyst, where the larger $\Delta G^\ddagger_{\text{cat}}$, the more catalytically efficient the enzyme is (Voet, 2012), as shown in Figure 2.7.

There are numerous different hypotheses for the progression of enzyme catalysis. However, the first step is common to all hypotheses, which is “an enzyme-catalyzed reaction always is initiated by the formation of an enzyme substrate (E·S) complex, from which the catalysis takes place” (Silverman, 2000, p. 2). This E·S complex is created when the substrate binds to one of the active sites on the enzyme. This step happens very quickly, and readers should notice from the depiction in Figure 2.7 that this step is in equilibrium.

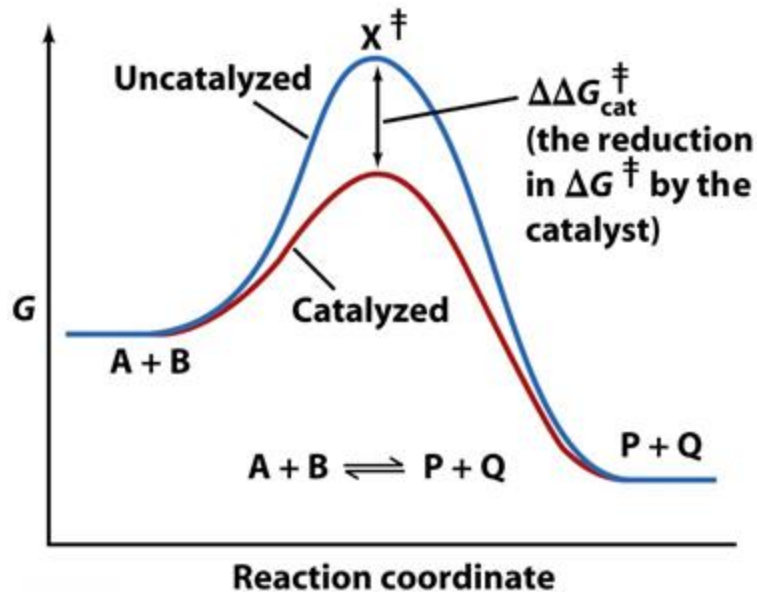


Figure 2.6. The transition state diagram of the catalyzed (red) and uncatalyzed (blue) reaction $A + B \rightarrow P + Q$ shows that the transition state, X^\ddagger , is the state with the highest free energy. The effect of a catalyst on the transition state diagram shows a decrease in activation energy (Voet, 2012, p. 322).

This binding of the substrate to the enzyme involves non-covalent interactions, such as van der Waals interactions, electrostatic interactions, hydrogen bonding, and hydrophobic interactions. Because of these weak forces, the binding process is reversible, which is important for the product release step (Bender & Brubacher, 1973; Silverman, 2000; Voet, 2012).

After this initial step, hypotheses diverge slightly. Two of the more well-known hypotheses of enzyme catalysis, lock-and-key hypothesis and induced-fit hypothesis, are described. The lock-and-key hypothesis is a crude description of how enzymes and substrates interact, stating that the enzyme is the “lock” into which the substrate, the “key,” would fit. A more nuanced explanation is the induced-fit hypothesis, which states that when a substrate begins to bind to an enzyme, interactions of various groups on the enzyme with each other

are initiated and produce a conformational change in the enzyme from a low catalytic form (poor catalyst) to high catalytic form (good catalyst). In bimolecular systems, such as in the reaction used in biodiesel production, the conformation resulting from the first molecule binding to an active site establishes an active site for the second molecule to bind (Silverman, 2000; Voet, 2012).

Transition-State Theory states that the substrate does not bind most effectively in the E·S complex; rather, as the reaction proceeds, the enzyme conforms to the transition-state structure, leading to the tightest interactions (increased binding energy) with the transition state structure. This conformation of the enzyme stabilizes the E·S complex, known as transition-state stabilization, increases the concentration of the E·S complex and increases the rate of the reaction. “The more tightly an enzyme binds its reaction’s transition state relative to the substrate, the greater is the rate of the uncatalyzed reaction relative to that of the uncatalyzed reaction” (Voet, 2012, p. 331). The ΔG between an E·S complex and an enzyme-transition state complex (ΔG_E^\ddagger) is less than the ΔG of a substrate and its transition state (ΔG_N^\ddagger) in an uncatalyzed reaction, or the $\Delta G_{\text{cat}}^\ddagger$ for the enzyme. This is illustrated in the transition state diagram in Figure 2.7. It has been suggested that all hypotheses of enzyme catalysis are just alternative versions of this theory involving the transition state of the substrate (Voet, 2012).

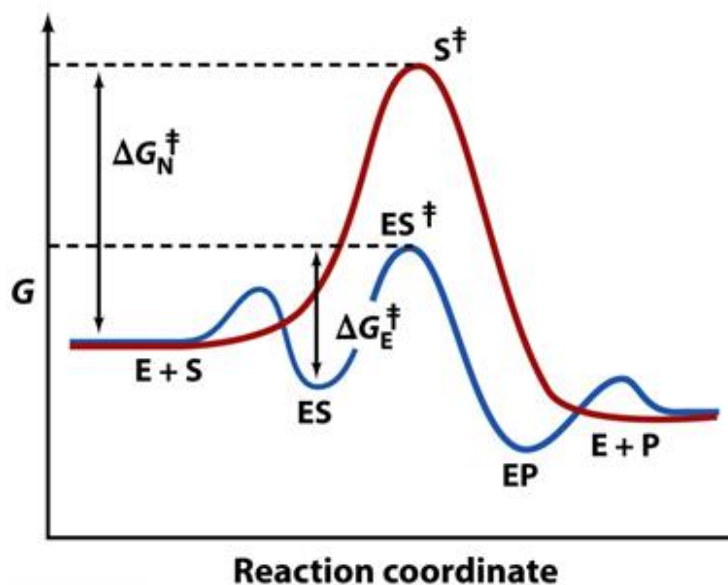


Figure 2.7. The transition state diagram for an uncatalyzed reaction with an activation energy of ΔG_N^\ddagger is shown in red, and for a catalyzed reaction with an activation energy of ΔG_E^\ddagger is shown in blue. The small dips in the diagram for the enzyme catalyzed reaction arise from the binding of substrate and product to the enzyme (Voet, 2012, p. 331).

There are several reaction parameters that affect the rate of an enzyme reaction. They include temperature, pH, enzyme concentration, substrate concentration, and the presence of inhibitors. Table 2.3 gives a brief description of each of these.

Table 2.3. Variables Affecting Enzyme Reactions

Temperature	With increased temperature, substrate and enzyme molecules increase collision frequency and kinetic energy and contribute energy to overcome the activation barrier. However, the temperature should not exceed a temperature that will destroy the enzyme or cause it to deactivate.
pH	pH affects the charge of amino acids at active sites which could alter the binding of a substrate. At the right pH, the enzyme will be able to bind at the active site faster so an increase of reaction rate is more likely to occur. Vice versa, if the pH is too high or low, that change the charge on the amino acid at the active site and that deactivates the active site which no longer allows the enzyme to bind.
Enzyme Concentration	An increase of enzyme concentration will also increase the chances of substrate-enzyme binding.
Substrate Concentration	An increase in substrate concentration will also increase the chances of substrate-enzyme binding.
Inhibitors	Enzyme inhibitors will decrease the activity of an enzyme and the rate of reaction. Inhibitors will bind to enzyme active sites and could modify the chemistry of an active site which can stop a substrate from entering.

Once the substrate binds to the active site of the enzyme, a variety of mechanisms are employed to catalyze the conversion of the substrate to product by stabilizing the transition-state or de-stabilizing the ground state (Silverman, 2000).

Enzyme kinetics.

The dynamics of enzyme catalysis are manifested in a reaction in two ways: rate acceleration and specificity or selectivity. The Michaelis-Menten Theory is used to describe the kinetics of an enzyme catalyzed reaction. The model serves to explain how an enzyme can cause kinetic rate enhancement of a reaction and why the rate of a reaction depends on the concentration of enzyme present.

The first step in the desired reaction (the one that produces free product) of the process is the binding of the substrate(s) to the enzyme to form the E·S complex. The product is then formed, released from the enzyme, and the enzyme is used to again bind to substrate(s) and the process starts over. Because of the reversibility of the reactions, unwanted interactions occur as well, such as the E·S complex undergoing the reverse reaction to give free E and S without the production of P. In the case of biodiesel production, this would lead to a smaller yield of FAME. The equilibrium between enzyme, substrate, and the E·S complex may be characterized mathematically by an equilibrium constants and rate equations derived from the formation and dissociation of the E·S complex as well as the production of product. The overall reaction equation is displayed in Figure 2.8.

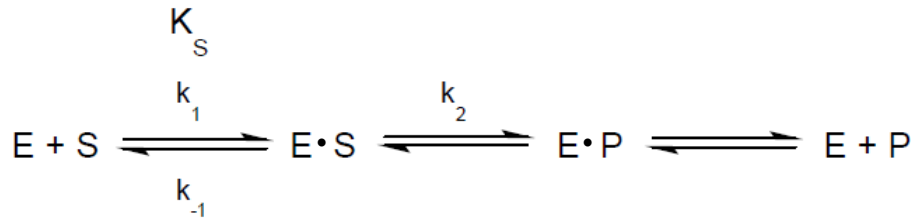


Figure 2.8. The simplest form of an enzyme-catalyzed reaction involves a single substrate converting to a single product where E=free enzyme, S=substrate, P=product, E•S=enzyme-substrate complex. There are several rate constants that dictate the overall rate of the reaction (Silverman, 2000, p. 563).

Rate of reaction.

The term k_1 is the rate constant for the binding of the enzyme to the substrate forming the E•S complex and is dependent on the concentration of the substrate and the enzyme. The term k_{-1} is the rate constant for the dissociation of the E•S complex to enzyme and substrate and is dependent on the concentration of the E•S complex, among other forces. The overall equilibrium constant, K_s , represents the formation and dissociation of the E•S complex. The term k_2 is the rate constant for the catalysis reaction which results in the product and regeneration of the enzyme.

Some simplifications can be made with the assumption that the concentration of substrate is much larger than the concentration of enzyme. This is a quite reasonable assumption because enzymes are such efficient catalysts it will typically be the case that only a small amount is needed, and in the production of biodiesel, this is desirable due to the enzymes' efficiency and cost. When this assumption is made, the enzyme is saturated with substrate and the rate of formation and dissociation of the E•S complex are equal. In this case, the concentration of the E•S complex changes much more slowly than does the concentration of substrate. This is referred to as the steady state approximation.

Under the steady state approximation, k_2 is the limiting step and is referred to as the catalytic rate, or k_{cat} . “The k_{cat} represents the maximum number of substrate molecules converted to product molecules per active site per unit of time, that is, the number of times the enzyme ‘turns over’ the substrate to the product per unit of time” (Silverman, 2000, p. 5). Typical k_{cat} values are 10^3 s^{-1} , which translates to about 1000 molecules of substrate converted to product every second.

Again, under the steady state assumption, K_s is referred to as the Michaelis-Menton constant, and is denoted by K_m . More specifically, K_m is the concentration of substrate that produces half the maximum rate, V_{max} , of which the enzyme is capable (Silverman, 2000). This value is an indicator of the stability of the E·S complex; the smaller the K_m value, the more tightly the substrate and enzyme are bonded, leading to a more stable and higher concentration of the E·S complex. The value of K_m can be calculated from the equation below. The K_m value for many E·S complexes are on the order of 10^{-6} to 10^{-3} (Bender & Brubacher, 1973)

$$K_m = \frac{k_{-1} + k_{cat}}{k_1} \quad (2.1)$$

Equating the rate of reaction to the rate constant times the concentration of the reactants, the rate of reaction can be derived to the equation below.

$$v = \frac{k_{cat}[E]_o[S]}{K_m + [S]} \quad (2.2)$$

Additionally, using the rate law to represent V_{max} , which is dependent only on the enzyme concentration because V_{max} is only attained at infinite (or very, very large) substrate concentrations, the maximum rate of reaction has the relationship to the initial enzyme concentration and k_{cat} that is depicted below.

$$V_{max} = k_{cat}[E]_0 \quad (2.3)$$

Substituting, the resulting equation given below is referred to as the Michaelis-Menton equation.

$$v = \frac{V_{max}[S]}{K_m + [S]} \quad (2.4)$$

From this relationship, increasing the substrate concentration will increase the rate of the reaction (Silverman, 2000). Additionally, V_{max} is reached when all enzymes are in the E·S complex, and can only be changed by the addition of more enzymes. This dependence is depicted graphically in Figure 2.9.

It is important to note that enzyme catalysis does not alter the equilibrium of a reversible reaction. If the enzyme accelerates the rate of the forward reaction, it likewise accelerates the rate of the reverse reaction.

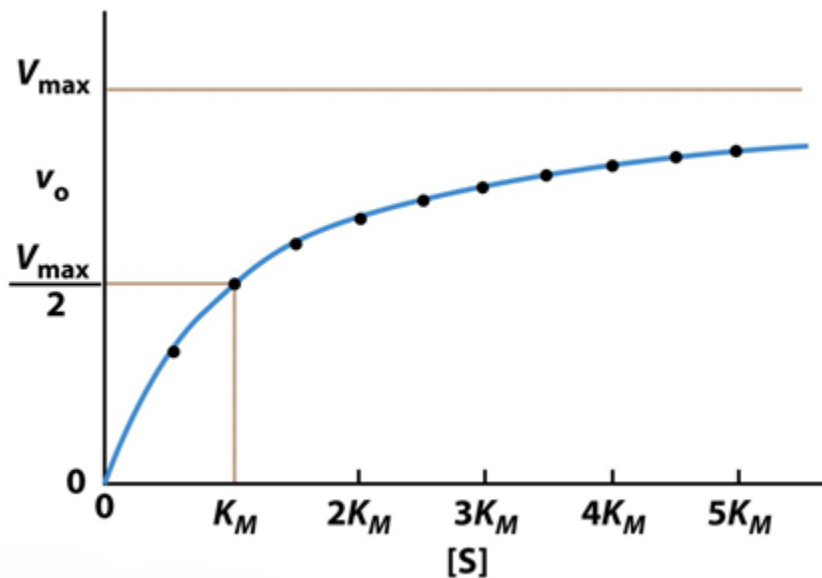


Figure 2.9. A graph of rate, v , versus substrate concentration, $[S]$, shows the non-linear dependence of the rate of an enzyme catalyzed reaction on the substrate concentration (Voet, 2012, p. 361).

Ping pong bi-bi mechanism.

This description of enzyme kinetics is for a fairly simple, one-step reaction. However, most enzymatic reactions are more complicated, as is the case of the reactions in biodiesel production. These reactions include the binding of a second substrate to the enzyme as well as multiple steps in the mechanism. This is referred to as a ping pong bi-bi mechanism and is depicted in Figure 2.10.

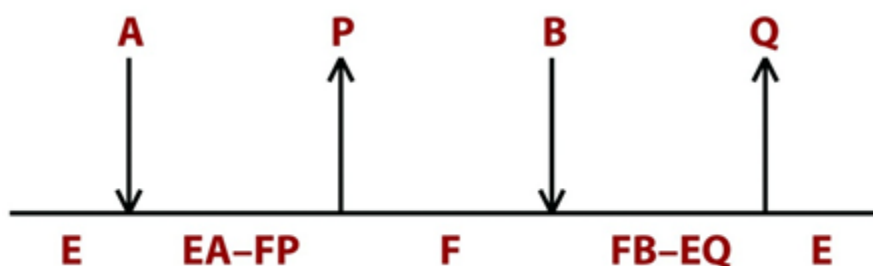


Figure 2.10. A ping pong bi-bi mechanism describes a group transfer reaction where one or more products are released before all substrates have been added where E=enzyme, A=1st substrate, P=1st product, F=stable enzyme conform, B=2nd substrate, Q=2nd product (Voet, 2012, p. 367).

In this type of reaction one or more products is released before all substrates have been bound. A functional group of the first substrate A is bound to the enzyme to produce the first product P and a stable enzyme complex tightly bound to the functional group. In the second stage of the reaction, the functional group is displaced from the enzyme by the second substrate B to yield the second product Q thereby releasing the original form of the enzyme.

Despite these complications, the Michaelis-Menton form of the rate equation is generally applicable for this mechanism. “For a more complicated mechanism the constants k_{cat} and K_m do not refer to a single step; they become composite constants incorporating the rate constants for several steps” (Bender & Brubacher, 1973, p. 29).

Specificity.

Two steps, besides the formation of product, dictate the effectiveness and efficiency of enzymatic catalysis: substrate binding and product release. “High turnover numbers are only useful if these two physical steps occur at faster rates” (Silverman, 2000, p. 5). In addition, the weak, non-covalent bonds formed during the E·S complex formation influence the effectiveness of the enzymatic catalysis. Several of these interactions combine to create an overall strong interaction. And because several types of interactions are involved, selectivity in enzyme-substrate interactions exists.

The specificity of an enzyme can refer to how it binds to the substrate or how it favors reacting molecules or atoms. Binding specificity is a broad term that can mean that only one substrate can bind to an active site on the specific enzyme or that only one substrate that binds to the active site converts to a product. Specificity is governed by geometry (shape) or electronic complementarity (charge). This is induced from the arrangement of specific amino acids forming the active site on an enzyme attracting specific substrates.

Specificity constant.

“The two constants k_{cat} and K_{m} are important parameters for the reaction of a particular substrate catalyzed by a particular enzyme since they indicate how susceptible the substrate is to the catalysis by the enzyme” (Bender & Brubacher, 1973, p. 27). The term $k_{\text{cat}}/K_{\text{m}}$ is the specificity constant. The specificity constant allows you to rank an enzyme on how good it is with different enzymes, how fast the enzyme might catalyze a reaction, and what concentration of the substrate would be required to reach V_{max} .

Enzyme inhibition.

Substances that combine with an enzyme and influence the binding of the enzyme to the substrate or turnover number, resulting in a negative effect on the enzymes activity are known as inhibitors. Inhibitors act through various mechanisms that can result in irreversible or reversible inactivation. “Irreversible enzyme inhibitors, or inactivators, bind to the enzyme so tightly that they permanently block the enzyme’s activity” (Voet, 2012, p. 368).

Reversible enzyme inhibitors are substances that diminish an enzyme’s activity by (a) structurally resembling a substrate and binding to the active site reducing the available enzyme and thus the concentration of the E·S complex; (b) binding to the E·S complex, distorting the active site and disallowing the substrate to form product; or (c) a combination of both mechanisms (Voet, 2012).

Enzyme Catalyzed Biodiesel Production

In the production of biodiesel, lipases are the family of enzymes used. Ideally, in the production of biodiesel, lipases should (a) be non-stereospecific (so all mono-, di-, and triglycerides will react); (b) catalyze both TGs and FFAs; (c) have low product inhibition with high FAME yield; (d) have a low reaction time; (e) be easily recovered and re-used; (f) react at mild temperatures; and (g) have minimal alcohol or glycerol inhibition. In studies of enzymatic catalysis of biodiesel, many lipases have been researched and their effect on several of the variables listed above have been analyzed and optimized. “In general, enzyme catalysts at 4-10 wt% result in FAME yields of 55-97% in 3-120 hours at 30-50 C” (Akoh et al., 2007, p. 8996). Table 2.4, compiled by Fjerbaek et al. in 2009, summarizes the research done up to that point.

Table 2.4. Summary of Research Conducted on Biodiesel Production With Various Lipases						
Lipase	Oil/fat	Alcohol	Yield	Form	Conditions and observations	References
<i>Pseudomonas fluorescens</i> ^a	Soybean oil	Methanol	90%	Free	35 C, 3:1 molar alcohol added in three steps, 90 h, 150 rpm	Kaideda et al. (2001)
<i>Pseudomonas cepacia</i> ^b			>80%	Free		
<i>Candida rugosa</i>			90%	Free		
<i>Pseudomonas fluorescens</i> ^a	Sunflower oil	Methanol	>95% (24 h, molar ratio 4.5:1)	Imm.	40 C, 200 rpm, 3:1 molar alcohol added in three steps, 10 wt% enzyme based on oil weight, 30 h	Soumanou and Bornscheuer (2003)
<i>Rhizomucor miehei</i> ^c			>80%	Imm.		
<i>Thermomyces languinosa</i> ^d			>60%	Imm.		
<i>Candida antarctica</i> ^e	Sunflower oil	Methanol	93.2% (1-propanol)	Imm.	40 C, 3:1 molar ratio of alcohol added in four steps, 10 wt% enzyme based on oil weight, 24 h	Deng et al. (2005)
<i>Rhizomucor miehei</i> ^c		Ethanol	79.1% (96% each)	Imm.		
<i>Thermomyces languinosa</i> ^d		1-Propanol	89.8% (methanol)	Imm.		
<i>Thermomyces languinosa</i> ^f		2-Propanol	72.8% (1-propanol)	Imm.		
<i>Pseudomonas cepacia</i> ^g		1-Butanol	88.4% (96% EtOH)	Imm.		
<i>Pseudomonas fluorescens</i> ^a		Isobutanol	45.3% (96% EtOH)	Imm.		
<i>Pseudomonas cepacia</i> ^b	Mahua oil	Ethanol	96% (6 h)	Imm.		
			92% (2.5 h)	CLEA ^m		
			99% (2.5 h)	PCMC ⁿ		
Porcine pancreatic lipase ^h	Babassu oil	Butanol	95%	Imm.	40-50 C, 150 rpm, 10:1 molar alcohol to oil, 20 wt%, of total substrate enzyme	Paula et al. (2007)
<i>Pseudomonas cepacia</i> ⁱ	Jatropha oil	Ethanol	98%	Imm.	50 C, 200 rpm, 4:1 molar alcohol to oil, 5wt% water based on enzyme weight, 10 wt% enzyme based on oil weight, 8 h	Shah and Gupta (2007)
<i>Candida antarctica</i> ^j	Tallow	Methanol	74%	Imm.	30 C, 200 rpm, 3-step addition of 3:1 molar alcohol to tallow, 10 wt% enzyme based on oil weight, 72 h	Lee et al. (2002)
<i>Candida sp. 99-125</i>	Rapeseed oil	Methanol	83% (36 h, 5 wt%, enzyme BSTR)	Imm.	40 C, 180 rpm, alcohol molar ratio 3:1 added in three steps. Solvent: n-Hexane for salad oil, otherwise petroleum ether	Deng et al. (2003); Nie et al. (2006); Tan et al. (2006)
	Salad oil		95% (30 h, 20 wt%, enzyme BSTR)	Imm.		

Lipase	Oil/fat	Alcohol	Yield	Form	Conditions and observations	References
Candida sp. 99-125, cont.	Waste oil	Methanol	92% (22 h, three PBRs in series)	Imm.	40 C, 180 rpm, alcohol molar ratio 3:1 added in three steps. Solvent: n-Hexane for salad oil, otherwise petroleum ether	Deng et al. (2003); Nie et al. (2006); Tan et al. (2006)
Pseudomonas cepacia mixed with Candida Antarctica	Vegetable oil	Ethanol 95%	96% (30 h, 15 wt%, enzyme BSTR)	Imm.	35 C, 200 rpm, 4:1 molar ratio of alcohol, 5 wt% enzyme based on oil weight, respectively; addition of CA after 1h, 24h	Wu et al. (1999)
Rhizopus oryzae mixed with Candida rugosa	Soybean oil	Methanol	>99%	Imm.	45 C, 200 rpm, 4.5:1 molar ratio of alcohol added in 10 steps, 30 wt% enzyme based on substrate, 10 wt% water, imm on silica gel, 1 wt% RO and 1 wt% CR, 21 h	Lee et al. (2006)
Thermomyces languinosa (TL) mixed with Candida Antarctica (CA)	Rapeseed and waste oil	Methanol	95%	Imm.	35 C, 130 rpm, 4:1 molar ratio alcohol to oil, tert-butanol to oil volume ratio 1:1, 3 wt% TL and 1 wt% CA, 12 h	Li et al. (2006)
Rhizopus oryzae – whole-cell	Soybean oil	Methanol	80% (Cao et al., 07)	Free	37 C, 150 rpm, 3:1 molar ratio of alcohol added in three steps air-dried cells	Matsumoto et al. (2001)
Rhizopus oryzae biomass particles supported by polyurethane foam	Soybean oil	Methanol	71% (165 h)	Imm,	35 C, 150 rpm, 3:1 molar alcohol added 6 times, 72 h	Ban et al. (2002)
<p>Solvent free if nothing else is stated. Imm., immobilized; PBR: packed bed reactor; BSTR, batch-stirred reactor. ^aLipase AK from Amano Enzyme Inc. ^bLipase PS from Amano Enzyme Inc. ^cLipzyme RM IM from Novozymes. ^dLipzyme TL IM from Novozymes. ^eNovozym 435 from Novozymes. ^fLipase LA201 from Novozymes. Adapted from Fjerbaek et al., 2009.(Fjerbaek et al., 2009)</p>						

Lipases.

In order to appreciate why lipases are the enzyme used to catalyze the production of biodiesel, an understanding of their structure and mechanism is useful. Lipases are a class of enzymatic biocatalysts that have proven to be of great use in many industries, including the biodiesel industry. There are many reasons for this including the fact that they (a) are stable in organic solvents; (b) do not require cofactors nor do they catalyze side reactions; (c) possess broad substrate specificity and display exquisite chemoselectivity, regioselectivity, and stereoselectivity; (d) are readily available in large quantities because many of them can be produced in high yields from microbial organisms, namely fungi and bacteria; and (e) have solved crystal structures of many lipases, facilitating considerably the design of rational engineering strategies (Jaeger & Eggert, 2002; Jaeger & Reetz, 1998).

α/β hydrolase fold superfamily.

Lipases belong to one of the 41 distinct families of the versatile and widespread α/β hydrolase fold superfamily (Lazniewski, Steczkiewicz, Knizewski, Wawer, & Ginalski, 2011). These enzymes, which range in molecular weight from of 19-60 kD, bind a variety of ligands including lipids, peptides and ethers to catalyze the hydrolysis of bonds that play an important role in the synthesis and degradation of a variety of compounds (Jaeger & Reetz, 1998; Lazniewski et al., 2011). The structural similarities, as well as the slight inconsistencies between these subfamilies play an important role in their function as described below and shown in Figure 2.11.

The canonical α/β hydrolase fold has been described as consisting of mostly parallel, eight-stranded β sheets surrounded on both sides by α helices (only the second β strand is anti-parallel). . .and it displays a left-handed superhelical twist, with the first and last

strands crossing each other at an angle of approximately 90 degrees. The degree of twisting can show significant differences, however, with the largest deviations usually localized between strands $\beta 5$ and $\beta 6$. Differences may also be present in the spatial position of the α -helices connecting the β -strands of the central β sheet. In some cases, one or more of these helices may even be completely absent. Only helix αC appears to be well conserved; it has a strategic position in the center of the β -sheet and plays a key role in the correct positioning of the nucleophilic residue in the active site. (Nardini & Dijkstra, 1999, p. 732)

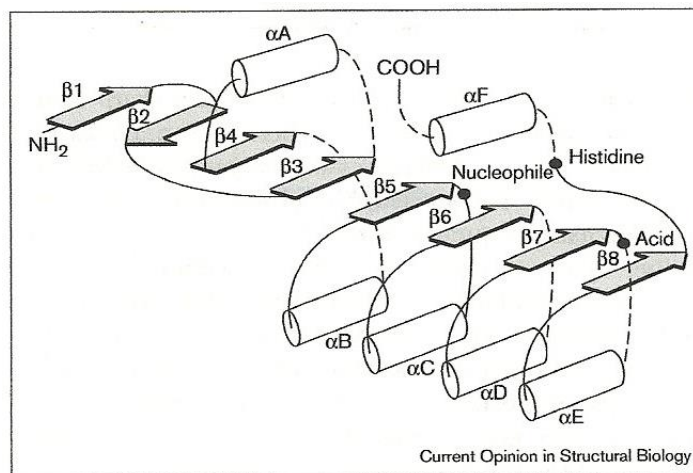


Figure 2.11. Secondary structure diagram of a ‘canonical’ α/β hydrolase fold. The location of the catalytic triad is indicated by black dots. Dashed lines indicate the location of possible insertions (Nardini & Dijkstra, 1999, p. 732).

The variability of the secondary structure in enzymes of the α/β hydrolase fold superfamily is shown Figure 2.12.

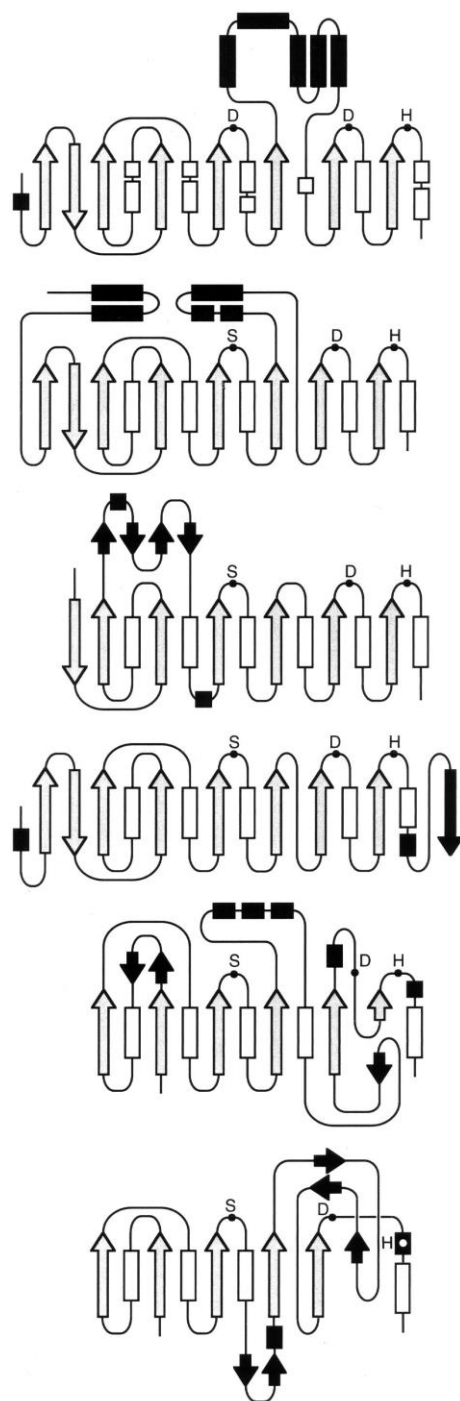


Figure 2.12. Variability of the secondary structure of various α/β hydrolase fold enzymes. α helices and β strands belonging to the ‘canonical’ fold are represented by white rectangles and gray arrows, respectively. Secondary structure elements that deviate from the ‘canonical’ fold are represented in black. The location of the catalytic triad is indicated by black dots and the corresponding single-letter amino acid code where S=serine, D=aspartic acid, and H=histidine (Nardini & Dijkstra, 1999, p. 733).

Lipase subfamily.

The lipase subfamily of the α/β hydrolase fold superfamily is a carboxylesterase that catalyzes the hydrolysis of long-chain acylglycerols, a class of lipids (Jaeger & Reetz, 1998). Lipids are characteristically any member of a class of biological molecules that are fatty acids (carboxylic acids that contain long chain hydrocarbon side groups) or their derivatives, and they are insoluble in water but soluble in organic solvents. Of all the α/β hydrolases, lipases are particularly useful in industry due to their structural and mechanistic properties.

Interfacial activation and the lid.

Since lipids are water insoluble due to their high hydrophobicity and lipases are water soluble, catalytic activity takes place at the water-lipid interface. This phenomenon is referred to as “interfacial activation.” “The determination of their 3D structure seemed to provide an elegant explanation for interfacial activation: the active site of lipases was found to be covered by a surface loop, which was called the lid” (Jaeger & Reetz, 1998, p. 397). The structure of the lid may vary among lipases from very small to quite large to a double lid. In any case, the lid moves to permit the interaction between the lipases’ hydrophobic face and residues that surround the lipase active site with the hydrophobic surface of the substrate. When contact occurs with a lipid/water interface, the lid undergoes conformational rearrangement which renders the active site accessible to the substrate (Fernandez-Lafuente, 2010; Schmid & Verger, 1998). The lid may also serve as a device to inhibit the proteolytic activity, or the breakdown of the protein, by the catalytic triad found at the active site, thereby protecting the enzyme itself (Brady et al., 1990).

Active site triad.

The active site that is exposed upon opening of the lid consists of a catalytic triad responsible for the cleavage reaction of the lipid's ester bond. The triad of catalytic residues is composed of (a) a nucleophile (serine, cysteine, or aspartic acid) positioned after strand $\beta 5$; (b) an acidic residue almost always positioned after strand $\beta 7$; and (c) an absolutely conserved histidine located after the last β -strand. These three residue positions are shown in Figure 2.11 as Nucleophile, Acid, and Histidine and in Figure 2.12 as S, D, H. The nucleophile residue is typically found in a Sm-X-Nu-X-Sm sequence motif referred to as the nucleophile elbow, where Sm stands for a small residue, typically glycine (Gly), X stands for any amino acid, and Nu stands for nucleophile, usually serine (Ser) (Jaeger & Reetz, 1998; Nardini & Dijkstra, 1999). The sequence variation within this motif is one of the factors distinguishing various lipolytic families (Lazniewski et al., 2011). The nucleophile elbow is found in a very sharp turn in a characteristic β -turn- α motif. This conformation positions the nucleophilic residue free of the active site surface and allows easy access on one side to the active site histidine (His) residue and on the other side to the substrate (Jaeger, Dijkstra, & Reetz, 1999). "The geometry of the nucleophile elbow also contributes to the formation of an oxanion-binding site, which is needed to stabilize the negatively charged transition state that occurs during hydrolysis. This 'oxanion hole' is usually formed by two backbone nitrogen atoms: the first is always from the residue immediately following the nucleophile, whereas the second is usually located between strand $\beta 3$ and α -helix" (Nardini & Dijkstra, 1999, p. 733).

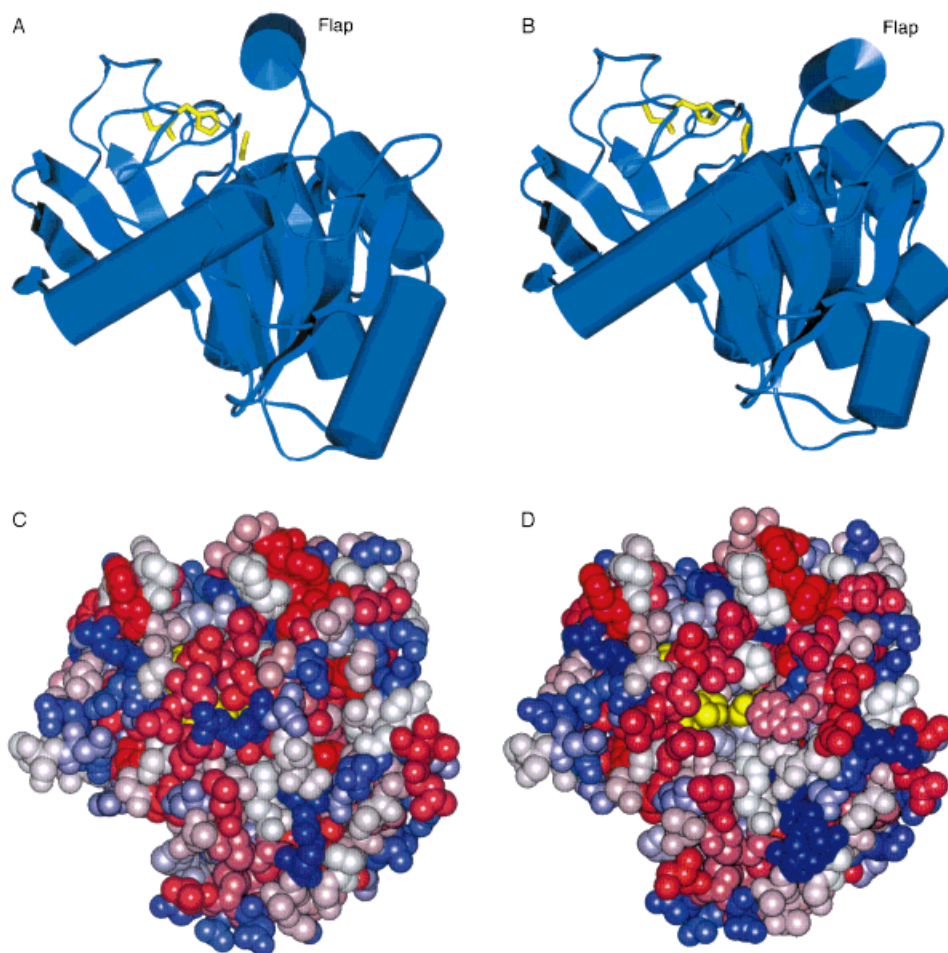


Figure 2.13. Structure of *Mucor miehei* lipase in closed (A, C) and open form (B, D). In A and B the catalytic triad (yellow) and secondary structure elements common to all lipases is shown. In C and D a space-filling model is shown, colored by decreasing polarity (dark blue - light blue – white – light red – dark red). Upon opening the lid or flap, the catalytic triad becomes accessible (D), and the region binding to the interphase becomes significantly more apolar (Schmid & Verger, 1998, p. 1613).

The characteristics of the structure, active site and interfacial activation of lipases have been found to be common in almost all lipases. Figure 2.13 illustrates the structure of the lid and active site triad, and Table 2.5 summarizes these important structural and functional features.

Table 2.5. Important Features of Lipases

Feature	Details	Remarks
Mechanism based on a “catalytic triad” made up of nucleophilic serine, histidine, and aspartate/glutamate	Found in over 30 lipases, including those from psychrophilic or thermophilic microorganisms; the only exception is replacement of aspartate for glutamate. Substitutions of serine for cysteine by site-directed mutagenesis led to strongly reduced activity	Related hydrolases show much greater variability in catalytic mechanism. In the case of proteases, the amide bond can be hydrolyzed through nucleophilic attack by hydroxyl (serine, threonine) or thiol groups (cysteine), or through electrophilic attack by a carboxyl group (aspartate/glutamate) or a metal ion, (Zn^{2+})
Consensus sequence at the active serine residue	The consensus sequence for over 30 closed lipases is a “nucleophile elbow” at the end of a theta sheet and is composed of -Gly/Ala-X-Ser-X-Gly/Ala-	Other hydrolases show greater variability
Most lipases feature a lid structure	A lid composed of an amphiphilic peptide loop covers the active site of the enzyme in the inactive state.	No lid was observed in esterases or proteases, but some lipases have no lid or just a small lid.
All lipases are members of the “ α/β -hydrolase fold” family	The structure is composed of a core of predominantly parallel β strands surrounded by α helices. The active nucleophilic serine residue rests at a hairpin turn between a β -strand and an α -helix.	Many other hydrolases (esterases, acetylcholine esterases, serine proteases, carboxypeptidases, dehydrogenases) and even a haloperoxidase show a similar structural motive, which suggests evolutionary relationships.

Adapted from Schmid & Verger, 1998, p. 1614

Lipase mechanism.

Lipases catalyze the chemical process of conversion of acylglycerols to fatty acids and glycerol by acting on the carboxyl ester bonds. The active site’s catalytic triad is similar to that observed in serine proteases, and therefore catalysis by lipases is thought to proceed along a similar path (Brady et al., 1990; Jaeger et al., 1999).

Because of the similarity of these two mechanisms and the far larger number of references that describe the mechanism of serine proteases versus lipases, the serine protease mechanism is shown in Figure 2.14 and Figure 2.15. The major difference between the two is the substrate and the bond that is broken. The serine protease family hydrolyzes the peptide bond of an amide where a lipase hydrolyzes the ester bond of an acylglycerol. In the

numbered list that follows, descriptions of the structures and bonds for a lipase catalyzed reaction (in parenthesis) versus a serine protease catalyzed reaction are provided.

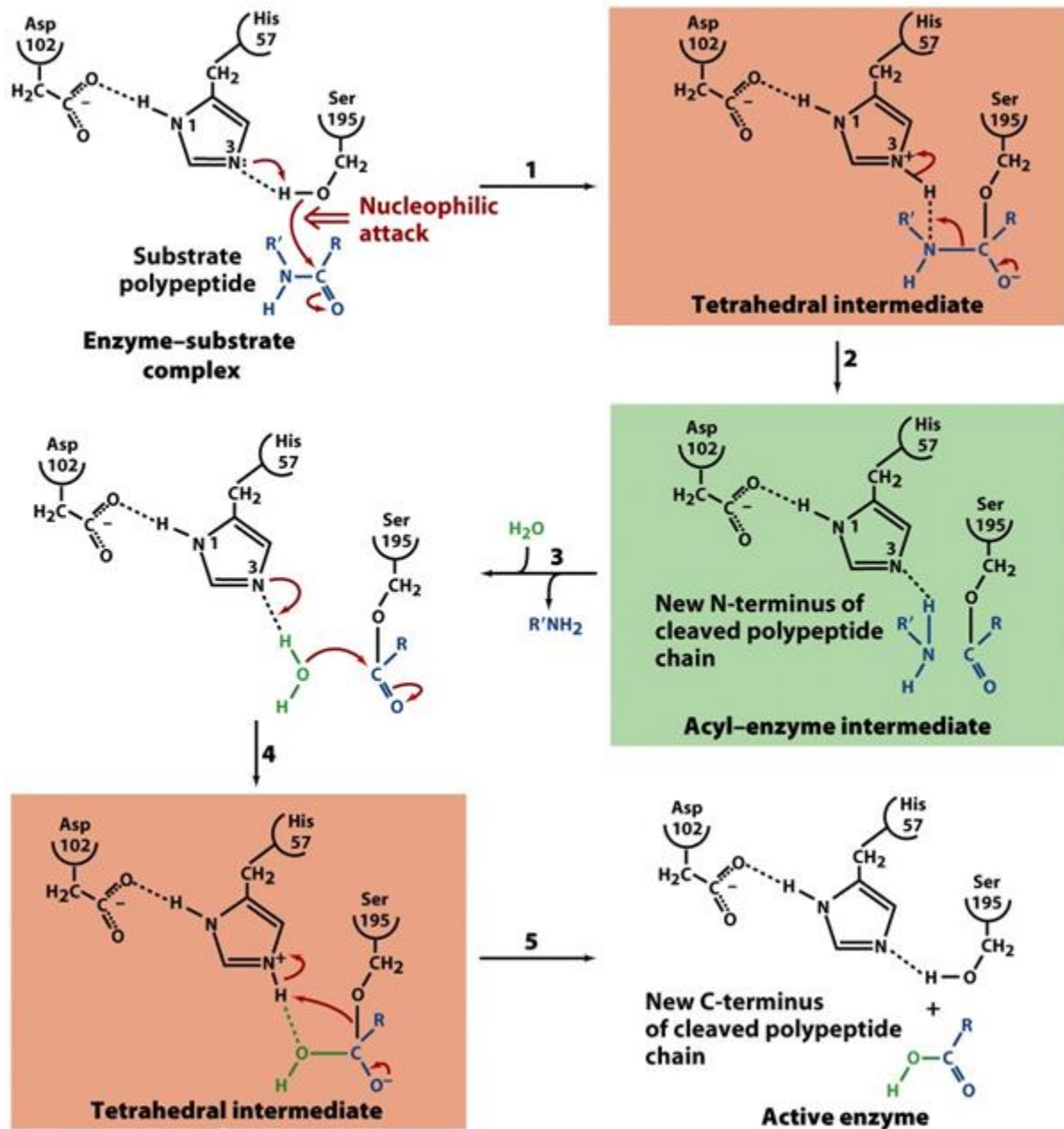


Figure 2.14. The catalytic mechanism of the serine proteases is very similar to the catalytic mechanism of lipases (Voet, 2012, p. 344).

1. Substrate hydrolysis starts with a nucleophilic attack by the catalytic-site-Ser on the scissile carbonyl's carbon atom of the peptide bond (ester bond), leading to the formation of a tetrahedral intermediate. The Ser residue is ideally positioned to carry out this nucleophilic attack as a result of proximity and orientation effects. The nucleophilic attack involves transfer of a proton to the imidazole ring of the catalytic-site-His, thereby forming an imidazole ion. This process is aided by the polarizing effect of the unsolvated carboxylate ion of catalytic-site-Asp or Glu, which is hydrogen bonded to the catalytic-site-His. The tetrahedral intermediate, to which the lipase shows preferential binding, has a well-defined, although transient, existence. This binding preference is due to the stabilization of the intermediate by hydrogen bonding to nitrogen atoms of main-chain residues that belong to the so-called "oxyanion hole" shown in Figure 2.15.
2. The tetrahedral intermediate decomposes to the acyl-enzyme intermediate under the driving force of proton donation from N3 of the catalytic-site-His facilitated by the polarizing effect of the catalytic-site-Asp or Glu on the catalytic-site-His.
3. The amine (alkyl) leaving group is released from the enzyme and replaced by water from the solvent.
4. The acyl-enzyme intermediate, which is highly susceptible to hydrolytic cleavage, adds water by the reversal of Step 2, yielding a second tetrahedral intermediate.
5. The reversal of Step 1 yields the carboxylate product (free fatty acid) thereby regenerating the active enzyme. In this process water is the attacking nucleophile and the catalytic-site-Ser is the leaving group (Jaeger & Reetz, 1998; Voet, 2012, p. 345).

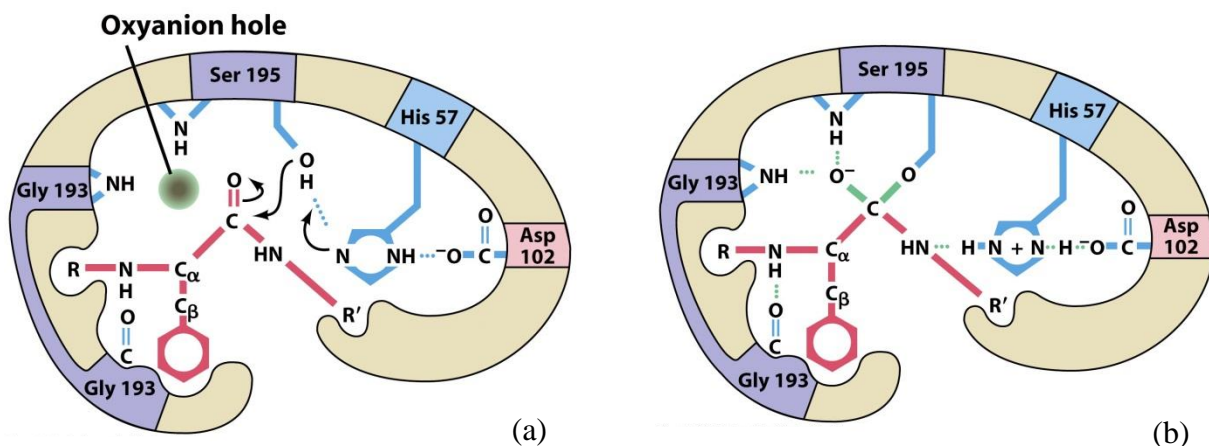


Figure 2.15. Transition state stabilization in the serine protease is similar to that in lipases. (a) When the substrate binds to the enzyme, the trigonal carbonyl carbon of the scissile peptide (ester) is conformationally constrained from binding in the oxanion hole. (b) In the tetrahedral intermediate, the now charged carbonyl oxygen of the scissile peptide (ester) enters the oxanion hole and hydrogen bonds to the backbone NH groups of the catalytic-site-Ser and the catalytic-site-Gly. The consequent conformational change permits the NH group of the residue preceding the scissile peptide (ester) bond to form an otherwise unsatisfied hydrogen bond to the catalytic-site-Gly. Therefore, serine proteases (lipases) preferentially bind the tetrahedral intermediate (Voet, 2012, p. 346).

Regioselectivity of lipases.

Another commonality among lipases is their specificity. Many lipases exhibit sn-1,3 specificity towards TG; however, the tendency towards acyl migration from the sn-2 to the sn-1 or sn-3 positions can lead to hydrolysis of all three ester bonds of the TG (Fernandez-Lafuente, 2010; Schmid & Verger, 1998). A suggested cause for this regioselectivity involves the structure of the enzyme in conjunction with substrate binding possibilities. “The enzyme contains a large hydrophobic groove in which the sn-3 acyl chain fits, a mixed hydrophilic/hydrophobic cleft for the sn-2 moiety of the substrate, and a smaller hydrophobic groove for the sn-1 chain. The difference in size and the hydrophilicity/ hydrophobicity of the various pockets determine the enzyme’s enantiopreferences and regiopreferences” (Jaeger et al., 1999, p. 336). In Figure 2.16, the four possibilities of substrate binding shown

demonstrate the regioselectivity of sn-1 or sn-3 positions due to binding of the substrate's acyl chains to the hydrophilic/hydrophobic grooves.

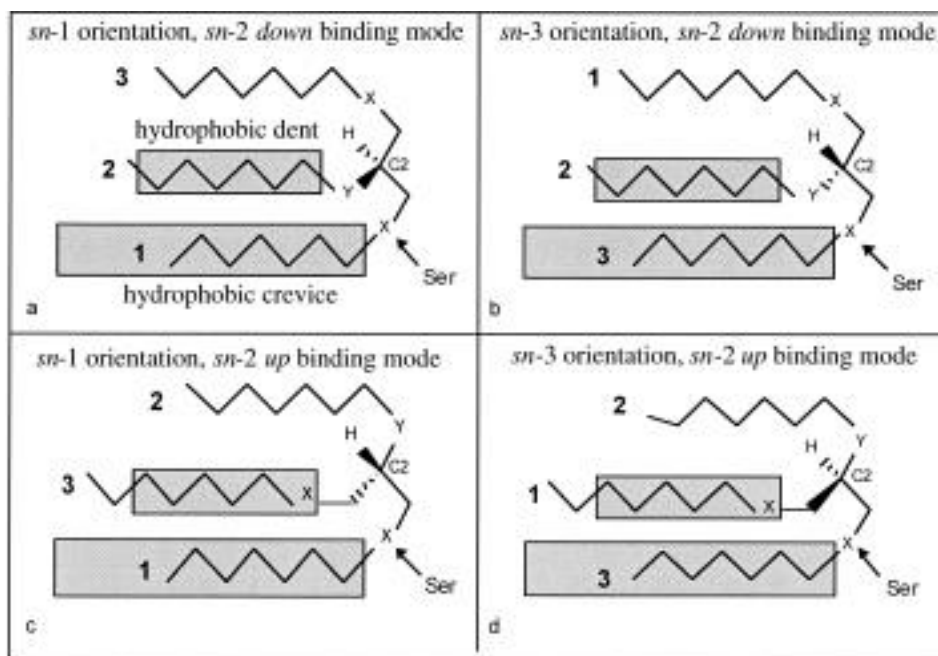


Figure 2.16. Four possibilities were suggested as to how a triacylglyceride substrate and analog can bind to a sn-1(3)-regioselective lipase. In the left column (a and c), the scissile sn-1 fatty acid chain binds to the hydrophobic groove. In the right column (b and d) the scissile sn-3 fatty acid chain binds to the hydrophobic groove. In the upper row (a and b), the sn-2 substituent binds to the hydrophobic cleft. In the bottom row (c and d), the non-hydrolyzed sn-3(1) fatty acid chain binds to the hydrophobic crevice. The sections a and d as well as b and c display the same configuration at the prochiral C2 of glycerol (Kovac et al., 2000, p. 68).

Enzyme inhibition and other considerations.

“The yield of biodiesel products through lipase catalysis is modulated by the substrate ratio (alcohol/oil), alcohol type, temperature of the reaction, water content, purity of the triacylglycerol and enzymes’ and whole cell immobilization” (Akoh et al., 2007, p. 9000). Because of an enzyme’s specificity, many of these variables (water content, methanol content, effect of glycerol, immobilized versus liquid formulation) react differently

depending on the specific lipase used. The following sections will describe generally how each of these variables is affected by lipase catalyzed reactions.

Alcohol inhibition.

One of the critical problems with using enzymes in biodiesel production is the deactivation of the enzyme by an alcohol. This is especially true in the commercial production because methanol is a particularly strong inhibitor and an excess amount of methanol is needed to drive the transesterification reaction forward. “There is an apparent connection between the solubility of the alcohol in oil” (Nielsen et al., 2008, p. 696). Low conversion is due to inactivation of lipases by contact with insoluble alcohols that exist as drops in the oil (Shimada, Watanabe, Sugihara, & Tominaga, 2002). A solution to this conundrum was presented by Shimada et al. (2002) as a three step or step-wise addition of methanol to the reaction. Also, Kaida, Samukawa, Kondo, and Fukuda (2001) reported that water or a solvent may help to alleviate lipase inactivation by methanol by solubilizing the methanol and drawing it away from the enzyme. Finally, use of alcohols other than methanol, help reduce alcohol inhibition, as Chen and Wu reported that the degree of enzyme inactivation is inversely proportional to the number of carbon atoms in the alcohol (Chen & Wu, 2003). However, when considering the economic viability of a biodiesel production facility the use of solvents, which must be recovered, and costlier alcohols compared to methanol makes these methods less economically competitive (Gog, Roman, Tosa, Paizs, & Irimie, 2012).

Ping pong bi-bi mechanism with competitive inhibition.

“Lipase transesterification of TG with an alcohol (alcoholysis) involves a two-step mechanism when looking at a single ester bond. The first step is hydrolysis of ester bond and

release of the alcohol moiety followed by an esterification with the second substrate” (Fjerbaek et al., 2009, p. 1301). The reaction mechanism for the esterification step conforms to a ping pong bi-bi mechanism, a widely accepted mechanism for alcoholysis of TG. (Al-Zuhair, 2006; Silverman, 2000).

Most of the kinetic models reported are based on the application of simple Michaelis-Menten kinetics, which seem to be valid for most simple enzymatic reactions. In the case of producing biodiesel, a step of liberating fatty acids from triglyceride should precede the esterification of free fatty acids. For simplicity, Michaelis-Menten kinetics will be used for the preliminary hydrolysis step to liberate the free fatty acids from the oil. However, for the esterification of the free fatty acids the most suitable kinetic model is the ping pong bi-bi kinetic model with competitive inhibition by the alcohol (Al-Zuhair, 2006). A diagram of the esterification reaction is shown in Figure 2.17. Other components of the reaction mixture that have exhibited inhibitory effects, and therefore should be included in the kinetics model, include fatty acid substrate and glycerol when using immobilized enzymes.

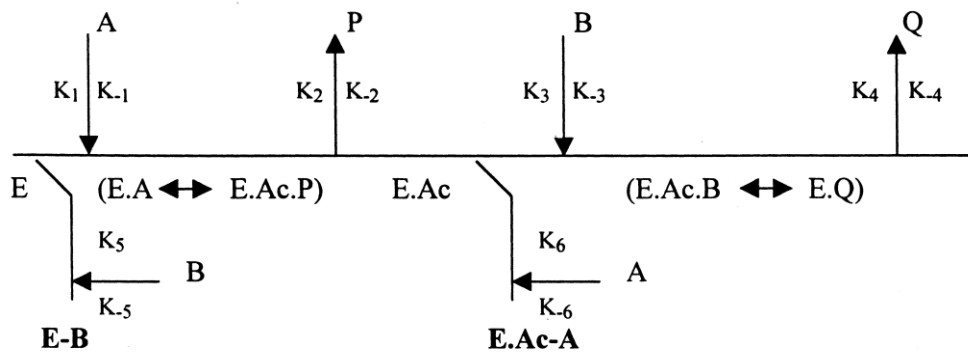


Figure 2.17. Schematic representation of the ping pong bi-bi mechanism with competitive inhibition by both alcohol and acid substrates where E=enzyme, A=fatty acid, B=alcohol, P=water, Q=FAME, and Ac=acyl group, and E-B and E.Ac-A are the deadend inhibition complexes of enzyme with alcohol and acid, respectively (Krishna & Karanth, 2001, p. 264).

Using this theory, the initial rate at the interface of the liquid enzyme that considers inhibition by both alcohol and substrate was derived by Al-Zuhair et al (2006).

$$v = \frac{V_{max}}{1 + \frac{K_A}{[A]} \left[1 + \frac{[B]}{K_{iB}} \right] + \frac{K_B}{[B]} \left[1 + \frac{[A]}{K_{iA}} \right]} \quad (2.5)$$

Where K_A = binding constant for the fatty acid, K_B = binding constant for the alcohol, K_{iA} = inhibition constant for the fatty acid, and K_{iB} = inhibition constant for the alcohol (Al-Zuhair, Jayaraman, Krishnan, & Chan, 2006, p. 213)

Fjerbaek et al. (2009) point out the limitation of using this model. “Steady-state kinetics, such as Michaelis-Menten, can possibly describe the enzymatic conversion satisfyingly with appropriate fitting to a long range of models of varying complexity, but the accuracy of this can be questioned” (p. 1301). Therefore, while this is a convenient model to apply, steady state kinetics may not accurately describe the kinetics of the reaction in biodiesel production. Additionally, neither the formation of mono- and diglycerides, the effect of temperature enzyme deactivation, nor the equilibrium limitations of the reactions are considered.

However, this model does deepen our understanding of the mechanisms and kinetics of this reaction, despite the less than perfect model. An examination of the other considerations mentioned in the review need to be included in order to fully understand how a specific enzyme behaves in this process.

Water content.

In a lipase catalyzed reaction with an insoluble substrate, such as oil, there is a need for some water to maintain and activate the lipase. Water contributes to the formation of a heterogeneous reaction medium where a liquid-liquid interface exists between the enzyme

and the substrate. The interface is the point where the lipase can access the substrate and catalyze the reaction. Lipase activity is influenced by the nature, size and properties of the interface. In general, an increase in interfacial area (i.e. an increase of water) increases the activity of the enzyme in a lipid/water solution (Akoh et al., 2007; Gamba, Lapis, & Dupont, 2008). In practical terms for a biodiesel production facility, “if the system is water free, no reaction takes place while the rate of reaction increased with increased water content (1-20 wt% water)” (Fjerbaek et al., 2009, p. 1302).

Too much water, however, may cause a reverse esterification reaction or hydrolysis of FAME to FFA and methanol leading to a lower yield of FAME (Al-Zuhair, Dowaidar, & Kamal, 2009; Lam et al., 2010). Additionally too much water may decrease the life of the enzyme (Fjerbaek et al., 2009). “The optimum water content is a compromise between minimizing hydrolysis and maximizing enzyme activity for the transesterification reaction” (Yucel, 2012, p. 101).

Use of solvents.

The purpose of using organic solvents is to “ensure a homogenous reaction mixture alleviating the problem of reactants in two phases; it reduces the viscosity of the reaction mixture increasing the diffusion rate reducing mass transfer problems around the enzymes; for immobilized enzymes non-polar solvents might force the residue water to stay around the enzyme increasing the water activity locally and solvents might help stabilizing enzymes” (Fjerbaek et al., 2009, p. 1302). Non-polar or hydrophobic solvents used in this capacity include isooctane, n-heptane, petroleum ether, n-hexane, cyclohexane and conventional diesel. (Al-Zuhair et al., 2009; Fernandez-Lafuente, 2010; Fjerbaek et al., 2009). It has also been observed that glycerol, a non-polar compound, is insoluble and remains in the reactor

where it absorbs to immobilized lipase causing the same level of inhibition as in a solvent-free reaction system (Gog et al., 2012).

Polar or hydrophilic solvents are typically much less useful as they strongly interact with the essential water layer coating the lipase that contributes to the lipases' interfacial activation. However, the use of 1,4-dioxane and tert-butanol have shown high transesterification yields. Tert-butanol, a molecule with moderate polarity, has been shown to be the most effective solvent because it does not interfere with the esterification reaction, it has the ability to dissolve oil, alcohol (to avoid inhibition by methanol) and glycerol (to avoid mass transfer problems) (Nielsen et al., 2008). For a commercial scale biodiesel production facility, solvents create potentially more problems than they solve, such as a need for larger equipment (solvents take up volume), environmental issues (solvents are volatile and potentially hazardous), and increased costs due to the necessary recovery of the solvent.

Liquid versus immobilized enzymes.

Liquid, soluble, or free enzymes are enzymes that are immersed in a liquid phase, typically water, and are not bound to each other or to another medium. The liquid may contain stabilizers to prevent enzyme denaturation as well as preservatives to prevent microbial growth. (Nielsen et al., 2008). Immobilized enzymes are bound to a carrier such as silica beads or gel, alumina beads, ceramic beads, ion-exchange resin, photo crosslinkable resin, and possibly nanoparticles (Fernandez-Lafuente, 2010). Some methods for immobilization include adsorption techniques, covalent bonding, entrapment, cross-linked enzyme aggregates (CLEAs), and protein coated microcrystals (PCMCs) (Fjerbaek et al., 2009; Lam et al., 2010).

Much of the recent research in enzymatic biodiesel production focuses on immobilized enzymes because of their ease of extraction and re-use and because of the added stability an enzyme has when it is immobilized (Akoh et al., 2007; Al-Zuhair, Ling, & Jun, 2007; Nielsen et al., 2008). “The purpose of immobilization is to provide a more rigid external backbone for lipase molecule which will result in a faster reaction rate” (Lam et al., 2010, p. 513). Immobilized enzymes may be used in a continuously stirred tank reactor (CSTR) followed by a simple filtration to extract the enzymes, or they have been used in packed bed reactor (PBR) columns (Al-Zuhair et al., 2011; Watanabe, Shimada, Sugihara, & Tominaga, 2001). “In general, the optimal temperature can be expected to increase when immobilizing an enzyme because binding to the carrier material gives stability to the enzyme and therefore decreases the effect of thermal deactivation compared to free enzymes” (Fjerbaek et al., 2009, p. 1303).

When using immobilized enzymes the effect that the immobilization has on internal and external mass transfer must be considered. Internal mass transfer refers to the fact that large molecules, such as TG and FAME, have to diffuse through small pores to reach the enzymes while only sparingly soluble reactants, such as methanol, have to travel through oil filled channels. External mass transport limitations arise when a film layer forms, particularly of glycerol, around the carrier (Fjerbaek et al., 2009). Internal mass transfer problems can be alleviated with pretreatment or washing techniques of soaking the enzymes in a solvent, such as n-hexane, water, ethanol or propanol (Fernandez-Lafuente, 2010). External mass transfer problems have been lessened with increased stirring in CSTRs or increased flow in PBRs (Fjerbaek et al., 2009), by the removal of glycerol during the reaction or the use of solvents to solubilize the glycerol and draw it away from the enzyme.

The removal of glycerol can also be accomplished with a hydrophilic ultrafiltration membrane, where the glycerol in the nonpolar reacting medium is pulled towards the membrane because of its stronger affinity for the polar membrane. This mechanism can be more easily and cheaply accomplished with the addition of water, as long as the above discussed effects of water are kept in mind. Additionally, pretreatment of the enzyme with a mixture of oil, methyl oleate, and methanol has shown to intrude the carrier and take up place where the glycerol would intrude if not pretreated (Fjerbaek et al., 2009). Finally, a hydrophobic, rather than a hydrophilic, carrier may lessen the external and perhaps internal mass transfer limitations.

Because of the difficulty of recovering liquid enzymes, there has been considerably less discussion and research focused on liquid enzymes in a production capacity. The advantages to using liquid enzymes are that the mass transfer resistances are negligible and the addition of an extra (solid) phase to the system, which may slow the reaction down, is avoided. (Fernandez-Lafuente, 2010; Nielsen et al., 2008). From an economic standpoint, liquid enzymes are less costly than immobilized. “The carrier itself, as well as the immobilization process, adds significantly to the cost of immobilized enzymes” (Nielsen et al., 2008, p. 695). Furthermore, lipase is already a quite stable enzyme, so the need for additional stabilization via immobilization is not necessary and can be detrimental. The lack of research in this area and the significant advantages to using liquid enzymes is the motivation for conducting this research to find an effective way to recover and reuse liquid enzymes.

Enzyme loading.

Applying Michaelis-Menten kinetics under steady state conditions, more enzyme present in a reaction results in a faster initial reaction. While other reaction parameters affect the extent of the rate increase, research has confirmed rate increases with higher enzyme loading for immobilized and liquid enzymes in conjunction with varied alcohol to oil ratios (Chen, Du, & Liu, 2008; Hernández-Martín & Otero, 2008; Xu, Du, Zeng, & Liu, 2004). A limiting factor in this trend observed with liquid enzymes is the available liquid-liquid interfacial area between the water and oil. “[W]hen the lipase concentration on the interface reached the maximum adsorptive capacity, the esterification rate could not be improved obviously with the increase in enzyme concentration” (Chen et al., 2008, p. 2099).

Recovery and Reuse of Liquid Enzymes

Research into the recovery of liquid enzymes in production of biodiesel is fairly limited, as most of the research done with enzymes in biodiesel has focused on the use of immobilized enzymes. A technique that has the potential to capture active enzymes from the glycerol/aqueous phase for reuse in enzymatic biodiesel production is membrane filtration. “Ultrafiltration is one of the methods used to concentrate, purify and recover enzymes” (Echavarria, Ibarz, Conde, & Pagan, 2012, p. 52). One such commercial process that uses ultrafiltration to successfully recover enzymes from a viscous solution is the clarification and filtration of apple juice (Kim, Meyssami, & Wiley, 1989; Sheu, Wiley, & Schlimme, 1987). This technique, which is novel to recovery of enzymes in the biodiesel industry, will be explored in this research, and will therefore be explained in more detail.

Membrane-based ultrafiltration.

Membrane filtration is a separation technique that can be classified depending on the size of the particles being separated. Figure 2.18 shows the range of particle sizes used in different types of membrane based bioseparation. Ultrafiltration, with a pore size between approximately 0.001 μm and 0.1 μm , is the most appropriate size for enzyme fractionation. Ultrafiltration membranes are typically characterized by molecular weight cutoff (MWCO) rather than pore size and range from 5kD to 1,000 kD. The MWCO value indicates the size of the molecule that the membrane can retain to 90% efficiency. For example, a MWCO value of 10 kD meant the membrane will most likely retain 90% of the molecules having a molecular weight of 10kD. Concurrent with the importance of particle size, the transport of material through an ultrafiltration membrane is primarily driven by a pressure gradient that typically ranges from 10 to 100 psig (Abdel-Latif, 2010).

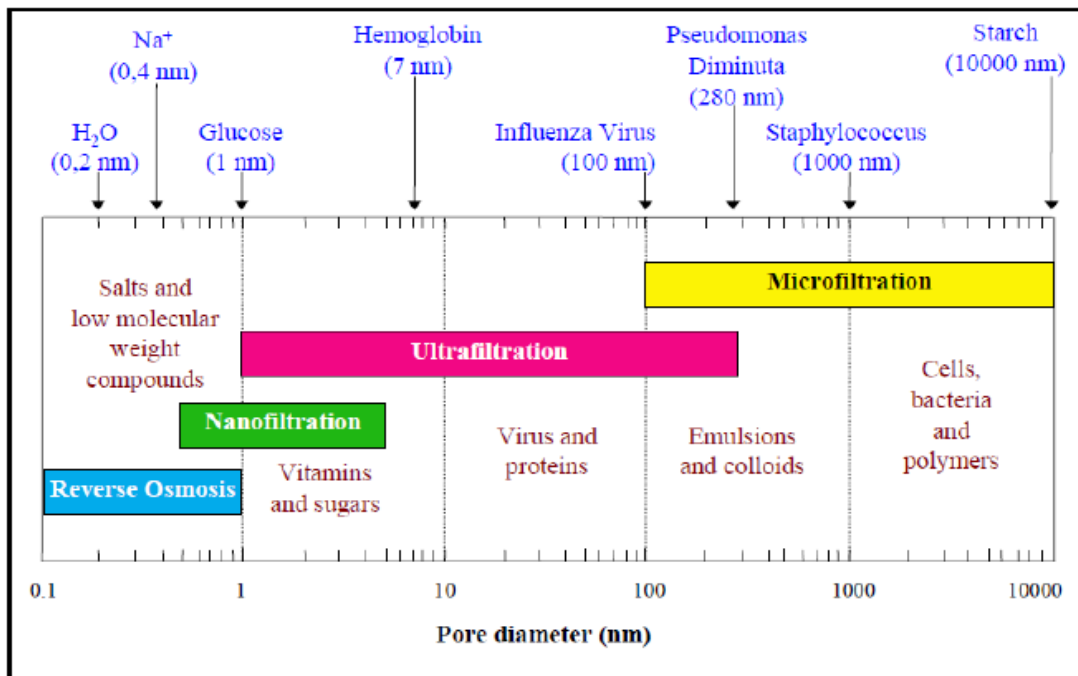


Figure 2.18. Filtration type versus pore size. Ultrafiltration is most appropriate for use with enzymes, which are proteins (Abdel-Latif, 2010, p. 1).

“A good general rule is to select a membrane with a MWCO that is 3 to 6 times lower than the molecular weight of the molecules to be retained... [I]f flow rate (or processing time) is a major consideration, selection of a membrane with a MWCO toward the lower end of this range (3x) will yield higher flow rates. If recovery is the primary concern, selection of a tighter membrane (6x) will yield maximum recovery (with a slower flow rate)” (Schwartz & Seeley, n.d.).

The modes of operations for membrane ultrafiltration are either direct flow filtration (DFF) or tangential flow filtration (TFF). In DFF the feed stream is perpendicular to the membrane face and attempts to pass 100% of the feed through the membrane. In TFF (also called crossflow filtration), the feed stream passes parallel to the membrane face, and is separated into a permeate (the portion containing smaller molecules that pass through the membrane) and a retentate (the portion retained by the membrane). Depending on the set-up and desired accuracy of separation, the retentate can either be pulled off or recirculated back into the feed. When size is the basis of separation, TFF can be a more efficient mode due to the fact that the flow of feed passing parallel to the membrane surface sweeps away larger aggregating molecules that would otherwise form a membrane-clogging gel to allow for smaller molecules to move toward and pass through the membrane.

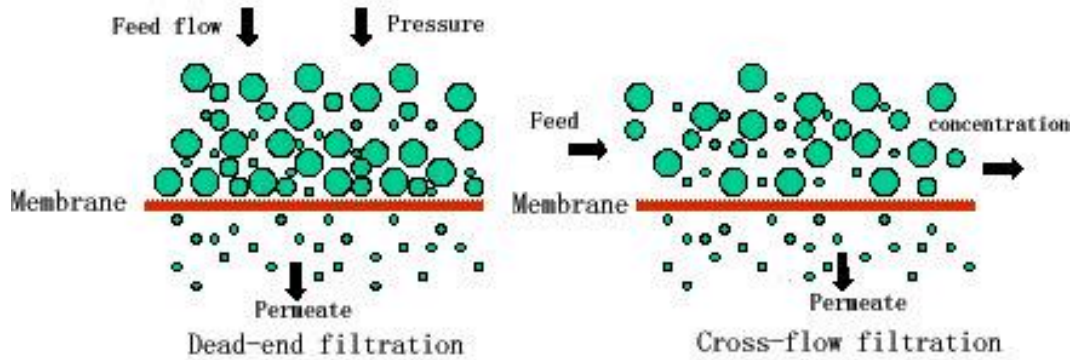


Figure 2.19. In dead-end filtration or DFF, the feed is directed into the membrane. Molecules larger than the pores accumulate at the membrane surface to form a gel, which fouls the surface, blocking the flow of liquid through the membrane. As the volume filtered increases, fouling increases and the flux rate decreases rapidly. In cross-flow filtration or TFF the feed channel directs solution along (tangent to) the surface of the membrane as well as through the membrane. The crossflow prevents build-up of molecules at the surface that can cause fouling. The TFF process prevents the rapid decline in flux rate seen in direct flow filtration allowing a greater volume to be processed per unit area of membrane surface (Schwartz & Seeley, n.d.).

Tangential flow filtration.

Two important parameters in TFF are the tangential velocity and the transmembrane pressure. The tangential velocity is the rate of flow of the feed stream/recirculated retentate across the membrane surface. It provides the force to sweep away aggregated molecules from the membrane surface that lead to a gel layer formation. However, the shear and turbulence caused by too high of a tangential velocity could damage the enzymes. Therefore, it is important to optimize the tangential velocity so that the filtration system can operate at the minimum tangential velocity that prevents gel layer formation.

The transmembrane pressure is the force that drives the fluid through the membrane, carrying along the permeate molecules. Transmembrane pressure results from the fluid flowing through the often narrow feed channels creating a pressure drop between the feed and retentate ports. The viscosity of the feed helps determine the channel height, which

typically falls between 0.5 mm and 2 mm. The tangential velocity and the transmembrane pressure are directly linked, where increasing the tangential velocity or restricting the tubing at the retentate increases the transmembrane pressure and vice versa.

The optimization of these two design parameters is crucial to allow the greatest volume of product to be filtered in the least possible time. The result of this is an optimum flux or permeate flux defined as the throughput of material a membrane or flow per unit membrane area. The common unit for flux is liter/m²/hour or LMH and is calculated using Equation 6.

$$J = \frac{V}{A \times T} \quad (2.6)$$

where J = Permeate flux rate (liters per m² per hour, LMH)

V = volume of permeate generated (liters)

A= Membrane area (m²)

T = Process time (hours)

Establishing baseline water fluxes for a specific set-up is a useful metric for characterizing new membranes and for assessing gel layer formation or fouling effects and the effectiveness of cleaning.

Tangential flow filtration unit.

TFF membrane modules are similar to plate and frame presses, where the flat membrane sheets are separated by narrow channels; this is referred to as the membrane cassette. Feed is pumped into the channels and the permeate crosses over the membrane into grooves in the membrane holder where it enters the permeate flow channel and is drained to a permeate reservoir. The retentate is recirculated to the feed reservoir to allow for multiple membrane passes. Figure 2.20 is a schematic of one such TFF membrane module.

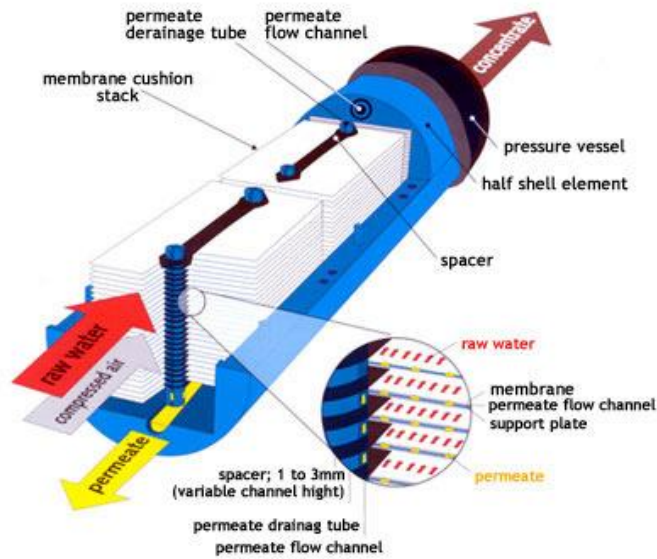


Figure 2.20. Tangential Flow Filtration module where feed stream flows tangentially to the membrane layers. Separation occurs as the smaller molecules that make up the permeate pass through the membrane into a drainage tube below and the retentate becomes more concentrated in enzyme (Abdel-Latif, 2010, p. 10)

Additional components of the filtration skid include pumps, tubing, valves, pressure gauges, and reservoirs. When handling thermally sensitive material (as in the case of *Thermomyces lanuginosus*) temperature sensors and heat exchangers may also be included. Figure 2.21 shows a diagram of what this type of system might look like. A system similar to this one will be used for this research, and is described in more detail in the description of the experimental design in Chapter 3.

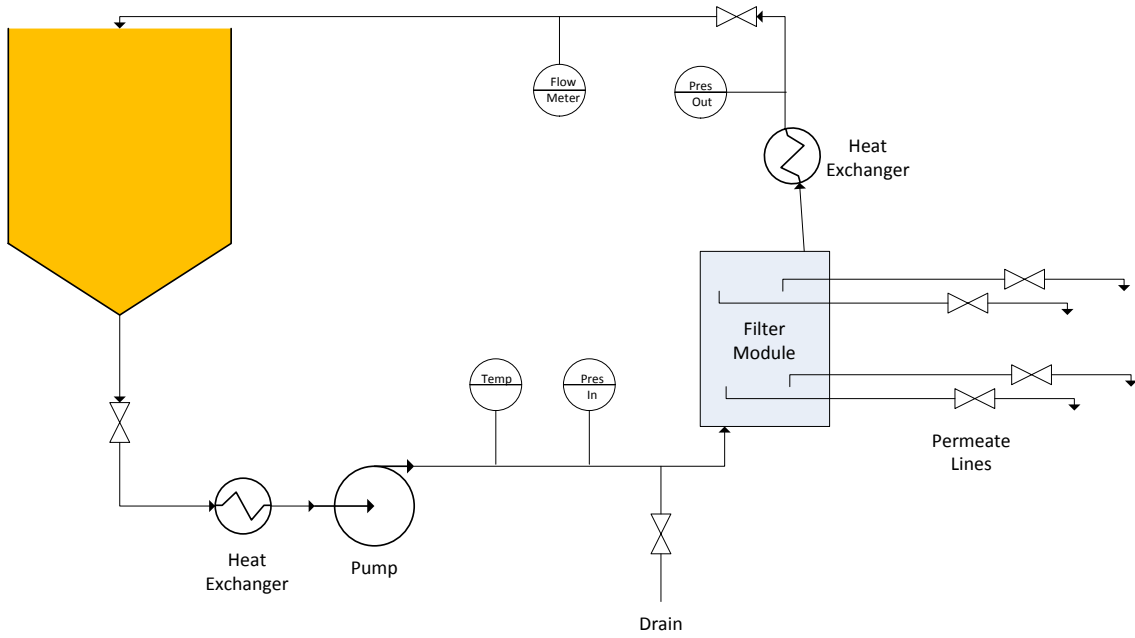


Figure 2.21. System design for TFF unit for thermally sensitive materials.

Chapter 3: METHODOLOGY

General Overview of the Research Design

This research aimed to compare the effectiveness of using Selective Aqueous Phase Reduction (SAPR) versus a Tangential Flow Filtration (TFF) system as a recovery technique for a commercially available liquid enzyme formulation of *Thermomyces lanuginosus* lipase (Liquid TL), after its use and subsequent re-use as a catalyst for the transesterification of triglycerides (TG) with methanol to make fatty acid methyl esters (FAME) or biodiesel. The SAPR method was a simple technique where gravity settling and decantation were used to remove a portion of the aqueous phase that formed as one of the three anticipated phases following the reaction of TG from lipid feedstock with methanol. The three phases included a top layer of FAME, a thin middle layer of primarily enzymes, and a bottom aqueous layer (Figure 3.1). The aqueous phase consisted primarily of glycerol, methanol, and water, although there may be some enzyme suspended as well. The reduction of aqueous phase (referred to as the “SAPR Reduction”) was necessary to remove glycerol formed during the reaction in order for the chemical equilibrium in the subsequent batch to favor FAME production, as well as to accommodate limited reactor volume. The remaining aqueous phase plus enzyme layer (referred to as the “SAPR Retentate”), was added to the subsequent batch. The TFF method used a Purostep Phoenix Pilot-Scale Filtration Unit (50 LPM) with a membrane filter designed and crafted by SmartFlow Technologies specifically for the aqueous phase (containing glycerol, methanol, water) and the enzymes. It was presumed that the filtered material (referred to as the “TFF Permeate”), analogous to the SAPR Reduction,

was going to be purely glycerol, water, and methanol. The filter would retain the enzyme along with some glycerol, methanol and water, in the retentate (referred to as the “TFF Retentate”), and was added to the subsequent batch. A series of four batches were run for each method. The effectiveness of conversion of TG to FAME was determined by the amount of bound glycerin in samples collected through-out and at the end of a 24 hour reaction window. The free fatty acid (FFA) content of each sample was tested to indicate the hydrolytic equilibrium and to better elucidate the rate mechanics of the reaction. Bench scale mini-batches using virgin soybean oil were conducted with the SAPR Reduction and the TFF Permeate to determine if enzyme was lost in the recovery stage of the process.

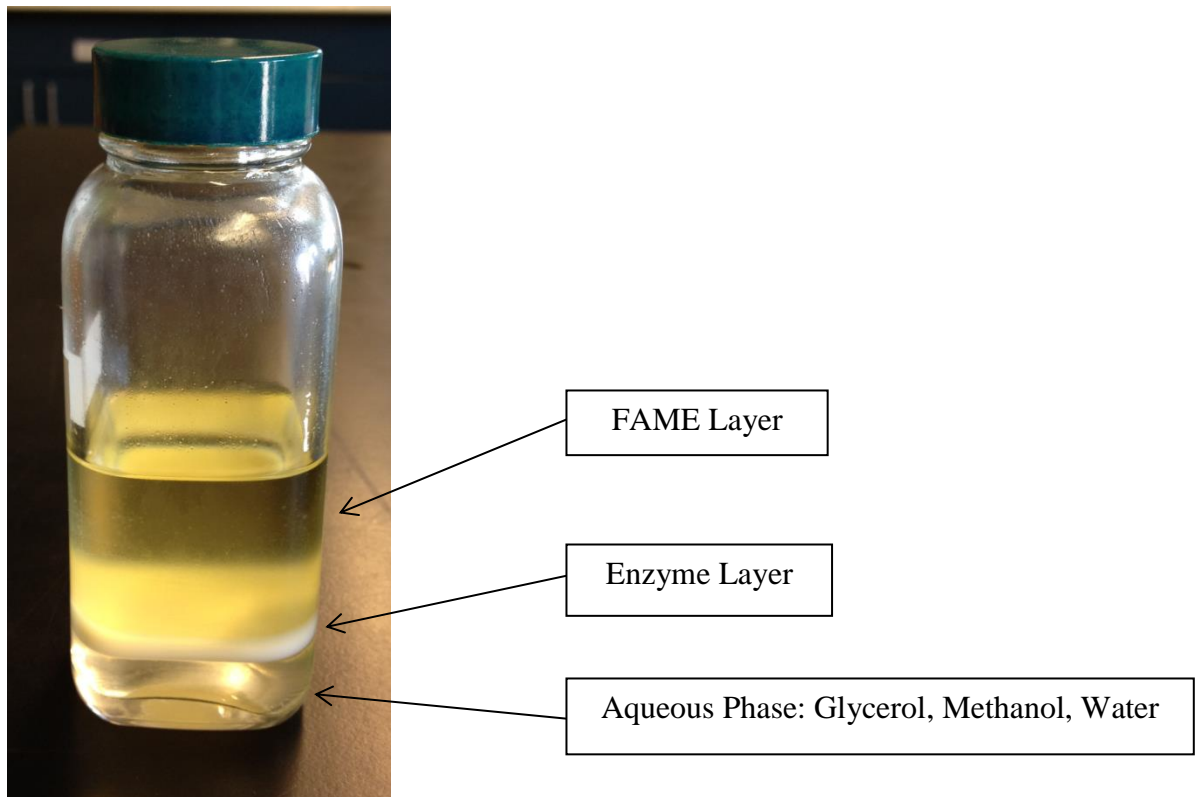


Figure 3.1. Three distinct phases formed during initial trials using Callera Trans to esterify virgin soy bean oil with methanol to produce FAME. The bottom glycerol layer is cleaner than the glycerol byproduct produced in traditional chemically catalyzed biodiesel production and considered technical grade following stripping of the residual methanol and water.

Collaboration with Piedmont Biofuels

Piedmont Biofuels is a small (1million gallons per year) biodiesel producer located in Pittsboro, NC that supplies biodiesel to customers across central and eastern North Carolina. Their mission is to lead the sustainability effort in North Carolina through the development and production of clean, renewable fuels. Their biodiesel feedstock is primarily used cooking oil from food service establishments throughout the region, but also includes poultry fat, sausage waste, brown grease, corn oil from distiller's dry grains (DDG), and fatty acid distillates, among other lower quality feedstocks. Much of the fuel Piedmont Biofuels produces is sold to oil companies, who then blend it with petroleum diesel and distribute it through gas stations and other channels. Another avenue Piedmont uses to bring biodiesel to local North Carolinians is through their fuel co-operative, where members have access to seven pumping stations maintained by Piedmont that provide B100.

In addition to Piedmont's production plant, there is a research division focused on developing technologies which make small scale production better, faster, and cheaper. Their focus on enzymatic catalysis has helped them stand out as a leader in development of cutting-edge, small-scale technologies. Their enzymatic FAeSTER (Fatty Acid eSTERification) process uses the CalB enzyme, developed and sold by Novozymes under the trademarked name Callera Ultra, to convert high free fatty acid feedstocks into quality fuel. "The FAeSTER process is a patent pending, fully continuous esterification technology using immobilized or liquid enzymes. The enzymes can be reused for multiple reactions, and [Piedmont] has achieved a catalyst cost of \$0.15 per gallon processed feedstock. This process is a direct replacement for acid esterification using sulfuric acid, or solid acid catalysts, and generates a dry (<1500ppm water), low FFA (<1%) feedstock ready for transesterification.

For very high FFA feedstocks like acid distillates or brown grease, this process is particularly cost effective. What differentiates FAeSTER from normal enzymatic esterification is [the] ability to continuously remove moisture to drive the esterification reaction towards methyl ester production” (Burton & Austic, 2011). This process is “a necessary component of full enzyme based biodiesel production process. Independent of feedstock, enzyme transesterification yields 2-3% FFA. The FAeSTER process can easily esterify or “polish” this FFA directly in methyl esters”, (Burton & Austic, 2011). In the spring of 2012 Piedmont opened the first full scale, continuous plant using the FAeSTER process at their facility in Pittsboro, NC.

In continued efforts to develop a fully enzyme catalyzed process, Piedmont’s research has turned to enzymatic transesterification. Research on the use of the *Thermomyces lanuginosa* liquid enzyme trademarked as Callera Trans, developed and sold by Novozymes, has shown to be promising. The research Piedmont conducted with Novozymes prior to collaboration for this thesis included optimizing the “recipe” at a bench scale. The point at which collaboration began for the content of this thesis was at the scale-up from bench scale to a 50 gallon reactor where research on the feasibility and logistics of recovery and reuse of the liquid enzyme were initiated.

Previous Research on Callera Trans

Previous bench scale research was conducted in an attempt to clarify the effects of methanol addition and enzyme loading on Callera Trans catalyzed transesterifications. From published Novozymes’ white papers entitled “Enzymatic large scale production of biodiesel” Nielsen and Rancke-Madsen (2011) describe a fully enzymatic two-step process for producing biodiesel. “The principle is that the first transesterification step is processing the

glycerides to esters and some FFA by use of Callera Trans. The FFA is esterified in the second step by use of Callera Ultra to achieve FFA according to ASTM specifications in the final biodiesel” (Nielsen & Rancke-Madsen, 2011, p. 231)

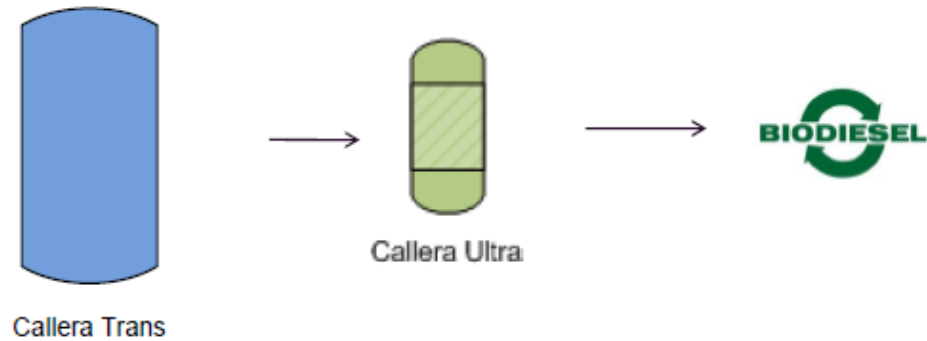


Figure 3.2. A fully enzymatic biodiesel production consists of two steps: transesterification of TG using the enzyme Callera Trans followed by esterification of FFA using the enzyme Callera Ultra (Nielsen & Rancke-Madsen, 2011).

In these trials, three batches were run back-to-back reusing the enzyme laden aqueous phase for catalysis of subsequent batches. The transesterification step used 1.4-1.5 molar equivalents of methanol to fatty acid dosed in a step-wise fashion with 0.5% enzyme loading (w/w) with respect to the oil mass. Reaction temperature was 45°C with a time between 4-24 hours. After the 3rd reaction FFA content post-transesterification with Callera Trans was approximately 7%, giving a fatty acid conversion of approximately 96% (Nielsen & Rancke-Madsen, 2011). The esterification step reduced the FFA to less than 0.25%. Details of this step are not presented because the research conducted for this thesis focuses on examining the transesterification step.

Further research was conducted by Piedmont Biofuels to determine a set of standard operating parameters and a recipe for transesterification with Callera Trans. This research focused on determining appropriate catalyst loading and the optimum rate of methanol addition, with the goal of minimizing deactivation due to excess methanol, while maximizing

the rate of reaction. This reaction used approximately 1.7 molar equivalents of methanol, where 25% was dosed initially and 75% was dosed over either 5 hours or 3 hours. For each methanol dosing scheme, enzyme loading of 0.5%, 1% and 2% (w/w) oil was used. The implications deduced from these trials include that a methanol concentration in excess of 6% in the reaction leads to deactivation of the enzyme and that a 5 hour dosing rate is most reasonable for 2% enzyme loading. However, additional research should be done to confirm and elaborate on these results. None the less, these findings were influential in determining the enzyme loading amount and methanol dosing scheme for the scaled-up batches conducted for this thesis.

Previous Research on Enzyme Recovery via TFF

Initial trials were conducted by Piedmont Biofuels using a TFF unit identical to the one used for this research to filter and reduce by 20% a “mock” aqueous phase comprised of FAME, glycerol, water, methanol, and enzyme. The retentate was then used to catalyze bench-scale batches to determine the effectiveness of retaining the enzyme. This process was repeated for a course of ten bench scale batches. Overall the data indicated that a vast majority (approximately 90%) of the enzyme was retained during the filtration process.

Characterization of Inputs

The feedstock used was a homogenous mixture of equal parts corn oil extracted from distiller’s dry grain and waste fryer oil from local restaurants collected by Piedmont Biofuel’s production team. The FFA content of the combined waste oils was determined by titration before each batch was run and was found to be approximately 9%.

The liquid form of a commercially available enzyme formulation of *Thermomyces lanuginosus* similar to Callera Trans was purchased from Novozymes by Piedmont Biofuels. This enzyme is thermally sensitive to temperatures in excess of 45°C.

Glycerol used was technical grade and obtained from Chemsolv. Methanol was also purchased from Chemsolv. Well water from the tap was used with a pH of 5.75.

Apparatus

Transesterification Reactor

The reaction vessel used was a Springboard BioPro 190 unit, which is a stainless steel all-in-one biodiesel production unit designed for homebrewing or small-scale batch making. The unit has a total capacity of 60 gallons, which allows for 50 gallons of oil feedstock to react with 10 gallons of methanol to produce 50 gallons of biodiesel and roughly 6 gallons of glycerol. The contents of the BioPro were agitated with a powerful tri-blade impeller that sits approximately mid-way down the volume of the unit. The unit is designed for an acid, base or two step process followed by a three stage water wash and evaporative drying cycle. The unit has a large covered opening to load the feedstock and separate inlet ports for loading methanol, and the base and acid catalysts. There is also a separate hook-up for a water source and an outlet port for the finished fuel.

For this series of experiments, the BioPro unit was used in its manual-mode, where the agitator was user controlled, and minor modifications were made to the BioPro unit to facilitate better control within the specified temperature range. An external methanol dosing system was also required for the enzyme catalyzed biodiesel reaction. The temperature control system of the BioPro was replaced with an off-the-shelf digital thermostat to allow a lower set-point temperature. As well, one of the ports on the BioPro was modified to allow a

continuous, relatively small methanol dose to be added over an extended period of time. This dosing system was achieved by a dosing pump configuration assembled from three lab scale dosing pumps: a 907MityFlex Fixed Speed Peristaltic Pump, contributing a constant rate of approximately 54 mL/min and two Stepdos 03 chemically resistant, diaphragm metering pumps whose rates could be varied from 0.3 – 30 mL/min and contributed the remainder of the total dosing rate. The inlets to the dosing pumps were connected to two 10 gallon carboys of methanol hooked up to a manifold of three tees. The outlets from the pumps were mated together to result in a single methanol feed.

Validating Dosing Pump Configuration.

The delivery rate of the dosing pump configuration was initially determined and was verified before and after each batch. Verification of the pump configuration was accomplished by filling a 1000 mL graduated cylinder with methanol for ten minutes and calculating the rate by dividing the volume collected in milliliters by ten minutes. If the rate had drifted from the required amount, it was corrected by adjusting one of the Stepdos diaphragm pumps. Due to the imperfect dosing system configuration, the methanol dosing rate fluctuated slightly during some runs. To account for this, the total methanol dosed was calculated from the integration of the final flow rate and the initial flow rate over time.

Tangential Flow Filtration Unit

The TFF unit (Figure 3.3) used included a Purosep Phoenix Pilot-Scale Filtration Unit designed and built by SmartFlow Technologies. Due to the thermally sensitive nature of the enzymes, an inline temperature probe was used to continuously monitor the temperature, and a jacketed filtration reservoir was added before the pump as well as an additional post-filtration heat exchanger after the membrane module to maintain a temperature below 40°C.

The unit was fit with a 3/4" retentate loop to be used in conjunction with the CONSEP® 3000 filter module and manifold. The CONSEP® 3000 filter module consists of alternating layers of "Permeate Packs" and "Retentate Channel Separators." A Permeate Pack consists of sheet membranes bonded to both sides of a single permeate screen separator. Retentate Separators are layered between Permeate Packs to form a single filter module. (Figure 3.4). The number of layers is proportional to the desired membrane surface area required.

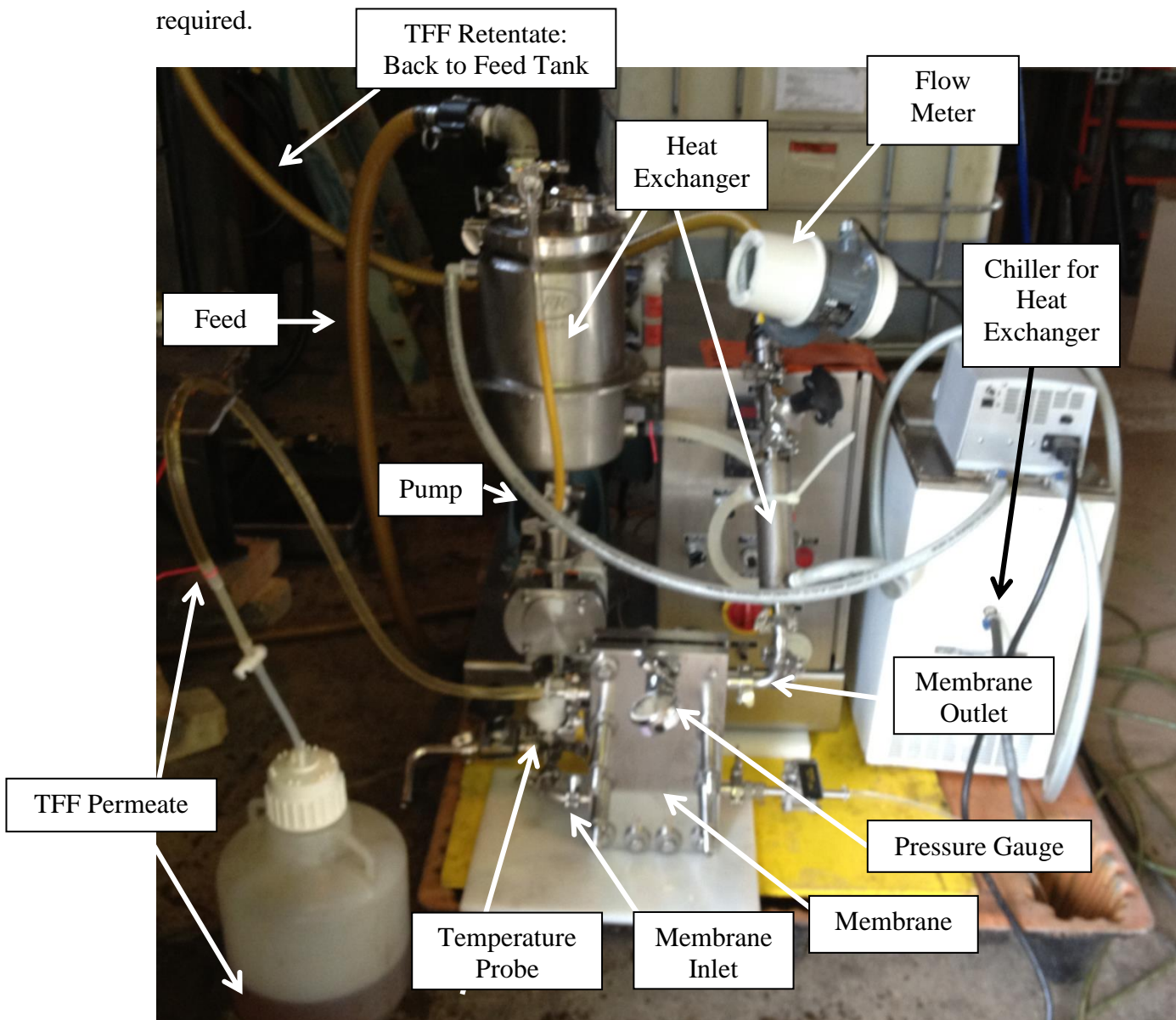


Figure 3.3. Purosep Phoenix Pilot Scale Filtration Unit in conjunction with the CONSEP® 3000 filter module and manifold.

For this particular application a regenerated cellulose membrane was used with a molecular weight cut off (MWCO) of 10 kD. The total membrane surface area was 0.19 m² and the channel height was 0.5mm. The CONSEP® 3000 module was sealed in the CONSEP® 3000 manifold by means of two terminal end silicone gaskets.

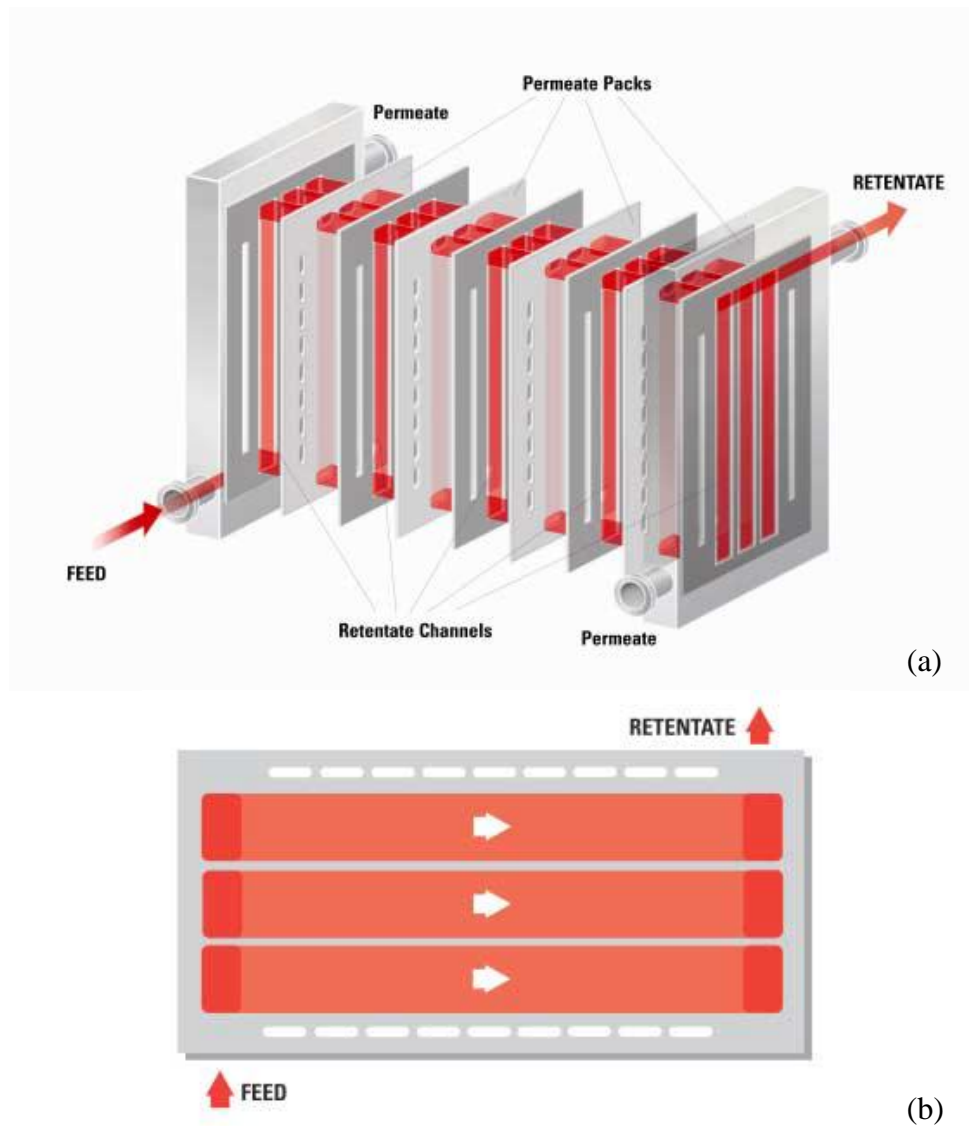


Figure 3.4. The feed channel directs a stream by the Permeate Packs where smaller molecules (glycerol, methanol, water) pass through the membrane and are directed to the permeate channel. The retentate contains the relatively large enzymes. (b)The unique flow channels of the CONSEP® 3000 allows for equal flow rates across the membrane surface.

CONSEP® 3000 filter is unique in that the flow channels use a patented rib design that creates uniform retentate channels that in turn produce equal flow rates across the membrane surface. This aids in minimizing gel layer formation on the membrane surface, which in turn greatly increases the permeate flow rate.

In Smartflow Technologies' optimization of this TFF system for the recovery of the enzyme Callera Trans, a tangential velocity or recirculation rate between 12.5-15 liters/min and an outlet pressure of 50 psi with an inlet pressure between 65-75 psi were recommended. The optimization trials were run using a mock aqueous phase comprised of FAME, glycerol, water, methanol, and enzyme. While this does not match exactly the aqueous phase from actual biodiesel batches, particularly when considering contaminants that may be suspended in the aqueous phase from the feedstock, it does give a decent suggestion of optimum tangential velocity and transmembrane pressures.

These two parameters were controlled by changing the pump speed to increase or decrease the velocity of the feed entering the membrane, resulting in a change in tangential velocity, and/or by opening or restricting a manual back pressure valve downstream from the filter module resulting in a change to the transmembrane pressure. Additionally, temperature was checked regularly and if it exceeded the recommended 40°C, the tangential velocity was slowed to allow for more residence time in the heat exchanger. The use of this unit required a balancing act between maintaining sufficiently low inlet pressure and temperature while achieving a sufficiently high permeate flux rate, which required constant manipulation of the controlling parameters.

Cleaning the tangential flow filtration unit between runs and NWP.

The Normalized Water Permeate (NWP), the term used for permeate flux when deionized water is run through the system, was used as a metric for any fouling that may have occurred on the membrane throughout the trials. The NWP was calculated as the unit was running by timing the collection rate of 100 mL of water from the permeate outlet, and then using Equation 3.1 to calculate a flux.

$$J = \frac{V}{A \times T} \quad (3.1)$$

where J = Permeate flux rate (liters per m² per hour, LMH)
V = volume of permeate generated (liters)
A = Membrane area (m²)
T = Process time (hours)

NWP was measured before the unit was used to filter any aqueous phase to be approximately 85 LMH, after cleaning of the membrane between batches, and whenever there was concern about gel layer formation indicated by slowing of the permeate flux.

Cleaning of the TFF unit occurred between each batch. The system was flushed with deionized water equivalent to approximately five times the system volume and a small amount of detergent. This mixture was drained, and the system was thoroughly flushed to remove any detergent. The membrane was stored wet in a 4% sodium bisulfite solution.

Procedure

First-Batch Transesterification Reaction

As this research aimed to compare the effectiveness of enzyme re-use using two enzyme recovery methods: selective aqueous phase reduction (SAPR) and a tangential flow filtration unit (TFF), there were a series of four consecutive batches run for each method.

Fresh enzyme was added only to the initial batch and the subsequent three batches were catalyzed by recovered enzyme from the previous batch. FAME and FFA from each batch were then analyzed to determine completeness of reaction, an indicator for enzyme activity.

At the start of each batch, the thermostat on the BioPro was adjusted to approximately 40°C while the oil was recirculated and allowed to equilibrate for 2 to 4 hours. For both the SAPR and TFF series of four batches, the first batch was slightly different from the three subsequent batches in the amount of enzyme, methanol, water, and glycerol additions. In the first batch an enzyme addition of 1% by feedstock weight was added. The target compositions for the other inputs in the first-batch, as well as all subsequent batches, were as follows: a 1.7 molar excess of methanol to TG, and an aqueous phase of 20% by feedstock weight, which itself was composed of 40% water and 60% glycerol by weight. The optimum amount of water was such that there was sufficient water present to activate the enzyme, while avoiding an overloading, which would have driven the hydrolysis reaction of converting TG to glycerol and FFA. Glycerol was used as an inert substance to bulk up the aqueous phase to allow for easier mixing in this size batch. The first-batch recipe by volume is listed in Table 3.1.

Table 3.1. *First-Batch Recipe*

	Feedstock	Enzyme	Initial Methanol, 25%	Dosed Methanol, 75%	Water	Glycerol
Volume (gallons)	42	1.3 L	2.3	6.8	3.1	3.6

An initial 25% of the total methanol, along with the water, glycerol, and the entire enzyme dose was added to the unit. With this addition, stirring of the reactor was initiated, and continuous methanol dosing of the remaining 75% of total methanol addition began. The

methanol was dosed continuously over a five hour period and was regulated by the dosing pump configuration to be approximately 86 mL/min.

Samples of approximately 80 mL of the oil/aqueous emulsion were taken from a port at the base of the BioPro at 1 hour, 2 hour, 4 hour, 6 hour, 8 hour, 10 hour, and 24 hour intervals. The samples were allowed adequate time to phase separated into an oil/FAME layer and an aqueous layer containing water, methanol, glycerol and enzymes. After these samples phase separated, the oil layer was analyzed for FFA content and bound glycerin levels.

Recovery and Reuse of Enzyme via Selective Aqueous Phase Reduction

After the 24 hours set to complete the reaction, the FAME/aqueous emulsion was pumped to a 150 gallon cone-bottom polyethylene tank. The mixture was allowed up to 2.5 hours to separate, which resulted in a two phase system. The total volume, as well as the volumes of each phase, were noted. The bottom layer of glycerol, water, methanol and enzyme was removed from the tank, the top layer of almost exclusively FAME was pumped into a holding tote. The aqueous layer was then pumped back into the cone bottom tank to settle for another 24 to 72 hours. This long settling period theoretically allowed for further stratification into three layers: a top layer of residual FAME, a thin, viscous enzyme-rich middle layer and a large bottom aqueous layer of glycerol, water and methanol (Figure 3.5). Samples of approximately 200 mL of the aqueous phase were taken and analyzed for methanol, glycerol, and water content. The expected trends are for the amount of methanol to decrease, glycerol to increase and water should remain constant.

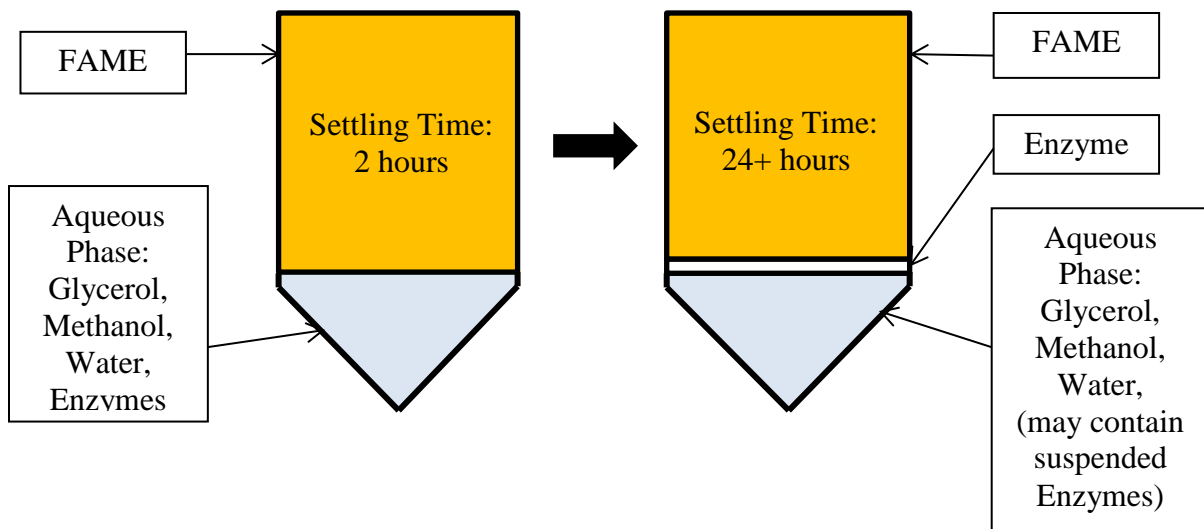


Figure 3.5. Phase separation after 2 hours of settling results in two phases, a FAME layer and an aqueous layer. After 24 - 72 hours an enzyme layer forms between the FAME and aqueous layers.

The volume of aqueous phase reduction was based on maintaining 3.6 gallons of glycerol in the aqueous phase that was to be added to the subsequent batch. This amount was slowly decanted to leave the enzyme layer as undisturbed as possible (Figure 3.6). The amount of methanol and water needed to bring the composition back up to target was calculated from the experimental results of the analysis of the aqueous phase and the theoretical production of each component (e.g., stoichiometric glycerol production). The reactor was again filled with 42 gallons of feedstock and heated to 40°C. The SAPR Retentate was added to the reactor, as was the make-up water and the initial methanol dose, before stirring was initiated and the continuous 5 hour dosing of methanol began. This process was repeated for the three batches subsequent to the first batch for a total of four batches using the same initial dose of enzymes.

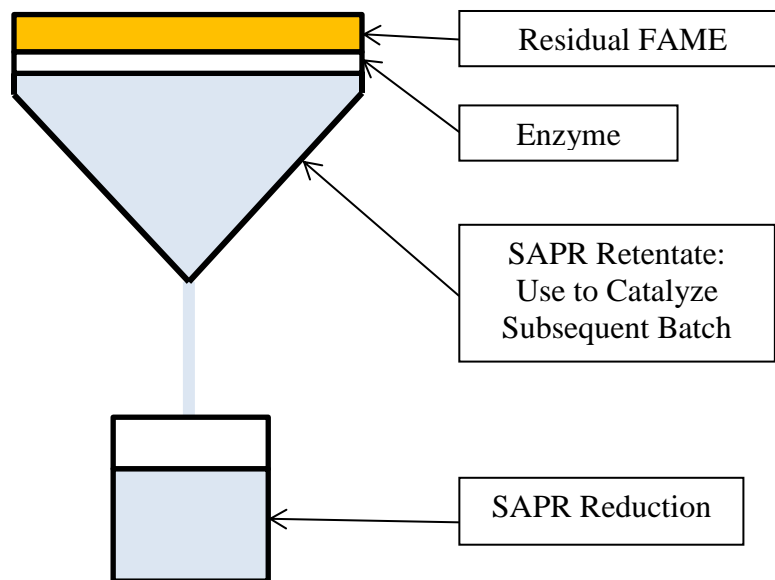


Figure 3.6. Diagram of the set-up for recovering enzymes using the SAPR technique.

Recovery and Reuse of Enzyme via Tangential Flow Filtration

After a 24 hour reaction period, the oil/aqueous emulsion settled in the BioPro for up to 2.5 hours and separated into two phases: FAME and an aqueous layer. The aqueous layer and a small amount of FAME that was emulsified in this layer were pumped into an 80 gallon cone-bottom polyethylene tank. Volumes of total aqueous phase pumped to the small cone-bottom were noted. The majority of FAME from the reaction was pumped from the BioPro into a holding tote. The aqueous layer was filtered for 14-76 hours to result in an enzyme rich TFF Retentate which also contained glycerol, water, and methanol, and a TFF Permeate consisting of glycerol, methanol, and water (Figure 3.7).

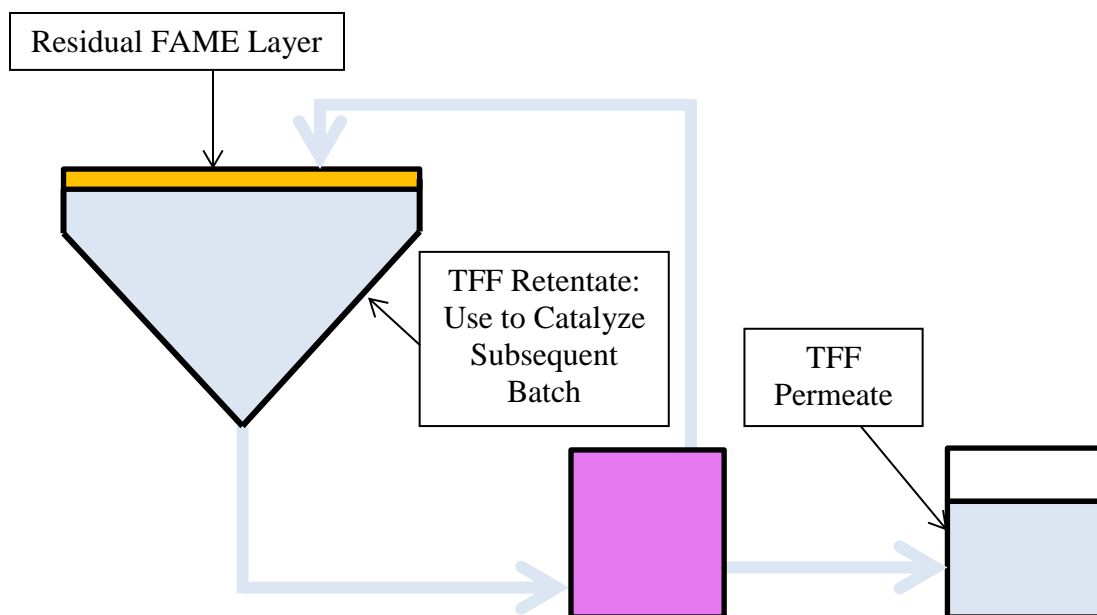


Figure 3.7. Diagram of the set-up for recovering enzymes using the TFF technique.

A sample of permeate collected early in the filtration cycle was analyzed for glycerol, water and methanol content, which was then used to estimate the total filtration time required for a reduction in aqueous layer resulting in a TFF Retentate with 3.6 gallons of glycerol. Again, the amount of methanol and water needed to bring the composition back up to target was calculated from the experimental results of the analysis of the TFF Permeate and the theoretical production of each component. The reactor was again filled with 42 gallons of feedstock and heated to 40°C. The TFF Retentate was added to the reactor, as was the make-up water and the initial methanol dose, before stirring was initiated, and the continuous five hour dosing of methanol began. This process was repeated for the three batches subsequent to the first batch for a total of four batches using the same initial dose of enzymes.

Analysis of Feedstock and Biodiesel

Determining Free Fatty Acids

The FFA content was determined by titration with KOH. This method is taken from the Acid Number Test defined in the ASTM Standard D6751: Standard Specifications for Biodiesel Fuel Blend Stock (B100) for Middle Distillate Fuels, specifically Test Method D664.

Determining Monoglycerides, Diglycerides, Triglycerides, Bound Glycerin

Gas chromatography (GC) analysis was used to analyze the amounts of mono-, di- and triglycerides in the samples, from which the total bound glycerin was calculated. The GC used was a HP 5890 Series 1 equipped with an open tubular column that was an Rtx-Biodiesel TG (15m x 0.32mm x 0.1 μ m) and an HP 7673 auto-sampler. The method and calculations used were based on the ASTM (2012) method D6584-2012: Standard Test Method for Determination of Total Monoglycerides, Total Diglycerides, Total Triglycerides, and Free and Total Glycerin in B-100 Biodiesel Methyl Esters by Gas Chromatography. This method functionalizes 0.1 g of biodiesel with 100 microliters of the silylating agent N-methyl-N-(trimethylsilyl)trifluoroacetamide (MSTFA), which converts the free hydroxyl groups the mono-, di-, and triglyceride into their more stable trimethylsilyl analogs, and is then followed by 100 μ L of the internal standard, tricaprin. This mixture was allowed to sit for 15 minutes, after which 8 mL of heptane was added. Approximately 1.5 mL of sample was transferred to a GC vial.

The temperature ramp for the GC oven was 50°C for 1 min, 15°C/min to 180°C, hold 0 min, 7°C/min to 230°C, hold 0 min, 30°C/min to 380°C, hold 8 min. The carrier gas was helium at a constant flow of 3.0 mL/min, the detector is a flame ionization detector (FID) at

400°C, hydrogen flow was at 35 mL/min, air was at 350 mL/min, He (make-up) was at 30 mL/min, and cool on-column injection with a sample size of 1 µL was used.

ChemStation software was used to identify and manually integrate peaks for mono-, di-, and triglycerides as well as the internal standard, tricaprins, peak. Using the previously established calibration curves for each class of compounds, the mass of the bound glycerin contributed by each type of glyceride (mono, di, tri) was calculated using Equation 3.2.

$$Gl_j = \left[\frac{W_{is2}}{a_{ol}} \right] \left(\left[\frac{A_{glj}}{A_{is2}} \right] - b_{ol} \right) \left[\frac{100}{W} \right] \quad (3.2)$$

where

- Gl_j = mass percentage of individual glyceride sample,
- A_{glj} = peak area of individual glyceride,
- A_{is2} = peak area of Internal Standard 2, Tricaprin,
- W_{is2} = weight of Internal Standard 2, mg,
- W = weight of sample, mg
- a_{ol} = slope of the calibration function for mono, di, or triolien, and
- b_{ol} = intercept of the calibration function for mono, di, or triolien.

The total bound glycerin is the summation of the glycerin contribution from the mono, di, and triglycerides, which are calculated using Equations 3.3, 3.4, and 3.5. The coefficients in these equations represent the average weight fraction of the glyceryl portion for each class of glyceride.

$$Gl_M = 0.2591 \times \sum \text{monoglyceride, mass \% determined in Eq. 3.2} \quad (3.3)$$

$$Gl_D = 0.1488 \times \sum \text{diglyceride, mass \% determined in Eq. 3.2} \quad (3.4)$$

$$Gl_T = 0.1044 \times \sum \text{triglyceride, mass \% determined in Eq. 3.2} \quad (3.5)$$

Determining Methanol

To determine if any methanol remained suspended in the final FAME layer, ASTM standard D93: Test Methods for Flash Point by Pensky-Martens Closed Cup Tester was used.

Analysis of Aqueous Phase

Determining Water

Moisture content of the aqueous phase used a Karl Fischer coulometric titrator produced by Metrohm International, which is typically used for samples with small amounts of water. Due to the fairly large amount of water in the aqueous phase, approximately 20-30%, the appropriate sample mass that could be analyzed was small and ranged from 12 mg to 15 mg.

Determining Glycerol

The glycerol content in the aqueous phase was determined using a rotary evaporator. The method used on a Buchi RotoVapor isolated the glycerol in a 100 g sample by vaporizing the methanol and water in the sample, and condensing it into a separate vessel. The equipment included a water bath to regulate temperature, a receiver flask connected to a vacuum gauge and a condenser. A pump connected to the condenser provided vacuum. The separation was performed in a 250 mL round-bottom, one neck flask. The temperature and pressure regiment started at 25 mbar and 25°C for 15 minutes, followed by 0 mbar and 50°C for 15 minutes and settled at 0 mbar and 80°C for two hours. The mass of the sample was taken at the 1, 1.5 and 2 hour mark. The mass percent glycerol was calculated as the final mass of the sample divided by the original mass of the sample

Additionally, the residual moisture content of the glycerol was acquired using the Karl Fisher methods described above.

Determining Methanol

Methanol content of the aqueous phase was calculated from the difference between the total sample and the glycerol plus water fraction. The considerations for discrepancy in this method include a possible low estimate of methanol amount due to losses from evaporation or methanol that may have stayed immersed in the FAME layer; a skewed result from enzyme in the aqueous phase in the SAPR batches; or incomplete vaporization of water in the RotoVapor method. Despite these possible discrepancies, this method gave a reasonable approximation of the aqueous phase composition.

Determining Enzyme Activity in Reduction and Permeate

To determine if any enzyme was extracted from subsequent reactions, a bench-scale mini-batch was conducted with the SAPR Reduction from each SAPR batch and TFF Permeate from each TFF batch. As this is the portion of the aqueous phase removed and not added to the subsequent batch the presence of enzyme (i.e., conversion of TG to FAME) indicated a loss of enzyme at that step in the series of four batches.

The bench-scale mini-batches reacted 40 g of virgin soybean oil with 8 g of SAPR Reduction or TFF Permeate and the amount of glycerol, methanol and water needed to reach the target compositions of 1.7 molar excess of methanol to TG, an aqueous phase of 20% by feedstock weight, composed of 40% water and 60% glycerol. The reaction was subject to transesterification conditions of 40°C and 300 RPM shaking via an SI-300 Incubated Shaker and was compared to three controls. Samples were taken at 2 hour, 6 hour, and 24 hour intervals and analyzed for total bound glycerin. The 24 hour sample was analyzed for FFA.

Filtration Performance

Data collected during the filtration processing time included recirculation rate (tangential velocity), inlet pressure, outlet pressure, temperature. Additionally, the permeate flux was calculated by timing the collection rate of 100 mL of permeate, and using Equation 3.1 to calculate the permeate flux. Collection of data was at random intervals, more frequently at the start of a filtration process and less frequently once the system had been operating for a while.

Chapter 4: FINDINGS AND DISCUSSION

Introduction

One aspect to remember when analyzing these data is the multitude of variables influencing the enzymatic biodiesel reactions and the complexity of their dependence upon each other. The findings presented here help to elucidate what is happening during an enzyme catalyzed biodiesel reaction and how this may affect the recovery and reuse of that enzyme.

An attempt was made to present the results and findings of these runs in a cascading progression of influential variables. The initial doses for both SAPR and TFF are first described, followed by an evaluation of efficacy for each technique, and ending with an analysis of the subsequent SAPR and TFF batches and how each reduction technique may have affected these batches. Because subsequent batches for both SAPR and TFF depend heavily on the experimental results of their respective previous batch, beyond the initial batches comparisons are only made between batches using the same reduction technique. In other words, comparisons were made between SAPR2, SAPR3 and SAPR4 and between TFF2, TFF3, and TFF4, but were not made between made between SAPR2 and TFF2.

Free Fatty Acid

The FFA content of the FAME throughout the reactions is an indicator for the state of equilibrium of the driving reactions in an enzyme catalyzed transesterification of TG to FAME. Those reactions are a hydrolysis reaction to convert glycerides into FFA followed by

the esterification or alcoholysis of FFA with methanol to produce FAME and water (Figure 4.1). As discussed in the Review of Literature, previous research proposes that these reactions follow a ping-pong bi bi mechanism.



Figure 4.1. Lipase transesterification involves hydrolysis followed by esterification.

At steady FFA levels, equal amounts of FFA are being produced from hydrolysis and being consumed by esterification. As shown in Figures 4.2 and 4.3, the FFA content quickly declined from an average starting amount of 8.92% until six hours into the reaction at which point the FFA effectively plateaus and there is only a slight decrease in FFA content level from 6 hours to the end of the 24 hour reaction window. The six hour point in the reaction is significant because it is the first data point after the completion of the five hour continuous methanol dosing and the entire methanol dose has been added to the reaction vessel by that point. FFA levels at the end of the 24 hour window for all batches (SAPR and TFF) range from 2.33% to 2.91%, a relatively modest difference. While water does play a role in these reactions as it is consumed and regenerated at presumably different rates, these data suggest that the methanol plays a more prominent role in reaching reaction equilibrium. This consistency in decline and end value indicates that all batches reached hydrolytic equilibrium in a similar time frame. Therefore, this metric, while offering insights about the enzymatic reaction equilibrium, does not play a role in the comparison of SAPR to TFF.

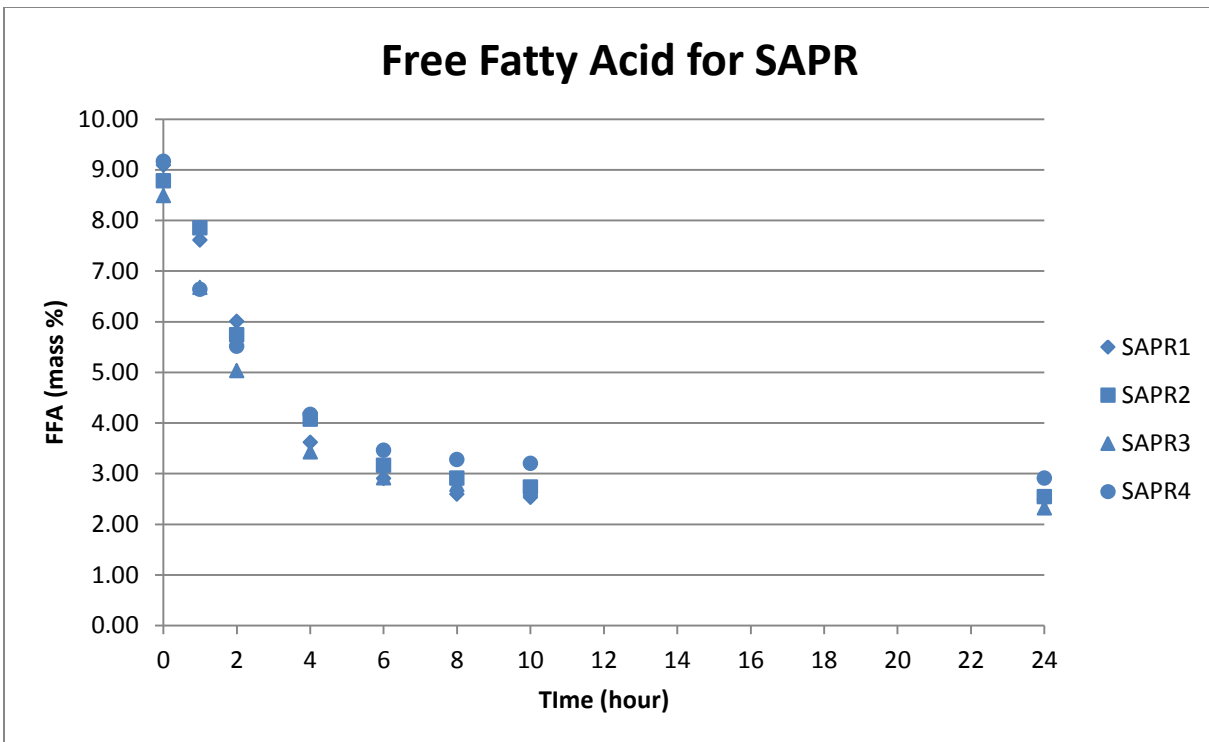


Figure 4.2. FFA content over the course of the initial reaction of the SAPR run.

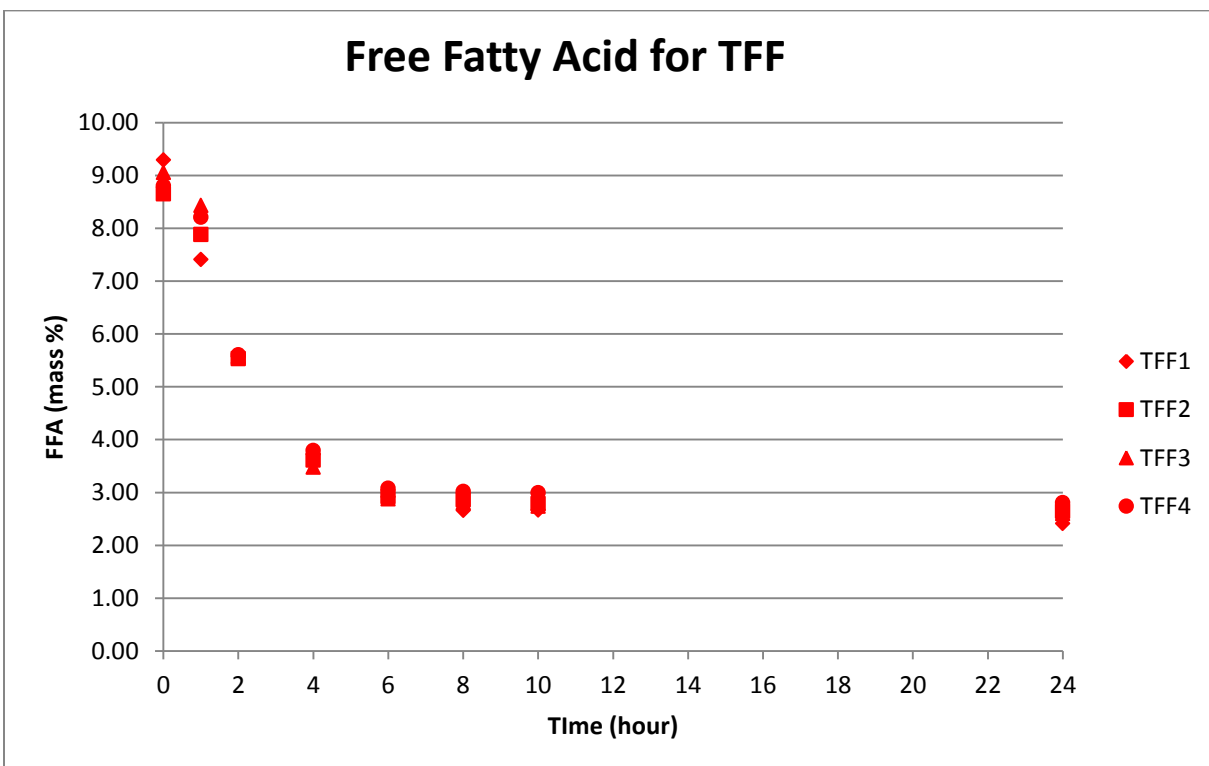


Figure 4.3. FFA content over the course of the initial reaction of the TFF run.

Initial Batches

The primary metric used to compare enzyme presence in both the initial batches and subsequent batches was the rate of bound glycerin (BG) consumed over the course of the reaction. The percent BG is the mass of the glycerin backbone from any mono-, di-, or triglycerides in a sample relative to the total mass present. For a batch of biodiesel to be within specifications according to ASTM standards, the percentage of BG must be less than 0.20%.

Because the rate BG is consumed directly correlates to the rate of the reaction and the activity of the enzyme is also directly correlated to the rate of the reaction, analysis of BG consumed is one good indicator of the active enzyme present in the reaction. The initial BG for all reactions was 8.02% as determined from analysis of the feedstock. Due to the rapid progression and the lack of equilibrium between the hydrolysis and esterification reactions, in conjunction with a lag time between collecting the sample and testing for BG at the 1, 2, and 4 hour data points, the BG experimentally determined for these points demonstrated poor precision and were deemed unreliable. Therefore, these points were not used in the derivation of a best fit model for BG at a given time.

In general the amount of BG consumed follows an exponential decline for all batches. The statistical analysis program JMP 10 was used to fit an exponential model to the 0, 6, 8, 10 and 24 hour data points that had been experimentally measured. A system of fitting two consecutive models was used to find a best fit model for determining BG at any time during the reaction: the first model determined the total BG consumed over the reaction and the second model used the calculated total BG consumed and the experimentally measured BG present at 24 hours to derive an exponential equation for each batch. The beauty of the JMP

program is that it allows the user to hold some variables in the proposed model constant while iteratively fitting the other variables in the model. In the models below, the variables with asterisks were iteratively fit while all other variables came from experimentally measured data.

1st Model:

$$BG = BG_{total}^* \times e^{rate^* \times time} + (8.02 - BG_{total}^*) \quad (4.1)$$

where $BG = BG$ at specified time

$BG_{total}^* = BG$ consumed over 24 hour reaction window

2nd Model:

$$BG = BG_{total} \times e^{rate^* \times time} + BG_{final} \quad (4.2)$$

where $BG = BG$ at specified time

$BG_{total} = BG$ consumed over 24 hour reaction window, determined from 1st Model

$BG_{final} = BG$ remaining at end of 24 hour reaction, difference of 8.02% and BG_{total}

The residual sum of squares error (SSE) is the objective that is minimized in fitting the model to the data. It is the error that is presented for each model fit to determine how well the model fit the data from each batch relative to one another.

Figures 4.4 and 4.5 show the model fit to all the data points collected for the initial SAPR batch and initial TFF batch. The SSE for the rate constant for the SAPR1 batch is 0.0165 and for the TFF1 batch is 0.0134.

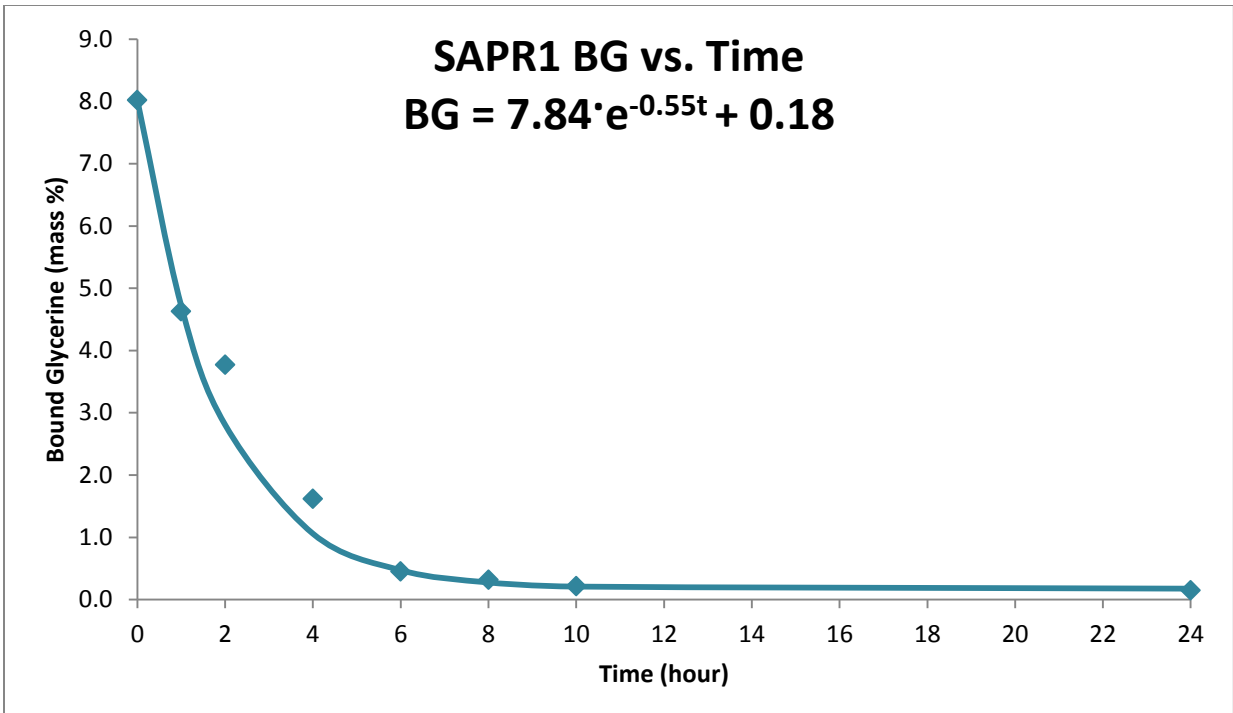


Figure 4.4. BG content over the course of the initial SAPR run. The model was fitted using only the 0, 6, 8, 10, and 24 hours. However, the less reliable 1, 2, and 4 data points were included in the plot to show the general overall trend.

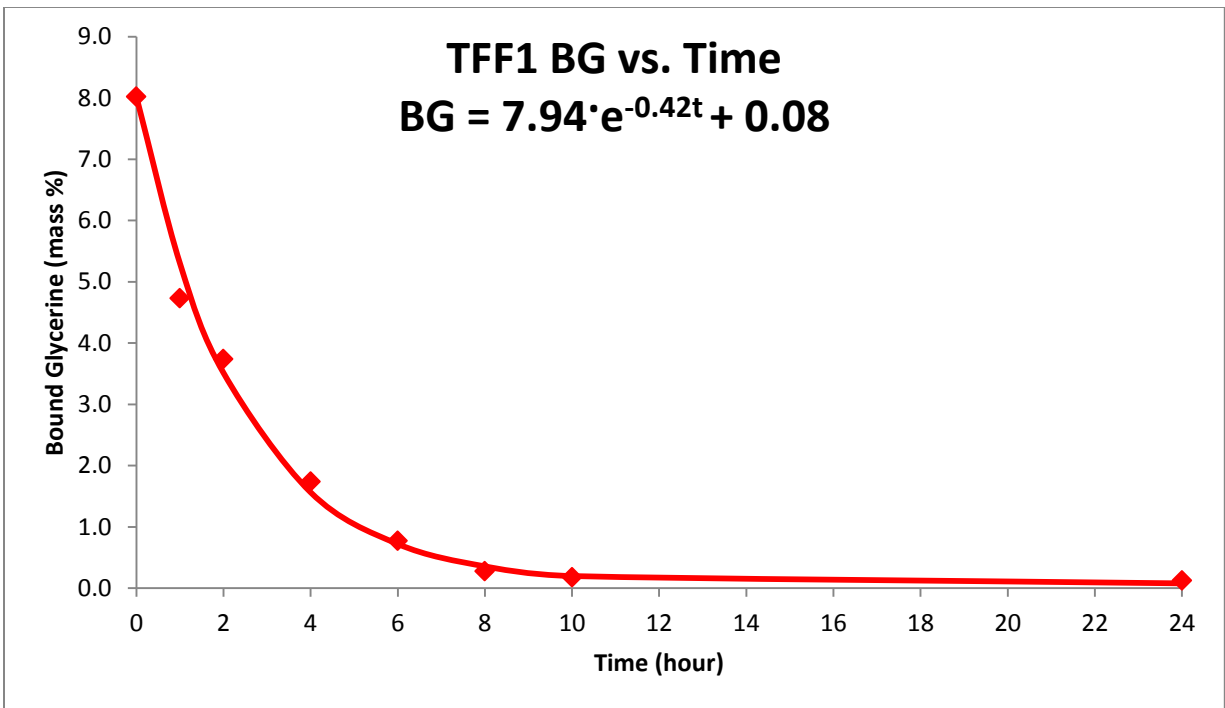


Figure 4.5. BG content over the course of the initial TFF run. The model was fitted using only the 0, 6, 8, 10, and 24 hours. However, the less reliable 1, 2, and 4 data points were included in the plot to show the general overall trend.

Both the recipe and reaction conditions for the initial batch for the SAPR run and TFF run were identical, therefore, the reaction kinetics and products were expected to be identical, within a small margin of error. A possible reason for the difference in rate of BG consumed was the discrepancy in methanol addition from the target methanol of 9.1 gallons. The initial SAPR batch was 0.92% in excess of the target methanol and the initial TFF batch was 1.24% below the target methanol. A more extensive analysis on the effect of methanol excess or deficiency on rate is discussed in another section below.

Selective Aqueous Phase Reduction

The SAPR Reduction volumes and the composition, as well as the separation times are listed in Table 4.1 for all SAPR batches. Based on the relatively quick stratification that was observed in previous bench scale experiments, the aqueous phase settling was expected to result in three distinct phases. After a 24 to 72 hour settling time, formation of only two distinct layers was observed. The top layer consisted of any FAME that remained suspended in the aqueous phase after the initial 2.5 hours and removal of the bulk of the FAME and a bottom layer of a glycerol heavy phase that also contained any excess of unreacted methanol and water. A more viscous middle layer was expected to form where the majority of the active enzyme would aggregate due to its attraction to the polar/non-polar or more specifically, aqueous phase/FAME interface. However, none of these pilot-scale batches had a distinct middle layer as was expected. The approximately 3,500 fold increase in volume from bench-scale to pilot-scale may have required longer than anticipated settling times. The larger volume of aqueous phase and the decrease in ratio of interface area to aqueous phase volume diminished the attraction of the enzymes to the interface and increased the distance through the aqueous phase the enzymes must travel to aggregate at the interface.

Additionally, the properties of the DDG corn oil used as feedstock may have influenced the migration of enzymes to the aqueous phase/FAME interface.

There is some indication that a portion of the enzymes migrated to the interface, as described below with the SAPR1 Reduction. However, this lack of distinct middle layer leads to ambiguity about how much of enzymes migrated to the interface (an important aspect influencing the effectiveness of the SAPR technique) versus the portion that remained suspended in the aqueous phase. The tests for enzyme activity in the SAPR Reduction (defined in this case as the material removed from the aqueous phase of a SAPR or TFF batch), described in more detail in a later section show that at least a portion of the active enzyme remained suspended.

Table 4.1. SAPR Reduction Content

	Hours for Separation	Aq. Phase Reduction	MeOH Content (mass %)	Glycerol Content (mass %)	Water Content (mass %)
SAPR1	26	6.0 gal	20.4%	60.3%	19.3%
SAPR2	41.5	6.2 gal	21.0%	55.3%	23.7%
SAPR3	46	5.6 gal	21.7%	56.2%	22.1%
SAPR4	47	NA	16.5%	58.6%	24.9%

A longer separation time for SAPR2 and SAPR3 compared to SAPR1 was due in part to the fact that after the 6.0 gallons of SAPR Reduction from SAPR1 sat in the laboratory for an additional 24 hours, a noticeable skim of enzymes formed. This enzyme was lost to subsequent reactions, whereas if the entire aqueous phase had been allowed adequate separation time, may have migrated to the aqueous phase/FAME interface and been retained in the SAPR permeate and thus added to the SAPR2 batch. This thin layer of enzymes was skimmed from the surface of the SAPR1 Reduction and added back to the SAPR run at the start of the SAPR3 batch. This discrepancy in method affected the rate of BG consumed

during SAPR2, but should not impact the overall decrease in enzyme activity, as it was added back to the SAPR run by SAPR3.

Another observation made of the aqueous phase was an increase in red pigmentation as batch numbers progressed. This difference can be seen in the comparison of samples from SAPR1 versus SAPR4 in Figure 4.6. Both of these phenomenon, the longer than expected separation time and pigmentation of the aqueous phase, could be due to the distillers dry grain (DDG) corn oil that made up 50% of the feedstock. Physical properties of the corn oil that may influence these include its reddish color and the fact that it was not degummed, both properties diverge from those of soy bean oil or yellow grease used at Piedmont Biofuels for previous experiments with enzymatic biodiesel production.

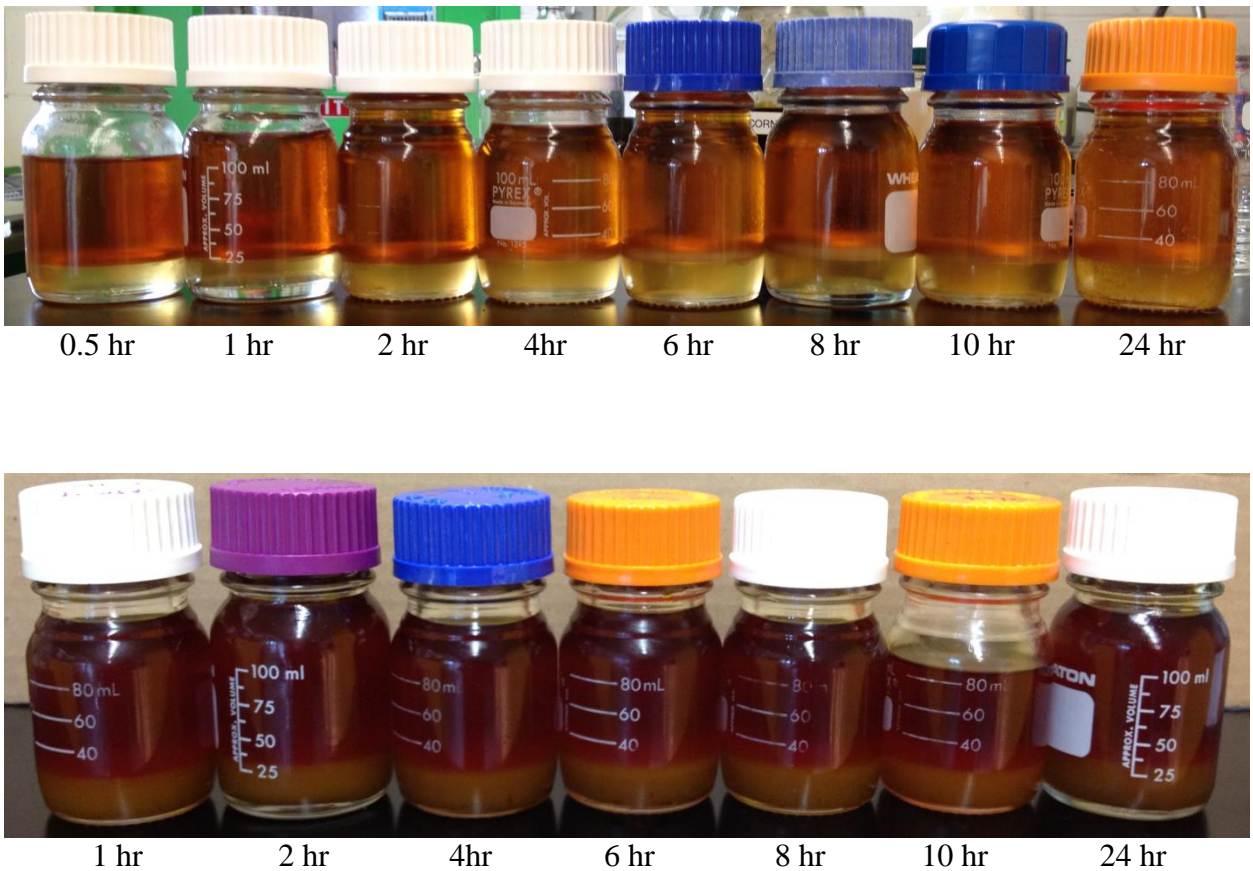


Figure 4.6. Samples from SAPR1 (top) versus SAPR4 (bottom).

Tangential Flow Filtration

The filtration times, the total volume of aqueous phase filtered, flow rate and flux of the TFF Permeate are listed in Table 4.2. Most noticeable in this table is the drastic increase in filtration time between TFF1 and TFF3. Because the filtration process had not been fully optimized for the specific *Thermomyces lanuginosus* lipase used, molecular weight cut-off of 10 kD for the filtration membrane was used to retain the approximately 30 kD enzyme. This MWCO turned out to be a highly conservative choice, and contributed to a diminishing permeate flux due to increased gel layer formation on the membrane surface as batches progressed. As enzymes deactivate and denature, they tend to aggregate. These large molecular clusters along with large, sticky molecular contaminants in feedstock from the DDG corn oil may have contributed to the formation of the gel layer on the membrane in the later TFF batches.

Table 4.2. *TFF Permeate Flux*

	Hours for Filtration	Aqueous Phase Filtered (Liters)	Permeate Flow Rate (L/hour)	Flux (LMH: L/m ² ·hour)
TFF1	14	23.2	1.7	8.7
TFF2	21	26.6	1.3	6.7
TFF3	43	24.3	0.6	3
TFF4	NA	NA	NA	NA

The filtration times, the volumes of total aqueous phase filtered, and compositions of the TFF Permeate (defined as the removed material for the TFF batches) are listed in Table 4.3. For TFF2 and TFF3 excess aqueous phase was filtered than was needed, and therefore, a portion of the TFF Retentate was added back to the TFF Permeate to ensure the appropriate amount of permeate was used to catalyze the subsequent batch.

Table 4.3. TFF Permeate Content

	Hours for Filtration	Permeate		MeOH Content (mass %)	Glycerol Content (mass %)	Water Content (mass %)
		Aqueous Phase Filtered (gallons)	Aq. Phase Removed (gallons)			
TFF1	14	6.1	6.1	18.9%	56.5%	24.6%
TFF2	21	7	5.4	16.6%	58.6%	24.7%
TFF3	43	6.4	5.9	18.4%	55.4%	26.2%
TFF4	NA	NA	NA	NA	NA	NA

The preliminary optimization work of the filtration system described in Chapter 3 was completed by SmartFlow Technologies with a mock aqueous phase comparable to the methanol, glycerol and water contents of the TFF aqueous phases prior to this research. The recommended parameters were a tangential velocity or recirculation rate between 12 - 15 L/min and a target transmembrane pressure between 55 psi and 65 psi. This optimization was aimed to result in an LMH (liters/m²/hour) that was sufficient to reduce the aqueous phase by approximately 20% in a reasonable amount of time (less than 12 hours). Between 9 and 16 data points were collected at random time periods during the runs. A summary of these data are presented in Table 4.4.

In an effort to increase the LMH of TFF2 and TFF3 and thus speed up the filtration process, the recirculation rate was increased. This increase in flow rate naturally increased the temperature of the viscous aqueous phase fluid moving through the narrow channels beyond the 40 °C limit recommended for the *Thermomyces lanuginosus* lipase used. The increase in temperature and extended filtration time were abuses suffered by the enzyme that likely led to a decrease in enzyme activity for subsequent TFF batches.

Table 4.4. TFF Parameters

		TFF1	TFF2	TFF3
Recirculation Rate (L/min)	Avg	10.6	10.2	14.4
	Min	6.5	6.3	11.6
	Max	12.7	13.6	16.7
Transmembrane Pressure (psi)	Avg	63.3	63.0	65.5
	Min	61.2	55.0	62.5
	Max	65.1	68.8	68.6
Temperature	Avg	33.2	36.3	36.9
	Min	24.0	27.0	34.0
	Max	38.0	45.0	38.0 ^a

^aDue to the long filtration time required, the TFF unit was run over night, and temperatures were not checked at regular intervals. Therefore, temperatures most likely exceeded the 38°C listed.

Enzyme Activity in Permeate

An important property by which the efficiencies of SAPR and TFF are evaluated is their ability to retain active enzymes in the aqueous phase retentate that is used to catalyze subsequent reactions. Lab scale mini batches were run using the aqueous phase permeates as catalysts. While this does not give the full picture of how much active enzyme is left in the retentate (some enzyme may have been retained, but deactivated), it does give some insight as to how much enzyme did not make it into the retentate either during the aqueous phase reduction process or the filtration process.

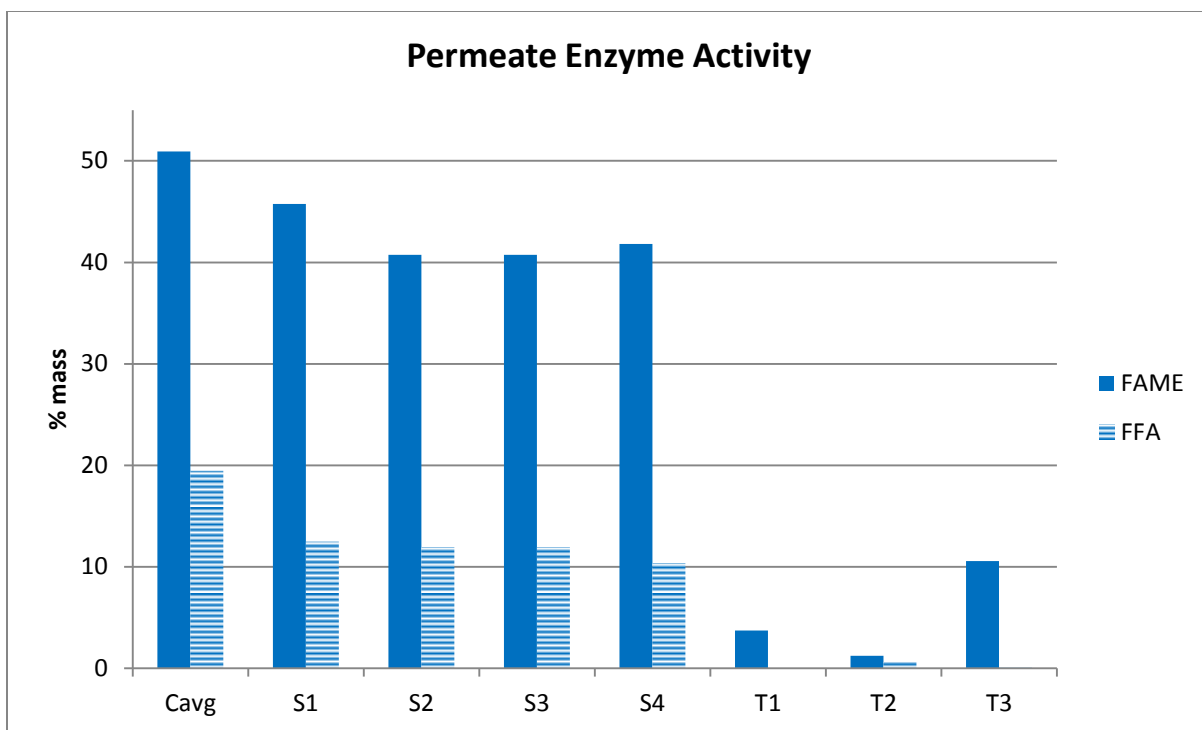


Figure 4.7. Enzyme activity in SAPR and TFF Permeates based on FFA and FAME

Because the feedstock for these batches was virgin soy oil, FAME content could be approximated by the difference of total reaction mass and glycerides and FFA present post reaction. As evident from the Figure 4.7, in general the SAPR permeate contained a substantial amount of enzyme, resulting in conversion of TGs to FFA via hydrolysis and ultimately to FAME via esterification. This supports the conclusion that at least a portion of the enzyme remained suspended in the aqueous phase rather than stratifying into a distinct middle layer after settling. This affects the efficiency of the SAPR method because it shows that enzymes were being drawn off in the SAPR Reduction and discarded, slowing down the rate of reaction for subsequent batches.

In contrast, the low production of FFA and FAME content of the TFF indicates that the TFF Permeates did not contain a substantial amount of enzyme. This is most notably shown by the FFA levels falling between 0.0 and 0.6%. However, there was an unexpected

increase in FAME in the TFF3 permeate. However, this FAME may be residual FAME in the aqueous phase from the TFF3 reaction that was not completely drained off prior to filtration or this could be the 90% efficiency associated with a MWCO value for most ultrafiltration membranes.

Reuse Batches

As with the initial batches, the primary metric used to compare enzyme presence in subsequent batches was the rate of BG consumed over the course of the reaction. A model was fit for each reaction in the same manner as it was for the initial batch. The point at which comparisons became most meaningful was after all the methanol has been added to the reaction vessel and equilibrium was reached between the hydrolysis and esterification reactions. The rate BG consumed at this point is most indicative of the amount of enzyme catalyzing the reaction in contrast to the first hours of the reaction when it was difficult to determine if the rate of BG consumption was a result of methanol dosing discrepancies or the amount of enzyme present.

Methanol discrepancy.

Table 4.5 shows the discrepancy in methanol addition from the target total methanol of 9.1 gallons for each reaction. In general the SAPR batches more consistently had an under-dosing of methanol beyond the initial batch; contrarily, the TFF batches had a consistent excess of methanol beyond the initial batch. It is difficult to pin point the exact effect these methanol discrepancies had on the BG consumption rate. A shortage of methanol to the point where it was a limiting factor in the esterification reaction, would have slowed down the overall BG consumption. While a slight excess of methanol may have contributed to a faster esterification reaction, an over-excess of methanol can deactivate the enzyme and

result in a slower reaction due to less enzymes catalyzing the overall reaction.

Additionally, the amount of methanol present in each batch may have been underestimated based on the fact that the aqueous phase retentates were left partially open to the environment post settling or filtration. This may have resulted in evaporative losses of methanol from the aqueous phase post determination of aqueous phase content.

Table 4.5. *Methanol Discrepancies in SAPR and TFF Runs*

SAPR1	0.92%	TFF1	-1.24%
SAPR2	-6.97%	TFF2	1.14%
SAPR3	-5.65%	TFF3	5.67%
SAPR4	-1.80%	TFF4	4.50%

SAPR reactions.

Figures 4.8 shows the SAPR reaction model from the completion of methanol dosing at the 5-hour mark to the 24-hour mark, and Figure 4.9 focuses on that portion of data where the greatest decrease in activity is occurring, between the 5-hour and 10-hour data points.

Based on these figures, we see there was an obvious decrease in BG consumed for each subsequent batch. Each reuse batch at five hours has a slightly higher level of BG. This trend, in conjunction with FFA levels being consistent between initial and reuse batches at the 5-hour point, suggests a slower overall reaction rate and thus a loss of active enzymes. Table 4.6 and Figure 4.12 presents the models calculated for each reaction and the decrease in BG consumption rate between each batch and a total rate decrease of 72.7% from the initial batch to SAPR4. The model fitting process for reuse batches became more difficult and the models calculated were less reliable as shown in the increase of SSE. However, the fitted models combined with the knowledge of what is happening in the reaction give an adequate representation and means of comparison of active enzymes between batches.

The very large decrease between SAPR1 and SAPR2 may be influenced by the skim of enzyme formed on the aqueous phase permeate of SAPR1 that was not re-introduced to the run until SAPR3, as was discussed in the above SAPR section of this report. Beyond SAPR1, the BG at 24 hours for the batches did not meet ASTM (2012) specs of below 0.24% mass.

Table 4.6. SAPR Model and Rate Decrease with Associate Residual Sum of Squares Error

	SSE	Model	Rate Decrease
SAPR1	0.0032	$7.84 * e^{-0.546t} + 0.176$	
SAPR2	0.0026	$7.81 * e^{-0.213t} + 0.210$	61.0%
SAPR3	0.0911	$7.63 * e^{-0.178t} + 0.395$	16.4%
SAPR4	0.1735	$6.98 * e^{-0.149t} + 1.04$	16.3%
Total			72.7%

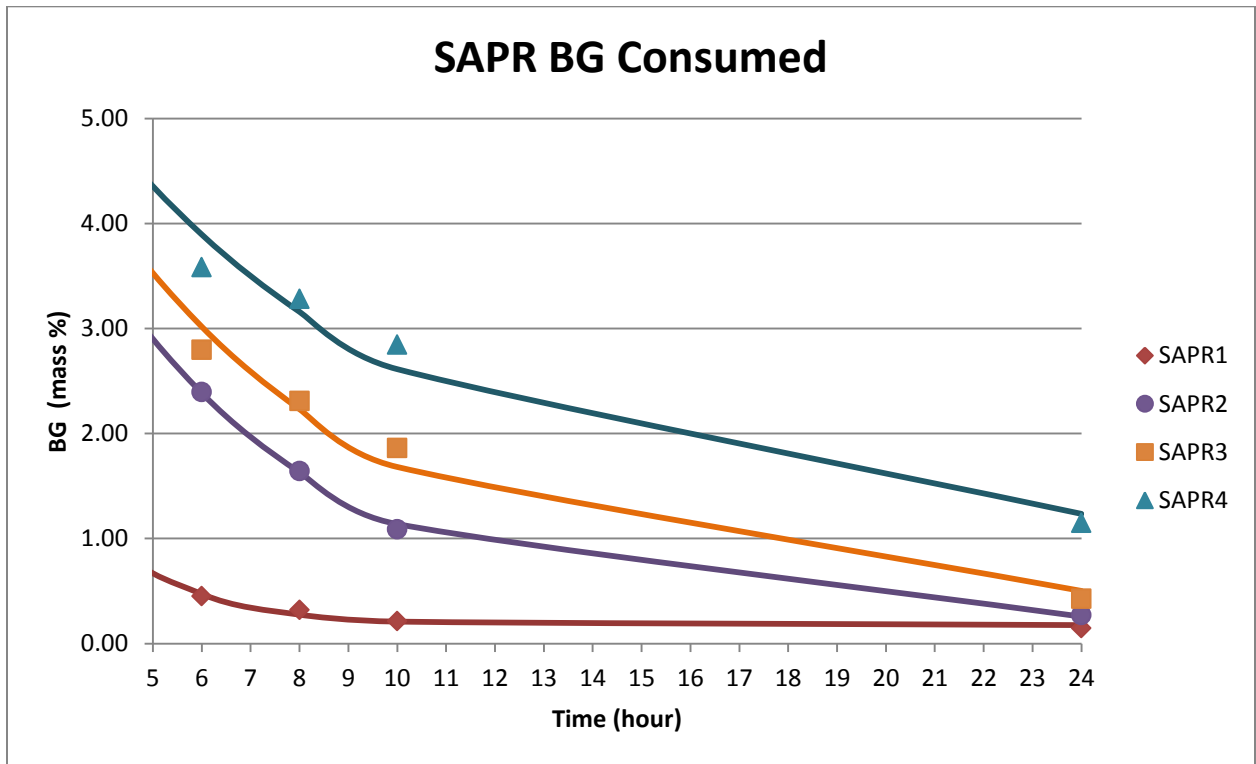


Figure 4.8. Rate of BG consumption post methanol dosing to 24 hour point for SAPR run.

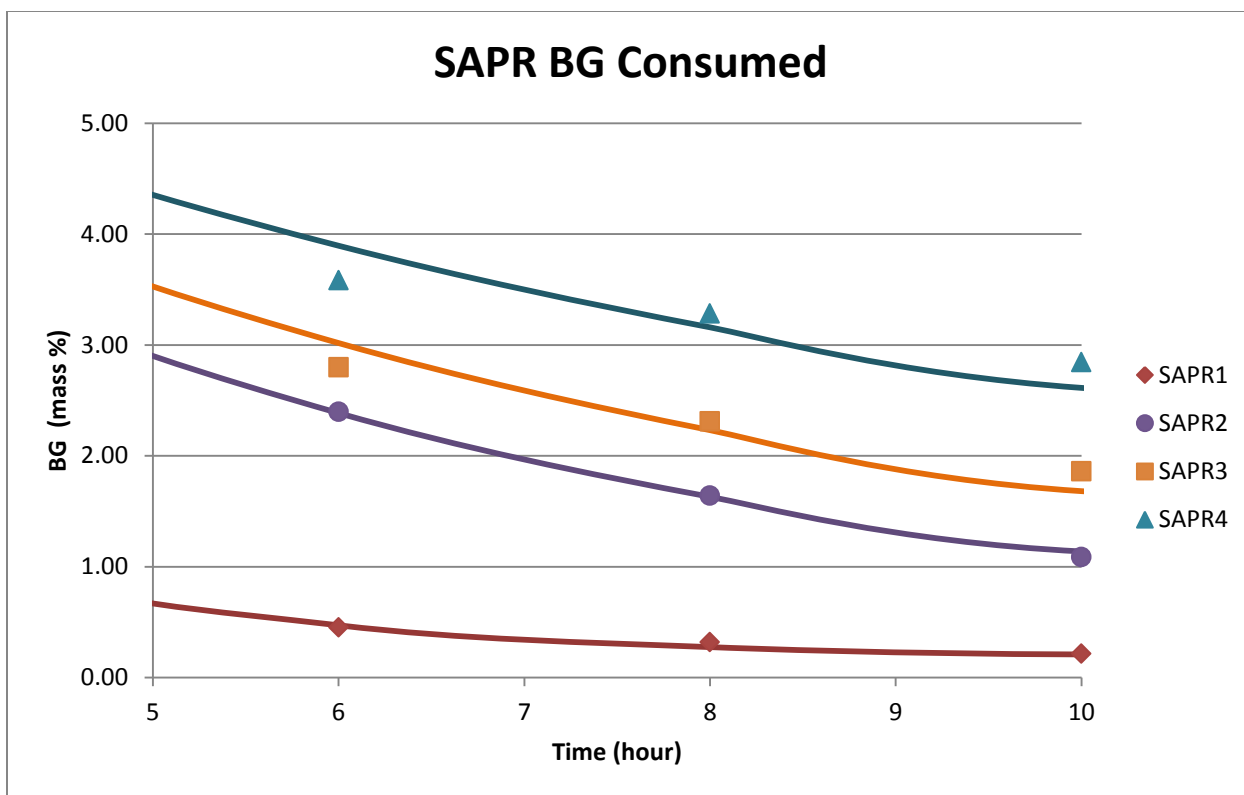


Figure 4.9. Rate of BG consumption post methanol dosing to 10 hour point for SAPR run.

TFF reactions.

Figure 4.10 shows the TFF reaction model from the completion of methanol dosing at the 5-hour mark to the 24-hour mark, and Figure 4.11 focuses on that portion of data where the greatest decrease in activity is occurring, between the 5-hour and 10-hour data points.

Fitting a model to the BG data points in the TFF batches was more reliable than for the SAPR batches, and the resulting total decrease in BG consumption rate was 46.8%, shown in Table 4.7 and Figure 4.12. The BG at 24 hours for all TFF batches fell below the ASTM (2012) spec of 0.24%. While there was some loss of enzyme activity in the TFF reuse batches, it is evident that the overall loss was less than in the SAPR reuse batches. It should also be noted that the greatest loss of enzyme activity appeared in the later TFF3 and TFF4 batches at which point the lengthy filtration process and increased temperatures during filtration may have been the main culprit in enzyme deactivation. This suggests that the

filtration process may not be flawed, but that batches run on an optimized process with the correct membrane size would be needed to better determine the effectiveness of TFF.

Table 4.7. TFF Model and Rate Decrease with Associate Residual Sum of Squares Error

	SSE	Model	Rate Decrease
TFF1	0.0115	$7.94 * e^{-0.419t} + 0.078$	
TFF2	0.0013	$7.89 * e^{-0.390t} + 0.128$	6.9%
TFF3	0.0007	$7.89 * e^{-0.313t} + 0.128$	19.7%
TFF4	0.0110	$7.85 * e^{-0.223t} + 0.172$	28.8%
Total			46.8%

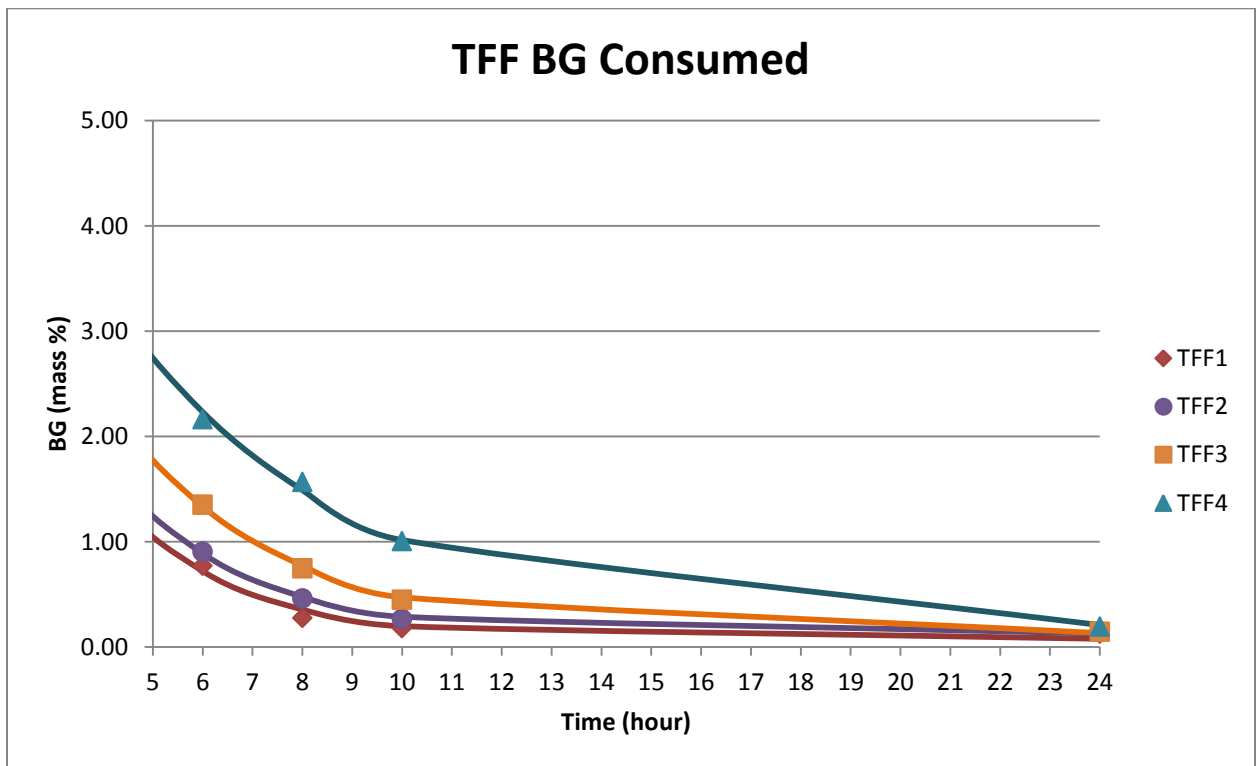


Figure 4.10. Rate of BG consumption post methanol dosing to 24 hour point for TFF run.

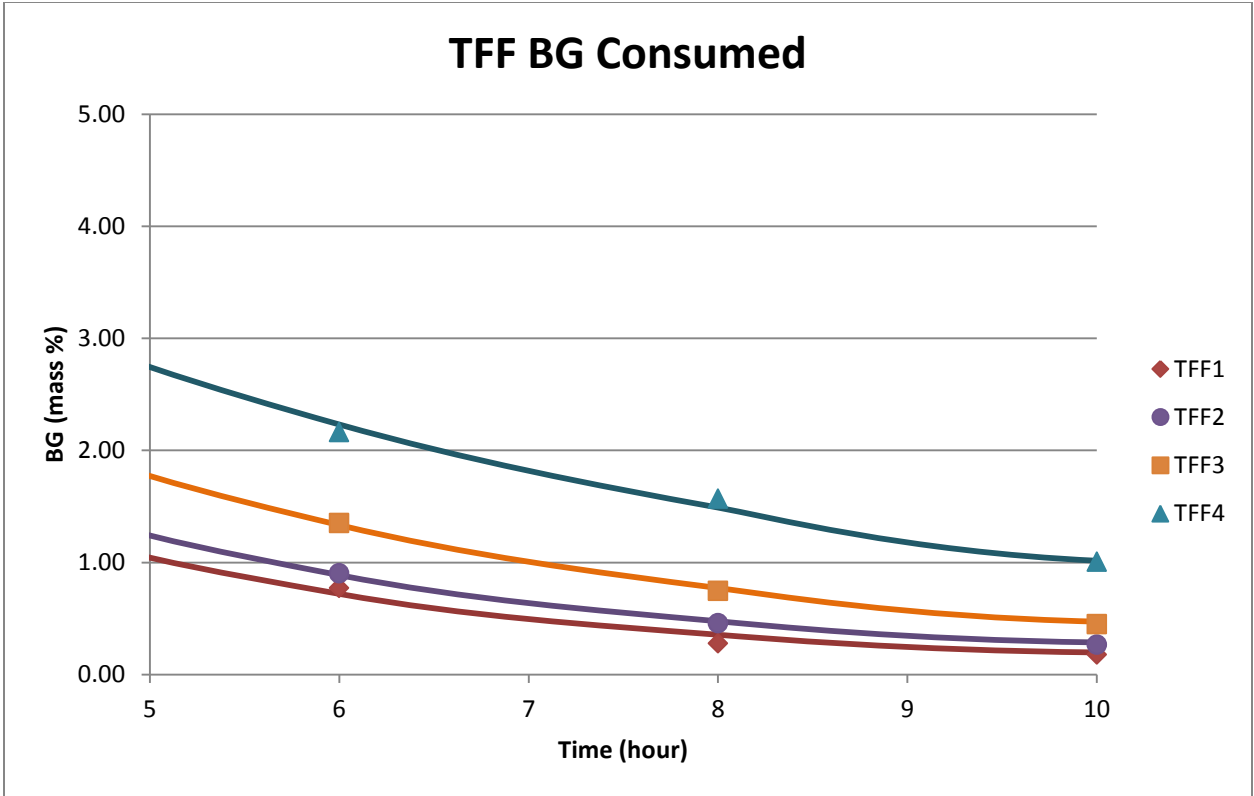


Figure 4.11. Rate of BG consumption post methanol dosing to 10 hour point for TFF run.

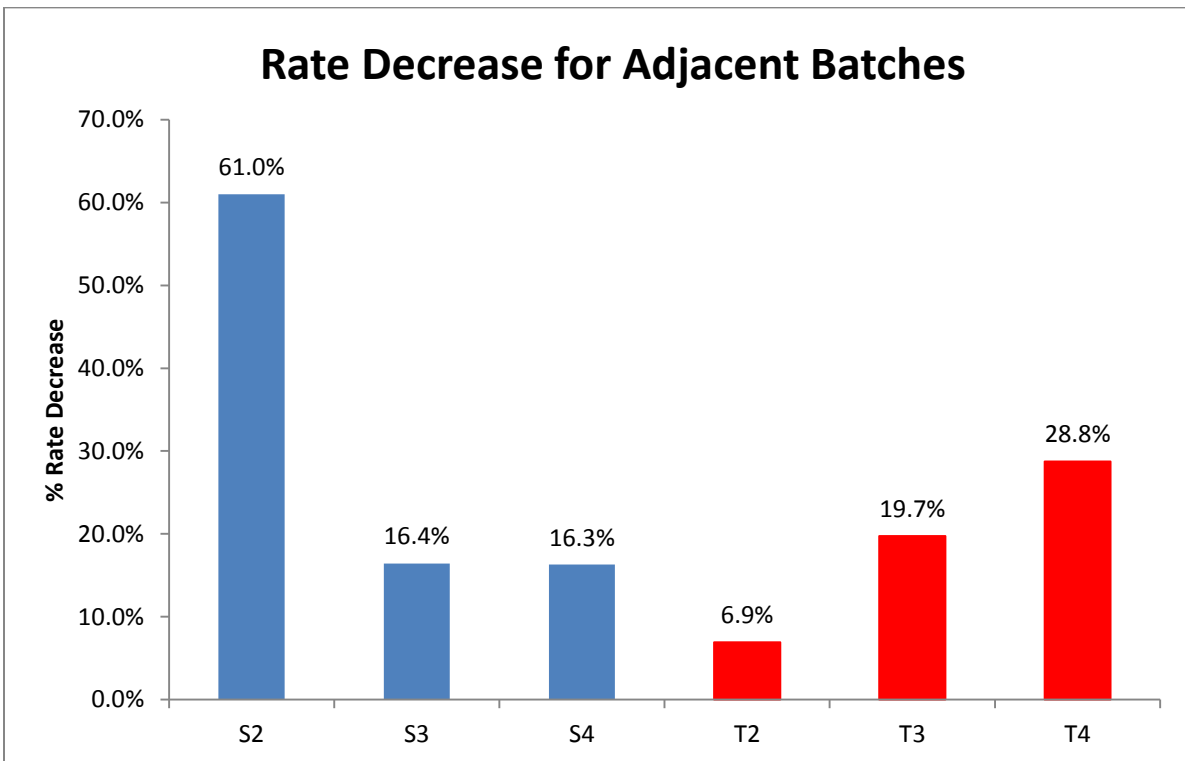


Figure 4.12. Rate decrease between adjacent batches for SAPR and TFF runs.

The overall rate decrease of bound glycerin consumption that was indicative of loss of enzyme activity from initial batch to final batch for both runs is compared in Figure 4.13. The loss of enzyme activity, as indicated by the rate decrease, is correlated to the settling time for the SAPR run and the filtration time for the TFF run. For the SAPR run, the general trend showed an indirect correlation where the longer the batches settled the smaller the rate decrease in the subsequent batch. This indicated that longer settling times allowed for more enzymes to concentrate at the aqueous phase/FAME interface, resulting in fewer enzymes lost in the SAPR Reduction, and therefore more enzymes remained in the SAPR Retentate to catalyze the subsequent batch. For the TFF run, the trend showed a direct correlation where the longer the filtration time, the greater the rate decrease in subsequent batches, indicating a greater loss of enzymes during longer filtration sessions. This may be due to an increase in abuses suffered by the enzyme during longer filtration sessions, particularly in the form of increased temperatures.

FAME Production

The FAME yield for both the initial SPAR and TFF batches was 97%. As the enzyme was recovered and reused, there was a greater loss in FAME yield for the SAPR batches than for the TFF batches. This is seen in the performance curve for the enzyme shown in Figure 4.14 where the FAME yield for SAPR decreases to 91% by the fourth batch, and TFF maintains a FAME yield of 96% by the fourth batch.

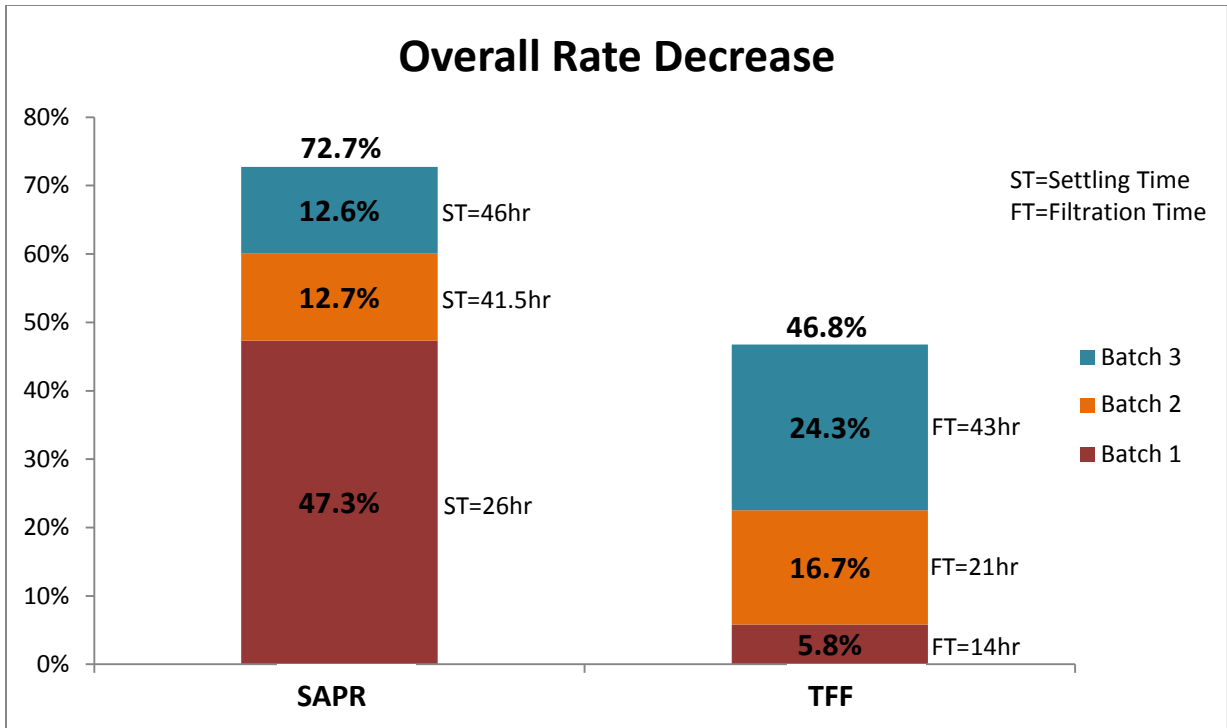


Figure 4.13. Overall rate decrease from initial to final batches SAPR and TFF runs. There is an indirect correlation between settling time and rate decrease and a direct correlation between filtration time and rate decrease.

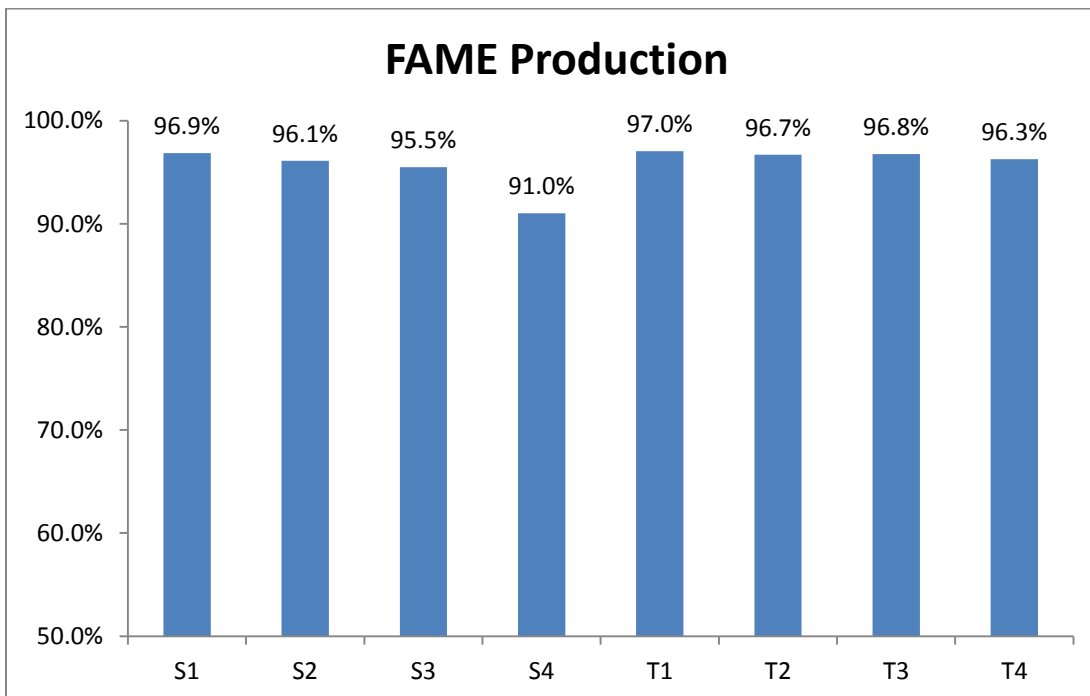


Figure 4.14. The performance curve for the enzyme indicates a greater loss of enzyme activity, therefore less FAME production, over the SAPR run versus the TFF run.

Chapter 5: CONCLUSIONS

Research Hypothesis

Tangential Flow Filtration (TFF) is a more effective method for the recovery of active, liquid enzymes from the transesterification of waste vegetable oil with up to 10% free fatty acid (FFA) into fatty acid methyl esters (FAME) catalyzed by a commercially available formulation of the enzyme *Thermomyces lanuginosus* lipase as compared to the simpler separation technique of selective aqueous phase reduction (SAPR).

Introduction

In determining if the findings support or reject the hypothesis, the primary metrics used were how much active enzyme is recovered in the retentate after each reduction technique and the rate of bound glycerin consumption in batches subsequent to the initial. The general trend of the data showed that while both SAPR and TFF retained active enzymes, and were thus able to catalyze subsequent batches, TFF was more effective than SAPR. While the findings from this research support this, the feasibility of implementing the use of liquid enzymes in the commercial production of biodiesel needs further discussion.

Implications for Enzyme Use in Biodiesel Production

The goal of this research was to contribute novel information to aid in the adoption of enzyme catalysts for the production of biodiesel on a commercial scale. Therefore, the effectiveness of the recovery and reuse of enzymes and the variances from bench-scale to

pilot-scale that arose were of particular interest. Effectiveness is based on the quantity of active enzyme recovered to catalyze subsequent batches as well as the time required to settle and/or filter the aqueous phase. These factors were examined in the context of the influence they have on the economic feasibility of using liquid enzymes as a catalyst.

In the scale-up from the bench-scale trials that used 8g (approx. 9 mL) of feedstock to pilot-scale batches that used 42 gallons (approx. 159 L) of feedstock, the phase separation was affected. The bench-scale batches quickly separated (within 2 minutes) into three distinct phases, giving a basis for considering gravity settling as an option to recover enzymes. However, the actual settling time was much longer in the pilot-scale batches (up to 72 hours), and a distinct middle enzyme-rich layer that could easily be retained did not form. More research should be conducted to elucidate why this occurred and possible techniques to increase the rate of separation.

While the TFF technique of enzyme recovery was more effective at recovering active enzymes, the filtration process took a considerable amount of time. This was due most likely to the conservative MWCO of 10 kD that resulted in gel layer formation. This gel layer formation in turn affected the transmembrane pressure, permeate flux rate, and, perhaps most detrimentally, it increased temperatures in the system causing deactivation to the thermally sensitive enzyme.

In an attempt to further optimize the use of TFF in this application, SmartFlow Technologies and Piedmont Biofuels filtered the aqueous phase from TFF4 using larger MWCOs and analyzed the permeate for enzyme activity. MWCOs of 30 kD and 100 kD were used and provided similar enzyme retention with greatly increased filtration rates. This implies that filtration sessions could be significantly shortened without risking thermal

deactivation of the enzymes. While further optimization of the membrane and filtration system will make TFF more feasible for commercial producers, determining the overall feasibility requires the cost of the filtration unit being weighed against the effectiveness of enzyme recovery and reuse.

Suggestions for Further Research

Techniques for enzyme recovery besides the two analyzed in this thesis should be considered for the recovery of liquid enzymes. For example, reacting multiple batches of biodiesel before any attempt to reduce aqueous phase would presumably ensure all active enzyme in the aqueous phase was recycled to the subsequent batch and it would avoid the abuse that the enzyme receives in the filtration process. This technique would require larger reactor volumes, as the aqueous phase would continually grow, and it may disrupt the equilibrium, but its possibility as a successful and economical enzyme recovery and reuse technique make this worthwhile research.

Optimization of batch recipe may improve the recovery of active enzyme, particularly in regard to the methanol dosing scheme. As discussed in Chapter 2, methanol is an enzyme inhibitor; therefore, the quantity of methanol in the reaction mixture at any one time has implications on the rate of the overall reaction. Methanol dosing schemes that have variable rates of delivery may better balance the reaction equilibrium and the enzyme inhibition.

Feedstock properties may also play a role in the effectiveness of enzyme recovery. In this research, the DDG corn oil that was used may have contributed to the lack of formation of an enzyme layer and thus the effectiveness of the SAPR technique. Additionally, contaminants in the feedstock may have contributed to a gel layer formation on the membrane. Other low quality, high FFA lipids are available as feedstocks for biodiesel

production, and may improve the SAPR and/or TFF techniques for active enzyme recovery. In addition, these feedstocks may be cheaper, and would further improve the economics feasibility.

Final Remarks

Liquid or soluble lipases have been used to catalyze the reactions that convert lipid feedstocks to biodiesel with promising results. Research has shown lipases to produce high FAME yields using lower quality, higher FFA feedstocks, require less downstream purification or biodiesel and co-products, and react under milder conditions compared to traditional acid or base catalysts. Combined with the prospect of producing technical grade glycerol, a higher value co-product, lipases have the potential to be a more economical option for biodiesel producers. The primary reason for looking to liquid lipases compared to immobilized is also driven by economics, as liquid lipases are significantly less expensive.

The major drawback of liquid lipases is the difficulty in their recovery and reuse. This research has taken the initial steps of analyzing techniques that can effectively and efficiently recover liquid lipases so they can be recycled and used to catalyze multiple batches. The use of ultrafiltration as well as gravity settling showed potential, although further studies are required to optimize these systems. While the use of ultrafiltration was more effective, it must be weighed against the capital equipment costs. This research focused narrowly on these two processes for making liquid lipases more economically advantageous. A larger body of research on processes and recovery technologies for liquid lipases in the production of biodiesel should be amassed to get a full picture of available, economically viable options. The impact of this study on the production of biofuels could be widespread if it allows the

industry to move closer to using lipases, a more environmentally benign, energy efficient and economically profitable catalyst for biodiesel production.

REFERENCES

- Abdel-Latif, M. (2010). *Membrane based bioseparation*. The Islamic University of Gaza. Retrieved from <http://www.monzir-pal.net/Bioseparation/Contents/Membrane%20based%20bioseparation%20chapter.pdf>
- Akoh, C. C., Chang, S. W., Lee, G. C., & Shaw, J. F. (2007). Enzymatic approach to biodiesel production. *Journal of Agricultural and Food Chemistry*, 55(22), 8995-9005.
- Al-Zuhair, S. (2006). The effect of substrate concentrations on the production of biodiesel by lipase-catalysed transesterification of vegetable oils. *Journal of Chemical Technology and Biotechnology*, 81(3), 299-305.
- Al-Zuhair, S., Almenhali, A., Hamad, I., Alshehhi, M., Alsuwaidi, N., & Mohamed, S. (2011). Enzymatic production of biodiesel from used/waste vegetable oils: Design of a pilot plant. *Renewable Energy*, 36(10), 2605-2614.
- Al-Zuhair, S., Dowaidar, A., & Kamal, H. (2009). Dynamic modeling of biodiesel production from simulated waste cooking oil using immobilized lipase. *Biochemical Engineering Journal*, 44(2-3), 256-262.
- Al-Zuhair, S., Jayaraman, K. V., Krishnan, S., & Chan, W. H. (2006). The effect of fatty acid concentration and water content on the production of biodiesel by lipase. *Biochemical Engineering Journal*, 30(2), 212-217.
- Al-Zuhair, S., Ling, F. W., & Jun, L. S. (2007). Proposed kinetic mechanism of the production of biodiesel from palm oil using lipase. *Process Biochemistry*, 42(6), 951-960.
- ASTM Standard D-6751-12. 2012. *Standard specification for biodiesel fuel blend stock (B100) for middle distillate fuels*. West Conshohocken, PA: ASTM International.
- Bender, M. L., & Brubacher, L. J. (1973). *Catalysis and Enzyme Action*: Michigan: McGraw-Hill Book Company.
- Brady, L., Brzozowski, A. M., Derewenda, Z. S., Dodson, E., Dodson, G., Tolley, S., . . . Menge, U. (1990). A Serine Protease Triad Forms the Catalytic Center of a Triacylglycerol Lipase. *Nature*, 343(6260), 767-770.
- Burton, R., & Austic, G. (2011). *FAeSTER enzymatic biodiesel process*. Piedmont Biofuels. Retrieved from <http://www.biofuels.coop/wp-content/uploads/2011/01/2012-FAeSTER-Letter1.pdf>

- Burton, R., & Fan, X. (2009). Recent development of biodiesel feedstocks and the applications of glycerol: a review. *The Open Fuels & Energy Science Journal*, 2, 9.
- Chen, J.W., Du, W., & Liu, D. H. (2008). Effect of several factors on soluble lipase-mediated biodiesel preparation in the biphasic aqueous-oil systems. *World Journal of Microbiology & Biotechnology*, 24(10), 2097-2102.
- Chen, X. & Wu, W. T. (2003). Regeneration of immobilized *Candida antarctica* lipase for transesterification. *Journal of Bioscience and Bioengineering*, 95(5), 466-469.
- Echavarria, A. P., Ibarz, A., Conde, J., & Pagan, J. (2012). Enzyme recovery and effluents generated in the enzymatic elimination of clogging of pectin cake in filtration process. *Journal of Food Engineering*, 111(1), 52-56.
- Fernandez-Lafuente, R. (2010). Lipase from *Thermomyces lanuginosus*: Uses and prospects as an industrial biocatalyst. *Journal of Molecular Catalysis B-Enzymatic*, 62(3-4), 197-212.
- Fjerbaek, L., Christensen, K. V., & Norddahl, B. (2009). A review of the current state of biodiesel production using enzymatic transesterification. *Biotechnology and Bioengineering*, 102(5), 1298-1315.
- Gamba, M., Lapis, A. A. M., & Dupont, J. (2008). Supported ionic liquid enzymatic catalysis for the production of biodiesel. *Advanced Synthesis & Catalysis*, 350(1), 160-164. doi: 10.1002/adsc.200700303
- Gog, A., Roman, M., Tosa, M., Paizs, C., & Irimie, F. D. (2012). Biodiesel production using enzymatic transesterification - Current state and perspectives. *Renewable Energy*, 39(1), 10-16.
- Hernández-Martín, E., & Otero, C. (2008). Different enzyme requirements for the synthesis of biodiesel: Novozym® 435 and Lipozyme® TL IM. *Bioresource technology*, 99(2), 277-286.
- Institute of Shortening and Edible Oils. (2006). Food fats and oil. Washington, DC: Author.
- Jaeger, K. E., Dijkstra, B. W., & Reetz, M. T. (1999). Bacterial biocatalysts: Molecular biology, three-dimensional structures, and biotechnological applications of lipases. *Annual Review of Microbiology*, 53, 315.
- Jaeger, K. E., & Eggert, T. (2002). Lipases for biotechnology. *Current Opinion in Biotechnology*, 13(4), 390-397.
- Jaeger, K. E., & Reetz, M. T. (1998). Microbial lipases form versatile tools for biotechnology. *Trends in Biotechnology*, 16(9), 396-403.

- Jain, S., Sharma, M. P., & Rajvanshi, S. (2011). Acid base catalyzed transesterification kinetics of waste cooking oil. *Fuel Processing Technology*, 92(1), 32-38.
- Kaieda, M., Samukawa, T., Kondo, A., & Fukuda, H. (2001). Effect of methanol and water contents on production of biodiesel fuel from plant oil catalyzed by various lipases in a solvent-free system. *Journal of Bioscience and Bioengineering*, 91(1), 12-15.
- Kemp, W. H. (2006). *Biodiesel basics and beyond*. Ontario, Canada: Aztext Press.
- Kim, K. H., Meysami, B., & Wiley, R. C. (1989). Pectinase recovery from ultrafiltered apple juice. *Journal of Food Science*, 54(2), 412-415.
- Kovac, A., Scheib, H., Pleiss, J., Schmid, R. D., & Paltauf, F. (2000). Molecular basis of lipase stereoselectivity. *European Journal of Lipid Science and Technology*, 102(1), 61-77.
- Krishna, S. H., & Karanth, N. G. (2001). Lipase-catalyzed synthesis of isoamyl butyrate - A kinetic study. *Biochimica Et Biophysica Acta-Protein Structure and Molecular Enzymology*, 1547(2), 262-267.
- Lam, M. K., Lee, M. T., & Mohamed, A. R. (2010). Homogeneous, heterogeneous and enzymatic catalysis for transesterification of high free fatty acid oil (waste cooking oil) to biodiesel: A review. *Biotechnology Advances*, 28(4), 500-518.
- Lazniewski, M., Steczkiewicz, K., Knizewski, L., Wawer, I., & Ginalski, K. (2011). Novel transmembrane lipases of alpha/beta hydrolase fold. *Febs Letters*, 585(6), 870-874.
- Marchetti, J. M., Miguel, V. U., & Errazu, A. F. (2007). Possible methods for biodiesel production. *Renewable & Sustainable Energy Reviews*, 11(6), 1300-1311.
- Nardini, M., & Dijkstra, B. W. (1999). Alpha/beta hydrolase fold enzymes: The family keeps growing. *Current Opinion in Structural Biology*, 9(6), 732-737.
- Ngo, H. L., Xie, Z. G., Kasprzyk, S., Haas, M., & Lin, W. B. (2011). Catalytic synthesis of fatty acid methyl esters from extremely low quality greases. *Journal of the American Oil Chemists Society*, 88(9), 1417-1424.
- Nielsen, P.M., Brask, J., & Fjerbaek, L. (2008). Enzymatic biodiesel production: Technical and economical considerations. *European Journal of Lipid Science and Technology*, 110(8), 692-700.
- Nielsen, P.M. & Rancke-Madsen, A. (2011). Enzymatic large-scale production of biodiesel. *Lipid Technology*, 23(10), 230-233.
- Saleh, J. (2011). *A membrane separation process for biodiesel production*. Unpublished doctoral dissertation. University of Ottawa, Ottawa, Canada.

- Schmid, R. D., & Verger, R. (1998). Lipases: Interfacial enzymes with attractive applications. *Angewandte Chemie-International Edition*, 37(12), 1609-1633.
- Schuchardt, U., Sercheli, R., & Vargas, R. M. (1998). Transesterification of vegetable oils: a review. *Journal of the Brazilian Chemical Society*, 9(3), 199-210.
- Schwartz, L., & Seeley, K. (n.d.). Introduction to tangential flow filtration for laboratory and process development applications. Retrieved from <http://www.pall.com/main/laboratory/literature-library-details.page?id=34212#34227>.
- Shah, S., Sharma, S., & Gupta, M. N. (2003). Enzymatic transesterification for biodiesel production. *Indian Journal of Biochemistry & Biophysics*, 40(6), 392-399.
- Sheu, M. J., Wiley, R. C., & Schlimme, D. V. (1987). Solute and enzyme recoveries in apple juice clarification using ultrafiltration. *Journal of Food Science*, 52(3), 732-736.
- Shimada, Y., Watanabe, Y., Sugihara, A., & Tominaga, Y. (2002). Enzymatic alcoholysis for biodiesel fuel production and application of the reaction to oil processing. *Journal of Molecular Catalysis B-Enzymatic*, 17(3-5), 133-142.
- Silverman, R. B. (2000). *The Organic Chemistry of Enzyme-Catalyzed Reactions*. San Diego, CA: Harcourt, Inc.
- Voet, D. , Voet, J. & Pratt. C.W. (2012). *Fundamentals of biochemistry: Life at the molecular level*. (4th ed ed.). Hoboken, NJ: Wiley.
- Wang, Y., Ou, P. L. S., & Zhang, Z. (2007). Preparation of biodiesel from waste cooking oil via two-step catalyzed process. *Energy Conversion and Management*, 48(1), 184-188.
- Watanabe, Y., Shimada, Y., Sugihara, A., & Tominaga, Y. (2001). Enzymatic conversion of waste edible oil to biodiesel fuel in a fixed-bed bioreactor. *Journal of the American Oil Chemists Society*, 78(7), 703-707.
- Xu, Y. Y., Du, W., Zeng, J., & Liu, D. H. (2004). Conversion of soybean oil to biodiesel fuel using lipozyme TL IM in a solvent-free medium. *Biocatalysis and Biotransformation*, 22(1), 45-48.
- Yan, S. L., Salley, S. O., & Ng, K. Y. S. (2009). Simultaneous transesterification and esterification of unrefined or waste oils over ZnO-La₂O₃ catalysts. *Applied Catalysis a-General*, 353(2), 203-212.
- Yucel, Y. (2012). Optimization of biocatalytic biodiesel production from pomace oil using response surface methodology. *Fuel Processing Technology*, 99, 97-102.

Zhang, Y., Dube, M. A., McLean, D. D., & Kates, M. (2003a). Biodiesel production from waste cooking oil: Process design and technological assessment. *Bioresource Technology*, 89(1), 1-16.

Zhang, Y., Dube, M. A., McLean, D. D., & Kates, M. (2003b). Biodiesel production from waste cooking oil: Economic assessment and sensitivity analysis. *Bioresource Technology*, 90(3), 229-240. doi: 10.1016/s0960-8524(03)00150-0

Vita

Rebecca Leigh Hobden was born to Jim and Bonnie Hobden in Metairie, LA in 1979. She graduated from the Louisiana School for Math Science and the Arts in Natchitoches, LA in June 1997. The following autumn, she entered Manhattan College in Riverdale, NY to study engineering. In the spring of 2001 she was awarded the Bachelor of Science in Chemical Engineering. That summer she joined AmeriCorps in Portland, OR to work in the Portland Public School system as a Resource Conservation Coordinator. In the summer of 2006 she enrolled at Western Carolina University in the NC Teach Program, and she received her license to teach secondary mathematics in the state of North Carolina in the fall of 2008. She taught mathematics at ArtSpace Charter School in Swannanoa, NC from 2007 to 2011. In the fall of 2011 she began studying towards a Master of Science degree in Technology with a concentration in Renewable Energy Engineering at Appalachian State University. That same year she accepted a research assistantship in the Technology Department working on biodiesel production. The M.S. was awarded in May 2013.